Regional geophysical investigation of the Sudbury structure

by

Oladele Folajimi Olaniyan

A thesis submitted in partial fullfillment
of the requirements for the degree of
Doctor of Philosophy (PhD) in Mineral Deposits and Precambrian Geology

The School of Graduate Studies
Laurentian University
Sudbury, Ontario, Canada

THESIS DEFENCE COMMITTEE/COMITÉ DE SOUTENANCE DE THÈSE

Laurentian Université/Université Laurentienne
School of Graduate Studies/École des études supérieures

Title of Thesis Titre de la thèse	REGIONAL GEOPHYSICAL INVESTIGATION OF THE SUDBURY STRUCTURE
Name of Candidate Nom du candidat	Olaniyan, Oladele Folajimi
Degree Diplôme	Doctor of Philosophy
Department/Program Département/Programme	Mineral Deposits and Precambrian Geology
Date of Defence Date de la soutenance	July 15, 2014

APPROVED/APPROUVÉ

Thesis Examiners/Examinateurs de thèse:

Dr. Richard Smith
(Supervisor/Directeur de thèse)

Dr. Bruno Lafrance
(Committee member/Membre du comité)

Dr. Harold Gibson
(Committee member/Membre du comité)

Dr. Bernd Milkereit
(External Examiner/Examinateur externe)

Dr. Ming Cai
(Internal Examiner/Examinateur interne)

Approved for the School of Graduate Studies
Approuvé pour l'École des études supérieures
Dr. David Lesbarrères
M. David Lesbarrères
Director, School of Graduate Studies
Directeur, École des études supérieures

ACCESSIBILITY CLAUSE AND PERMISSION TO USE

ABSTRACT

The ca. 1850 Ma Sudbury structure (SS) lies in the Canadian Shield at the paleocontinental margin between the Archean Superior province and the Proterozoic Southern Province. It comprises the Sudbury Igneous Complex (SIC), underlying brecciated footwall rocks, and the overlying sedimentary sequence of the Whitewater Group that occupy the central depression of the SIC. Having gone through a series of syn- and post-formation orogenies, the hypothesized initial circular shape of the SIC has been deformed into an elliptical shape of about 28 km by 60 km. Contacts qualitatively interpreted from the computed directional and tilt derivatives of the magnetic field are mostly coincident with the mapped geological contacts, especially in the North Range, but show some inconsistencies in the South Range probably due to extensive alteration and deformation processes. Interpreted magnetic lineaments further highlight the continuity of some previously known faults and dykes and also revealed some new lineaments probably buried or otherwise obscured. Two-and-a-half dimensional joint magnetic and gravity forward modelling consistent with the magnetic contacts and a new interpretation of the Lithoprobe seismic section incorporated a north-verging fold into the basal portion of the SIC in the South Range. The location of the basal deformation is coincident with and could be related to a linear gravity high observed within the Sudbury Basin. Geological interpretation along six profiles was used to develop a three-dimensional geological model of the Sudbury structure and forward gravity computation suggests the existence of a dense feature, interpreted to be mafic volcanic rocks of the Elliot Lake Group, at about 5-6 km depth under the Sudbury Basin. Sulfide-rich sublayer norite could lie above this deformed zone, suggesting it to be a deep prospective zone for future investigation. Northwest-directed closure and reversal of the Huronian rift basin during the Penokean orogeny is suggested to explain the development of

structures at the base of the SIC. This interpretation is consistent with most reflectors of the Lithoprobe seismic section.

KEYWORDS

Sudbury structure, magnetic, gravity, interpretation, 2.5-D, 3-D, geological modelling, basal deformation, Lithoprobe section, forward modelling

ACKNOWLEDGEMENTS

This thesis is the most important product of my Ph.D. research work. It has been a very challenging research project that has enriched my life, but also a task that turned out to be tedious at times, long, demanding and often hard to combine with other important things in life. This research work would not have been completed without help of God and the support of many people, therefore I wish to express my sincere appreciation to them all.

First of all, I would like to thank my thesis supervisor, Richard Smith, for believing in me. Through his NSERC Industrial Research Chair (IRC) funding, he financially supported this research work. Of more importance to me is the fatherly support, patience and the valuable and promptly provided comments on my drafts and ideas. He took his time to listen and attend to most of the challenges I encountered during this research work; taught me the basics of exploration geophysical and research techniques; how to read scientific papers; how to write scientific statements that would not be provocative. I learnt a lot of valuable things from you that will take me very far in life.

Secondly, I would like to thank my other thesis supervisor, Bill Morris. In his busy schedule, he was still able to provide me with valuable corrections and suggestions that moved the research work forward to success. His critical statements and comments on my drafts got me thinking very deep several times on how to improve the research work. Though the distance did not allow us to relate very well, I gain a lot from the little interactions I had with you via emails and whenever we met in person.

Am also deeply grateful to Bruno Lafrance for the structural geology tips he suggested to me during the interpretation of the Lithoprobe section and geological modelling. His comments

helped to shape my thoughts and relate the geophysical interpretations to the observed geology. Thank you so much Darrel Long for teaching me about rocks, sedimentary basins and the geology of the Sudbury structure. Those huge volumes on Sudbury Geology were of great assistance to me. I am also grateful for the editorial assistance you rendered when you were on my PhD research committee before you went on sabbatical.

Harold Gibson, thank you so much for taking me round the Sudbury structure to show the different rock types in-situ. That field trip with you enhanced my geophysical interpretation process. To other faculty members like Mike Lesher, Phillips Thurston, Elisabeth Turner, and Douglas Tinkham that I interacted with in the course of this study and probably asked me questions during my series of seminar presentations that further helped my thinking process, you are really appreciated. My appreciation goes to all staff of Wallbridge Mining and Alan King for the industry experience I gained while working there as a geoscientist. To all the geophysics research students, our weekly interactions at the departmental project-progress meetings were very valuable. Thank you.

This research was financially supported by NSERC, Vale, Sudbury Integrated Nickel Operations, a Glencore company, KGHM International, Wallbridge Mining and the Centre for Excellence in Mining Innovation (CEMI).

To my wife, Oreoluwa Olaniyan who has been carrying the parental load during the past four years and taking care of our two boys, while am here in Canada for study, I am really grateful for your support and highly indebted to you. Indeed, your type of woman is rare and I love you. My kids, David and Daniel, you are loved so much. To all my family and well-wishers, thank you for your support and prayers. God bless you all.

TABLE OF CONTENTS *Page*

LIST OF FIGURES

LIST OF TABLES

CHAPTER 1: INTRODUCTION TO THESIS

1.1 Introduction

In an effort to unravel the subsurface geometry of the enigmatic Sudbury structure as an aid to understanding its origin, most of the past geophysical interpretations focused on quantitative interpretation of seismic data and modeling of gravity and magnetic profiles. Accordingly, this section provides a brief overview of the regional geological setting of the Sudbury structure and past geophysical interpretations that are broadly related to this study.

The event that formed the Sudbury structure (SS) occurred at about 1850 Ma (Krogh, 1984) at the paleocontinental margin between the Archean Superior Province to the north, the Proterozoic Southern province to the south and the Mesoproterozoic Grenville Province to the south-east (Figure 1.1). The centre of the Sudbury structure hosts the elliptical-shaped Sudbury Igneous Complex (SIC), which encloses an approximately 3 km thick pile of basal igneous rocks, breecias, and sediments of the Whitewater Group in its current central depression (Dresler, 1984). The Main Mass of the SIC consists of norite, quartz gabbro and granophyre, and is geographically divided into North, East, and South Ranges (Giblin, 1984). Archean basement rocks, comprising the Levack Gneiss Complex (LGC) and other granitiod rocks gently dip southwards under the SIC in the North and East Ranges, wheras Huronian metasedimentary rocks, in excess of 12 km in thickness, overlie it to the south (Milkereit et al., 1992; Long, 2004). The Huronian rocks extend south of the SIC and extend north-east along the SIC and thin northwards on the Archean basement to form the foot to the South Range. Xenolith-bearing, sulfide-rich sublayer norite occurs as a discontinous unit that is localized in paleo-topographic

depresions below the Main Mass of the SIC and upon the breeiated footwall rocks (Naldrett et al., 1984).

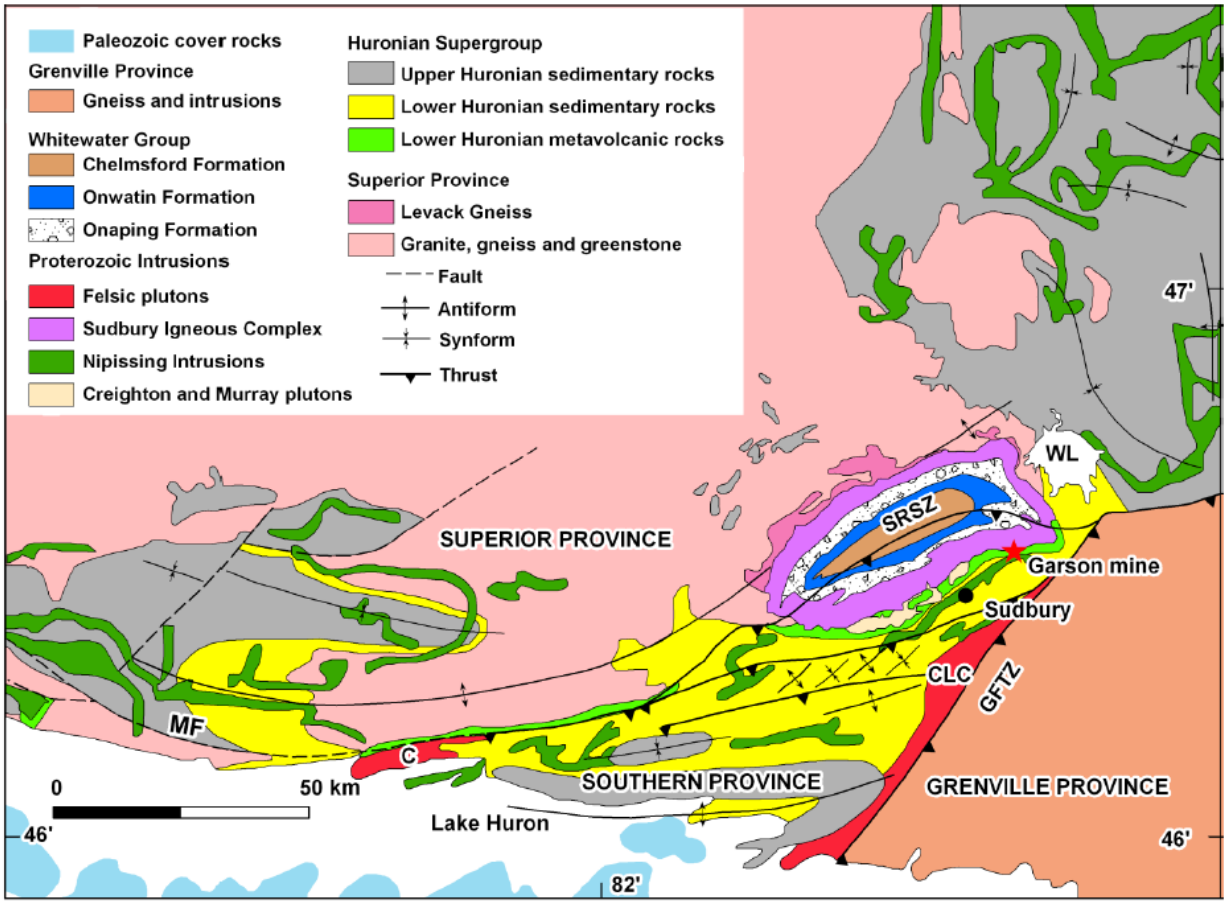

Figure 1.1: Regional geological setting of the Sudbury Structure (Mukwakwami et al., 2014). Map has been modified after Card et al., 1984; Riller 2005; Ames et al., 2005. GFTZ: Grenville Front Tectonic Zone, MF: Murray Fault, C: Cutler granite, CLC: Chief Lake Complex.

Early work by Popelar (1972) interpreted a gravity dataset and proposed three different models for the Sudbury structure: i) a funnel-shaped asymmetrical model of norite and norite-gabbro (2.83 g/cm^3) embedded in a lighter granitic crust (2.63 g/cm^3); ii) folded sills of overturned

norite on a gneissic substratum (2.73 g/cm^3); and iii) a folded-sill norite layer (2.83 g/cm^3) on lighter granitic material (2.65 g/cm^3). Popelar's models have been described by Gupta et al. (1984) to be gravitationally unstable, as heavier rocks are underlain by the lighter rocks and furthermore, the background density value of 2.63 g/cm^3 employed in Popelar's models is too low.

Gupta et al., (1984) modelled nine gravity and magnetic profiles across the SIC (in a north-south direction) using a background density value of 2.73 g/cm^3 for the crustal rock. Their models used a large, buried, dense intrusive sill-like body located at a depth between 5 and 8 km to explain the magnetic and gravity anomalies of the Sudbury Igneous Complex (SIC). They acknowledged the method used for the regional-residual separation was very subjective and could have introduced inconsistencies into the models (Gupta et al., 1984). Later, McGrath and Broome (1994) used a Lithoprobe seismic section to constrain gravity models of the SIC. They assigned a density value of 2.73 g/cm^3 to the Levack gneiss, but they had to introduce an additional 3.0 g/cm^3, 2-3 km thick layer of denser Levack gneiss immediately below the SIC, in order to satisfy the gravity response. It was acknowledged that their approach caused the gravity response of the model to tend toward zero over the Levack gneiss and that the value of the base-level shift required to compare the observed and the calculated gravity data is dependent on the selected density of the Levack gneiss (McGrath and Broome, 1994).

Hearst et al. (1994) carried out magnetic modeling of the SIC using an interpretation of the Lithoprobe seismic data by Milkereit et al. (1992) as a geometric constraint of the subsurface. Their model attributed the three main sources of magnetic anomalies along the Lithoprobe profile to the Levack Gneiss Complex, Onwatin-Onaping contact and the South Range norite.

They suggested that the modelling of the magnetic response of the Sudbury structure requires a more detailed geologic section than provided by the seismic section developed by Milkereit et al. (1992). Mueller and Morris (1995) attempted to constrain the geometry of the base of the norite using a set of cubes parameterised with physical properties such as density, susceptibility and remanent magnetisation. They developed 3-D models of the SIC with the south range dipping steeply south and proposed a deformed and upthrusted configuration for the base of norite in the North Range. These deductions are not consistent with recent geological and Lithoprobe seismic reflection interpretations (Milkereit et al., 1992).

The regional gravity study by Hearst and Morris (2001) suggested that i) the regional-residual separation techniques used by past workers are not optimal, due to the spatial overlap of the short and long wavelength structures of the SS; and ii) a portion of the near-surface geology has the same orientation and dimension as more deep-seated sources, therefore frequency-domain filtering introduces errors into the interpretation of the data. Of all the numerical methods they applied to determine the regional component, upward continuation seems to give a clearer view of the structural trend of the deeper parts of the SIC (Hearst and Morris, 2001).

The Lithoprobe seismic survey across the structure reported by Milkereit et al. (1992) contained five 2-D profiles. Data were acquired along these profiles to define the deep structure and refine existing knowledge of the SIC at depth. The structure of the North Range was well defined and consistent with drill holes in the eastern part of the North Range; however, the southern structure at depth was interpreted to be more complicated (Milkereit et al., 1994). Further seismic sections were acquired to better understand the geometry of the faults, shear zones and rock fabrics at depth (Boerner et al., 2000). Four of the seismic profiles were used by Boerner et al. (2000) to

construct a schematic 3-D model of the South Range Shear Zone (SRSZ). It was noted that the seismic image of the deformation was more developed in the Onaping Formation and since none of the sections crossed the SE lobe where the foliation trajectories turn almost EW, the geometry of the SRSZ in the SE lobe of the SIC remains poorly studied from a geophysical perspective. Also as part of the Lithoprobe Abitibi-Greenville transect experiment, Moon and Jiao (1998) studied seismic profiles in directions that were almost N-S and E-W across the Sudbury basin. Results from forward and inverse modelling of seismic data, tomographic inversion and preliminary interpretation suggest a high velocity lenticular shape below the SS at a depth range of approximately 4.5 – 9.0 km (Moon and Jiao, 1998).

A more detailed 3-D survey was used to estimate the structure in a small (4 by 6 km) area around the Trill deposit (Milkereit et al., 2000). Also, Synder et al. (2002) carried out downhole seismic studies on the NE lobe of the SIC and used a vertical seismic profile to map out the top and bottom of the Sublayer-norite unit. The areas covered by these 3-D and vertical seismic surveys are very small and don't provide regional scale structural information.

Dreuse et al. (2010) determined the thickness of the SIC, variations in the topography of the crater floor and the extent of post-impact tilting of layers. They extracted strike and dip measurements from the existing geological map of the Sudbury basin (Ames et al., 2005) and used high resolution topographical data to model the base of the norite, quartz gabbro-granophyre and granophyre-Onaping contacts. The 3-D topographical model constructed by Dreuse et al. (2010) revealed two main points. i) The dip magnitude of the SIC is not constant down dip and changes at depth. The shallow part of the SIC dip at 27^{o}, while the dip magnitude gets steeper near the centre of the SIC (41^{o}) at depth. ii) The crater floor depressions are

associated with the mineralisation in the quartz gabbro-norite layer and the sublayer. The study of Dreuse et al. (2010) was solely based on topographical information and surface measurements with no subsurface constraint or geophysical data. Furthermore, the investigation was only to the depth of about 3 km and only the North Range and the East Range were considered in the study.

1.2 Problem Statement

Extensive geological studies by individuals and mining companies have defined the lithological contacts and structures at surface in the Sudbury area (Pye et al., 1994; Dressler et al., 1994). This information has been compiled into a bedrock geological map of the Sudbury structure (Ames et al., 2005). Geological maps are generally based on discrete and sparse observations, due to lack of outcrop and accessibility. In addition, the location accuracy of early mapping techniques were lower in most cases, before the advent of the global positioning system. It is probable that some lithological and structural inaccuracies and generalizations in the original field maps have been propagated into the final compilation. Qualitative studies of airborne geophysical data can complement the geological observations and interpretations. Maps generated from qualitative geophysical interpretations showing contacts, faults, dykes etc. can assist the geologist to correlate structures and contacts between outcrops and subsequently enable comparison of geophysical contacts and mapped contacts to delineate the geology.

Furthermore, in the last decade, over $100 billion was spent in exploration worldwide with just 524 new discoveries made (Osmond et al., 2014). This reiterates the increased difficulty of finding large, high-grade and economic ore bodies near surface and the need to expand the search volume to greater depth (Salisbury and Snyder, 2007); for example, mining activities at TauTona Mine, South Africa have reached about 4 km depth. Exploration and mining of Ni-Cu-

PGEs in the Sudbury structure (SS) is currently close to 3 km depth at the Creighton mine. This implies the existence or continuity of high-grade sulfide mineralisation to greater depths in the SIC. These deep-seated deposits are likely to be controlled by pre-existing and syn- and post-impact structures as well as the brecciated footwall rocks that are related to the impact event.

In the absence of detailed geological information about the subsurface, the knowledge base of the deep-seated structures in the basal part of the Sudbury Igneous Complex (SIC) can be improved by interpreting the available potential-field data. The gravity and magnetic potential-field data comprise both short and long wavelength information generally reflecting near-surface and deeper structures, respectively. These fields can be forward modelled and inverted to develop subsurface 3-D models of the density and magnetic susceptibility that could be related to lithological structures. At the beginning of this project, a number of high-resolution magnetic and electromagnetic data sets were made available. These were compiled to make a single high resolution magnetic grid covering the SS and the rocks to the north. Preliminary visual inspection of the high-resolution airborne magnetic grid and the GSC gravity dataset highlights some regional geophysical anomalies in the SIC that previous geological mapping and near-surface interpretations had not adequately explained. What could be the source or cause of these regional magnetic and gravity anomalies? How much more can we learn from these unexplained geophysical anomalies?

Therefore, this thesis work exploits the recent advancements in airborne geophysical data acquisition and availability of geophysical processing packages to compile, process and interpret high-resolution potential-field and frequency-domain electromagnetic (FDEM) data in and around the Sudbury structure; carry out both qualitative and quantitative geophysical studies to develop surficial geophysical interpretation maps; and undertake constrained 2.5-D and 3-D

geophysical modelling of the subsurface to provide insights into the source of some previously unexplained gravity and magnetic anomalies in the SS.

1.3 Research Questions Addressed by the Study

The ultimate aim is to develop a 3-D geological model that best represents the deeper portion of the Sudbury structure in a manner consistent with available geological information.

Critical questions that were addressed in this study include:

- How does the interpreted magneto-stratigraphic lithologies, contacts, lineaments and other structures compare to the existing surface geological map of the basin? Can these produce new structural information?
- What are the structural styles and relative ages of intersecting structures?
- Can a seismically constrained 2.5-D integrated gravity and magnetic model provide structural information about the underlying rocks?
- Using the limited subsurface geometrical constraints and potential field data, how best can a 3-D geological model be developed to provide an insight into some previously unexplained geophysical anomalies observed in the gravity and magnetic data?
- What is the cause of the linear gravity high observed under the Sudbury Basin in the South Range? Can this be related to the interpreted basal deformation of the SIC?
- Are the proposed basal deep structures compatible with the known deformation history of the SIC?

- Based on the developed 3-D geological model, are there zones that could be prospective for Ni-Cu- PGE at the basal part of the SIC?

1.4 Structure of Thesis

Each chapter of this thesis, except the introduction and the final chapter has been written as an individual stand-alone manuscript for peer-reviewed journals. Chapter 2 has been published in the Society of Exploration Geophysicists' journal *Interpretation*. Chapter 3 has been submitted to the *Canadian Journal of Earth Sciences*, and is accepted subject to revisions. Chapter 4 is being prepared for submission. Being a single project documented with three manuscripts, some sections such as the 'regional geology' and part of the 'introduction' may be similar in content to enable each chapter to stand alone.

Chapter 2 presents the results of the qualitative geophysical interpretation of the high-resolution magnetic compilation and an Aerodat frequency-domain electromagnetic survey. It is written as a manuscript entitled "**Qualitative geophysical investigation of the Sudbury structure**" (Interpretation, volume **1**: pages 25-43). It starts with an overview of the geology of the Sudbury structure, then summarises the attributes of the available geophysical datasets in a table. The next section discusses the different data pre-processing and enhancement methods, which include merging of the different magnetic datasets, microleveling and subsequent directional filters and tilt derivative mapping to enhance the shorter wavelength information in the magnetic data. GIS-based information extraction of magnetic contacts and lineaments is described in the next section. This chapter also presents a comparison of the newly interpreted magnetic contacts and lineaments with those on the latest geological compilation in a tabular commentary that describes

the differences and similarities as well as the new features. The rationale for the conductivity mapping and the results of the regional electromagnetic interpretation are discussed.

The co-authors on this publication are Richard S. Smith, Department of Earth Sciences, Laurentian University, 935 Ramsey Lake Road, Sudbury, Ontario, Canada, P3E 2C6 and Bill Morris, Applied Geophysics Group, School of Geography and Earth Sciences, McMaster University, 1280 Main Street West, Hamilton, Ontario, Canada L8S 4M1.

Chapter 3 is written as a manuscript entitled "**A constrained potential field data interpretation of the deep geometry of the Sudbury structure**". It builds on the qualitative interpretation presented in Chapter 2, using the interpreted contacts as surface constraints in a constrained 2.5-D investigation of the deeper portion of the Sudbury structure along the Lithoprobe seismic section. Other constraints are a new interpretation of the Lithoprobe seismic section as well as new physical properties from published sources. In order to explain the potential field data a block of dense Elsie Mountain formation is hypothesized to be thrusted along the base of the Sudbury structure. The potential-field-profile data is magnetic data from compilation and airborne gravity data provided by Vale. The co-authors on this publication are Richard S. Smith and Bruno Lafrance, Department of Earth Sciences, Laurentian University, 935 Ramsey Lake Road, Sudbury, Ontario, Canada, P3E 2C6.

Chapter 4 focuses on the extrapolation of the constrained geological interpretation generated from the Lithoprobe line and the perpendicular line (Chapter 3) to four other sub-parallel profiles using the gravity and magnetic data as constraints. The six modelled profiles are then used to construct a 3-D geological model of the Sudbury structure in Geomodeller software. 3-D forward modelling shows that the thrust block of dense Elsie Mountain formation is laterally extensive.

The last part of the chapter initiates a discussion on the timing of the proposed basal deformation of the SIC and the sequence of events that deformed the initial circular shape of the SIC. The co-authors on this publication are Richard S. Smith and Bruno Lafrance Department of Earth Sciences, Laurentian University, 935 Ramsey Lake Road, Sudbury, Ontario, Canada, P3E 2C6.

Chapter 5 discusses how the major outputs of this current study can be further used to investigate the deeper geometry of the SIC and also outlines some more specific future research work related to geophysical data acquisition, processing and interpretation that might resolve some new questions generated by this current study.

1.5 Statement of Original Contributions

My supervisor Richard Smith conceived the initial concept of the carrying out a regional geophysical study of the Sudbury structure with the Industrial research chair (IRC) sponsors, but I developed the scope of the project, identified the core issues, and the research questions that were addressed in this study. Richard Smith supervised all aspects of this project, Bill Morris suggested improvements and edited the first two manuscripts and Bruno Lafrance critiqued the last two manuscripts of this thesis. Harold Gibson reviewed and edited all the chapters of this thesis.

Specifically, I merged and microleveled the available airborne magnetic data to produce the currently most extensive high-resolution magnetic data of the Sudbury structure. It covers the entire SIC at 20 m cell size and extends about 10 km into the North Range at 50 m grid cell size. I processed the merged airborne magnetic data to generate directional and tilt derivatives that

enhance the shorter wavelengths in the magnetic data. A GIS-based lineament interpretation was performed to map out all major contacts of rocks and discontinuities such as fault and dykes; I generated the magneto-stratigraphic map of the Sudbury structure based on the distribution of magnetic minerals, using magnetic derivatives. This map was compared to the published geological map to highlight their similarities and differences. Some magnetic lineaments correspond with well mapped geological structures, some are further extensions of partially mapped structures, while other new linear structures were identified. A large amount of time was spent interpreting 1881 profile lines of the frequency-domain airborne electromagnetic data of the Sudbury structure and I selected 7940 EM anomaly peaks to generate a regional conductivity map of the Sudbury structure. Some of these EM anomalies were interpreted to be due to responses from conductive ore bodies, faults, dykes, lithological contacts and cultural objects. I reinterpreted the Lithoprobe seismic section to include a north-verging fold under the Sudbury Basin in the South Range. The re-interpreted Lithoprobe section was used to constrain a 2.5-D density and magnetic susceptibility model. This 2.5-D model revealed that the north-verging fold is likely related to the linear gravity high under the Sudbury Basin,while the normal fault in the Sudbury basin is related to the interpreted E-W faults interpreted from the qualitative magnetic map. I further investigated these preliminary deductions to see if similar models could be constructed to explain the gravity and magnetic data on another 4 sections across the SIC. I use my quantitative surficial interpretation to guide the construction of the sections away from the Lithoprobe line. Subsequently, I used all the sections to develop a 3-D common earth geological model of the Sudbury structure. I then assigned density values to the different lithological units to compute a 3-D forward response of the developed 3-D geological model. The calculated response compared well with the measured free air gravity of the Sudbury

structure obtained from the Geological Survey of Canada (GSC). Removing the dense feature associated with the north-verging fold structure from the model removed the linear gravity high. Finally, I proposed a sequence for the deformational events that changed the initial circular shape of the SIC.

References

1. Ames, D.E., Davidson, A., Buckle, J.L., and Card, K.D. 2005. Geology, Sudbury bedrock compilation, Ontario. Geological Survey of Canada, Open file 4570, Scale 1:50,000.
2. Boerner, D.E., Milkereit, M., and Davidson, A. 2000. Geoscience impact: a synthesis of studies of the Sudbury structure. Canadian Journal of Earth Sciences, **37**: 477-501.
3. Card, K.D., Gupta, V.K., McGrath, P.H., and Grant, F.S. 1984. The Sudbury structure: Its regional geological and geophysical setting. *In* The Geology and Ore Deposits of the Sudbury Structure . *Edited by* E.G. Pye, A.J. Naldtrett, P.E. Giblin. Ontario Geological Survey Special Volume 1, pp. 25–44.
4. Dressler, B.O. 1984. General Geology of the Sudbury area. *In* The Geology and Ore Deposit of the Sudbury Structure, Ontario Geological Survey, Special Volume **1**: 57-82.
5. Dreuse, R., Doman, D., Santimano, T., and Ulrich, R. 2010. Crater floor topography and impact melt sheet geometry of the Sudbury impact structure, Canada. Terra Nova, **22**: 463-469.
6. Gupta, V.K., Grant, F.S., and Card, K.D. 1984. Chapter 18, Gravity and magnetic characteristics of the Sudbury structure. *In* The Geology and Ore Deposits of the Sudbury structure. *Edited by* E.G. Pye, A.J. Naldrett and P.E. Giblin. Ontario Geological Survey, Special Volume 1, pp. 381-410.

7. Hearst, R.B., and Morris, W.A. 2001. Regional gravity setting of the Sudbury structure. Geophysics, **66**: 1680-1690.
8. Hearst, R.B., Morris, W.A., and Thomas, M.D. 1994. Magnetic interpretation along the Sudbury structure Lithoprobe Transect. *In* Proceedings of the Sudbury-Noril'sk Symposium. *Edited by* P.C. Lightfoot, and A.J. Naldrett. Ontario Geological Survey Special Volume 5, pp. 33-43.
9. Krogh, T.E., Davis, D.W., and Corfu, F. 1984. Precise U-Pb zircon and baddeleyite ages for the Sudbury area. *In* The Geology and Ore Deposit of the Sudbury Structure, Ontario Geological Survey, Special Volume 1, pp. 431-446.
10. Long, D.G.F. 2004. The tectonostatigraphic evolution of the Huronian basement and the subsequent Basin fill: geological constraints on impact models of the Sudbury Event. Precambrian Research, **129**: 203-223.
11. McGrath, P.H., and Broome, H.J. 1994. A gravity model of the Sudbury structure along the Lithoprobe seismic line. Geophysical Research Letters, **21**(10): 955-958.
12. Milkereit, B., Berrer, E.K., King, A.R., Watts, A.H., Roberts, B., Adam, E., Eaton, D.W., Wu, J., and Salisbury, M.H., 2000. Development of 3-D seismic exploration technology for deep nickel-copper deposit- A case history from the Sudbury basin, Canada. Geophysics, **65**(6): 1890-1899.
13. Milkereit, B., Green, A., and Sudbury working group. 1992. Deep geometry of the Sudbury structure from seismic reflection profiling. Geology, **20**: 807-811.
14. Milkereit, B., Green, A., Wu, J., White, D., and Adam, E. 1994. Integrated seismic and borehole geophysical study of the Sudbury igneous complex. In Lithoprobe Sudbury Project. Geophysical Research Letters, **21(**10): 931-934.

15. Moon, W.M., and Jiao, L.X., 1998. Sudbury meteorite-impact structure modeling with Lithoprobe high resolution seismic refraction results. Geoscience Journal, **2** (1): 26-36.
16. Mueller, E.L., and Morris, W.A. 1995. A 3-D model of the Sudbury Igneous Complex. In Society of Exploration Geophysicists, 65th annual international meeting, expanded abstracts. SEG Annual Meeting Expanded Technical Program Abstracts with Biographies, **65**, pp. 777-780.
17. Mukwakwami, J., Lafrance, B., Lesher, C.M., Tinkham, D.K., Rayner, N.M., Ames, D.E. 2014. Deformation, metamorphism and mobilisation of Ni-Cu-PGE sulfides ores at Garson Mine, Sudbury. Ph.D. Thesis, Laurentian University, Sudbury Ontario, Canada.
18. Osmond, R.T., Montoya, R., and Pare. P. 2014. Exploration success- A business model and case study. KEGS geophysical symposium delegate program.
19. Popelar, J. 1972. Gravity Interpretation of the Sudbury Area. *In* New Developments in Sudbury Geology. *Edited by* J.V. Guy-Bray, Geological Association of Canada, Special Paper Number 11, pp. 103-115.
20. Riller, U. 2005 Structural characteristics of the Sudbury impact structure, Canada: impact induced and orogenic deformation. Meteoritics and Planetary Science, **40**: 1723-1740.
21. Salisbury, M., and Snyder, D. 2007. Application of seismic methods to mineral exploration, in Goodfellow, W.D., ed., Mineral Deposits of Canada: A Synthesis of Major Deposit-Types, District Metallogeny, the Evolution of Geological Provinces, and Exploration Methods: Geological Association of Canada, Mineral Deposits Division, Special Publication No. 5, pp. 971-982.

22. Synder, D., Perron, G., Pflug, K., and Stevens, K. 2002. New insight into the structure of the Sudbury igneous complex from downhole seismic studies. Canadian Journal of Earth Sciences, **39**: 943-951.

CHAPTER 2: Qualitative interpretation of the airborne magnetic and electromagnetic data of the Sudbury structure

2.1 Abstract

The Sudbury structure is one of the most studied geological features in the world due to its enigmatic nature and mineral wealth. The available geological work from literature and mining industry operations accumulated for over a century was recently assessed and compiled into a bedrock geological map. Most regional geophysical investigations of the Sudbury structure have been quantitative – modeling and depth estimation without clear definition of surface control.

Airborne total magnetic intensity data (TMI) over the Sudbury structure were compiled, processed and interpreted, to define magnetic stratigraphy boundaries and near-surface lineaments. Traditional directional and normalized derivatives were computed to enhance the high-frequency information in the magnetic field. Available airborne frequency-domain electromagnetic data was also interactively interpreted along profiles and in gridded format, to isolate conductive structures. On screen GIS-based information extraction from multiple derivatives was used to interpret the magnetic contacts, dykes, and lineaments.

The magnetic interpretation was compared with published bedrock maps of the Sudbury structure. Magnetic contacts based on the qualitative classification of the magnetic texture do

not always correspond to the geological boundaries on the existing maps. Some magnetic lineaments correspond with well-defined geological structures, some are further extensions of partially mapped structures, while others are newly identified linear structures. Conductive locations identified from the EM profiles are probably due to responses from conductive ore bodies, faults, dykes, lithological contacts and cultural objects.

2.2 Introduction

Genesis of the current morphology of the Sudbury structure involved a number of geological events: 1) a large scale meteorite impact event generated a thick melt body overlain by a breccia complex (Dietz 1964, French 1972), 2) turbidite sediment infill of the crater basin or Penokean foreland basin; and c) deformation of an originally circular crater to its current elliptical shape. While the age of the impact event has been well-established by radiometric age dating (1849 +/- 0.5 Ma, Krogh et al., 1984), the timing and spatial extent of the sedimentation and the deformation events continue to be the subject of on-going discussion. Critical to achieving a better understanding of the evolution of the Sudbury structure is having a geological map, which is capable of revealing details about the stratigraphic relationships between individual lithological units, and the disposition, displacement and distribution of faults and folds which modified the original structure.

Geological maps of the Sudbury structure were first published in the late 1880's (Bell 1891, Giblin 1984). Over the following 100+ years revised geological maps at varying scales have been published by many authors (Burrows and Rickaby 1930, Collins 1937). Mining companies active in the Sudbury area were also producing detailed studies of their individual mineral deposits (for example Lochhead, 1955). Compilation maps that summarised the geology of the Sudbury area began to appear with the work of Card (1978a). These were followed by a detailed

basin study by Dressler (1984a). Following publication of the 1984 Ontario Geological Survey Volume 1, there was a dramatic increase in the number of geological studies of the Sudbury structure. The culmination of these studies was the publication of the 2005 bedrock geology compilation map reported by Ames et al., (2005) (Figure 2.1).

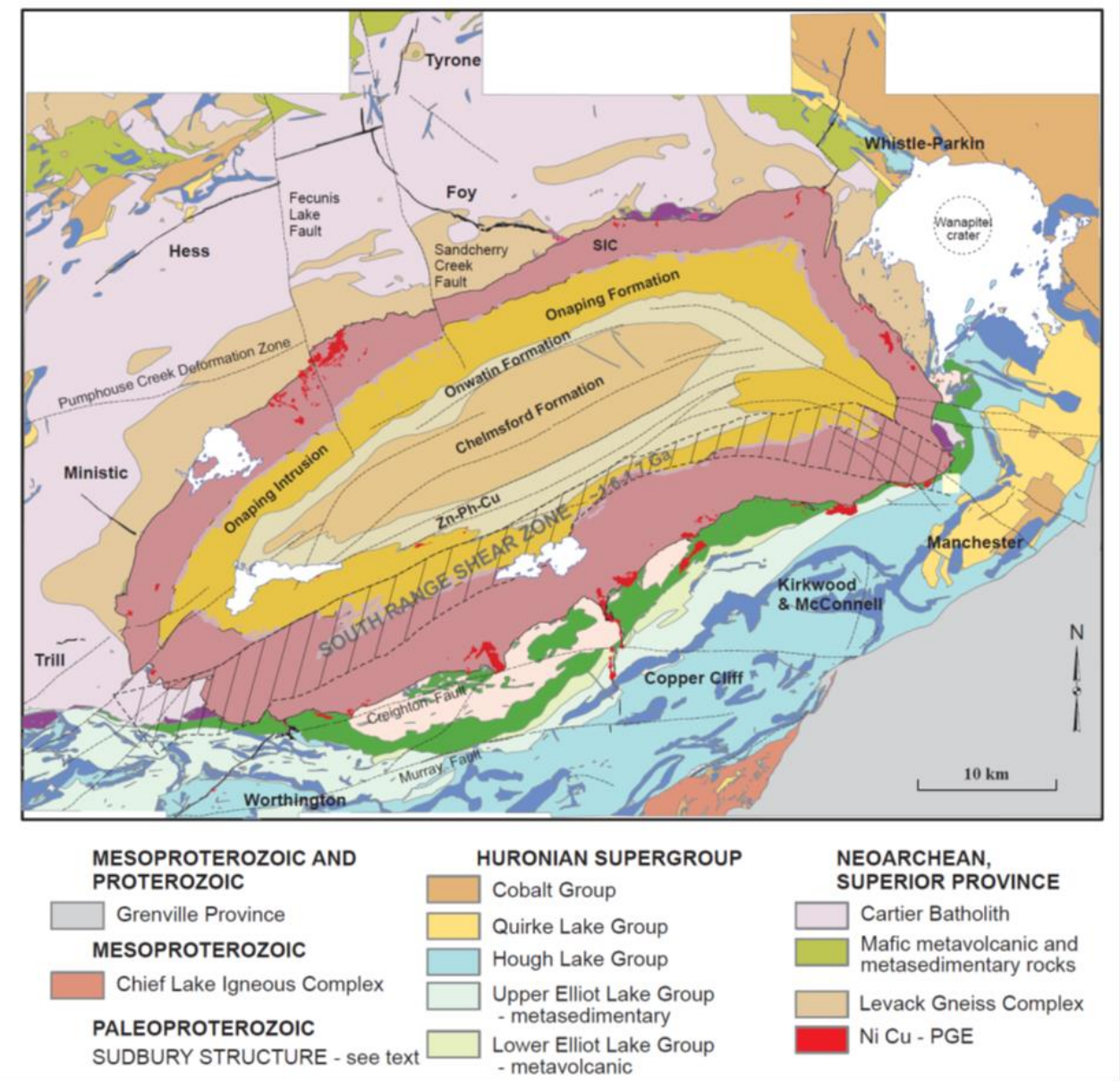

Figure 2.1: Geological map of the Sudbury structure (Ames et al., 2005).

The earliest geological maps of the Sudbury Basin were constructed purely on discrete and sparse field observations. As in many other areas of the Canadian Shield outcrops are limited (less than 1% outcrop in some areas), and access is difficult. Compounding the problem was the need to render these maps in a coherent reference frame, because over the years poorly

constrained air photograph mosaics have been used as a base for field mapping projects. It must be noted that it is only within the last twenty or so years that global positioning system (GPS) sensors have been used to provide locational information at decimetre scales in globally defined projection and datum reference frames. Yet even with high resolution locational information a field geologist is still faced with the problem of having to decide how to link observations made at isolated outcrops.

Airborne geophysical data acquisition and satellite imagery have provided the overview information that permits field geologists to link outcrop information through the continuity of a characteristic geophysical, or spectral signature. Recent advances in data acquisition systems have increased the sensitivity and spatial resolution of remote sensing platforms, it is now possible to perceive features that a few years back were undetectable. For example, at the time that Dressler (1984) produced his compilation map of the Sudbury structure the best resolution aeromagnetic data available was based on 800m flight line spacing.

In addition to advances in instrumentation, there have also been great improvements in data processing packages, which in turn have led to changes in map production. Geophysical data processing with embedded edge detection routines allow the interpreter to quickly locate bounds of regions with a similar geophysical response. Introduction of Geographical Information System (GIS) protocols permits the user to rapidly integrate responses from multiple sensor packages and to interrogate individual data sources for locational constraints. In this context it is worth noting that the recent Ames et al. (2005) compilation is available as ESRI ArcGIS shapefiles, while the Dressler (1984) map was original only available as a print copy.

It is not clear what geophysical data was used in the Ames et al. (2005) compilation map. However, it is known that since that map was published more high resolution geophysical imagery of the Sudbury structure has become publicly available. The authors of the present study are of the opinion that a qualitative geophysical interpretation of magnetic contacts, lineaments and discontinuities based on magnetic mineral distribution will provide better surface control for a subsequent quantitative study. The aim of this project is to process, interpret and integrate the available aeromagnetic and electromagnetic data of the Sudbury structure, in order to: i) extract contact information: ii) define a magneto-stratigraphy based on the distribution of the magnetic anomaly amplitudes and textures; iii) delineate magnetic lineaments (faults); and iv) identify locations of conductive bodies. This interpretation provides a viable geophysics-based map of the bedrock geological contacts and fault distribution within the Sudbury structure. Modifications suggested in the new geophysical interpretation map are discussed through comparison with the currently accepted geological map, which was constructed from geological outcrops, and an older poorer resolution magnetic anomaly map.

2.3 Geology of the Sudbury structure

The Sudbury structure (Giblin, 1984) is typically considered to have formed by a meteorite impact at ~1850Ma (Krogh et al., 1984). It lies regionally at a continental margin, developed adjacent to the Archean Superior Province, with Paleoproterozoic metasediments of the Southern Province occurring to the south. Lithologies associated with the Sudbury structure include a basal Archean high grade metamorphic terrain, and weakly metamorphosed late Precambrian diabase dikes. When discussing the geology of the Sudbury structure, it is common practice to subdivide the outcrop pattern into three areas: the North Range - the elliptical curved northern edge which is mostly dipping to the south; the South Range - the less elliptical southern edge

which is dipping vertically to slightly overturned to the south: and the East Range - the arcuate eastern end of the Basin that links the North and South Ranges.

The oldest rocks in the Sudbury region form the footwall to the Sudbury Igneous Complex on the North and East Ranges. Archean rocks of the Levack Gneiss complex which include high metamorphic grade, granitoids, metavolcanic and metasediments rocks, were uplifted in advance of the meteorite impact event (2711 Ma, Krogh et al., 1984, Milkereit et al., 1992). Sitting unconformably above the Archean is a thick metasedimentary sequence of the Huronian Supergroup (>2450 to 2200 Ma, Krogh et al. 1996; Young et al., 2001), which defines the Southern Province. Locally on the South Range the contact of the Huronian Supergroup and the Sudbury Igneous Complex is marked by mafic and felsic volcanic rocks (Peredery and Morrison, 1984).

Internally the Sudbury structure includes two lithological sequences: a) rocks directly related to the Sudbury Impact event, such as 1) the Sudbury Igneous Complex (SIC), 2) Sudbury breccia and 3) offset dykes; and b) rocks, such as sedimentary rocks and dikes, that were emplaced at a later time (Figure 2.1).

The SIC is a 28 km by 58 km elliptical collar of ‘layered’ igneous rocks that encloses the Sudbury basin. This includes a unit known as the Main Mass that contains the economically important contact Sublayer (Naldrett and Hewlins, 1984). The Main Mass of the Sudbury igneous complex consists of hypersthene bearing Norite at the base, a transition zone of Quartz Gabbro and the uppermost Granophyre unit (Naldrett 1984a). Xenolith and Ni-Cu-PGE ore bearing gabbro-noritic rocks of the Sublayer unit occur as sheets and lenses between the main mass Norite and the outermost footwall rocks (Naldrett et al., 1984a).

Dykes and irregular bodies of Sudbury breccia, consisting of subrounded clasts in an aphanitic textured matrix, occur from the outermost contact of the SIC, to up to 80 km into the footwall of the SIC (Peredery and Morrison 1984). The quartz dioritic offset dykes occur as sulphide-bearing radial dykes that radiate from the SIC and concentric dykes that are sub-parallel to the SIC (Grant and Bite, 1984).

The sedimentary basin is filled with hypabyssal intrusions, overlain by pelagic mudrocks and proximal turbidite sedimentary rocks of the Whitewater Group. The Whitewater Group is 2900 m thick and is made up of four formations. At the base of the group is a hypabyssal intrusion and upward fining complex sequence of breccia (the Onaping Formation), which is in places overlain by a sulphide-rich carbonate (the Vermilion Formation), a pyritic and carbonaceous laminated mudstone (Onwatin Formation) and finally the muddy sandstone of the Chelmsford Formation (French 1972; Ames et al., 1998)

Subsequent to crater formation, it is generally thought that deformation of the Sudbury structure occurred during two separate prolonged episodes of ductile and brittle deformation: the Penokean orogeny (1900-1700Ma, Deutsch et al. 1995; Riller 2005) and the Grenville orogeny (1000Ma, Zolnai et al., 1984). Unfortunately, the geological record of the Sudbury structure contains few rocks that were formed between the 1850Ma SIC and the 1238Ma Sudbury olivine diabase dikes, so the timing of deformation remains somewhat speculative. Recently Tschirhart and Morris (2012) have shown that the Grenville Orogeny only resulted in a broad scale fault segmentation of the basin. Further geochronological data reported by Bailey et al. (2004) has suggested that the basin was also deformed during a Mazatzal age event (1700-1600Ma). This interpretation is in agreement with seismic (Wu and Milkereit, 1994) and paleomagnetic

evidence (Morris 2002), which have both indicated two distinct periods of deformation, both of which occurred prior to the late Grenvillian event.

Furthermore, extensive deformation has resulted in a series of faulting, folding, fracturing, and shearing of rocks within the Sudbury structure (Rousell 1975). The faults within the Sudbury structure have been grouped into sets based on their geographic location and strike (Rousell et al., 2002). The fault sets include the Murray set (77^0 strike, Card 1978a), the Vermilion set (065^0 strike, Thompson 1957), the Fecunis set (346^0 strike, Cochrane 1991), the Norduna set (300^0 strike, Dressler et al., 1991), and the Errington set (034^0strike, Paakki 1992).

Weak zones in the Sudbury rocks, such as faults and fractures resulting from brittle deformation, and contacts of the rock units, have been intruded by series of dykes of different composition and age. These dykes include: i) the NW trending Matachewan mafic dykes (2.454 Ma, Heaman 1997), ii) Nipissing diabase dykes (2219 Ma, Corfu and Andrews, 1986), which intruded the Huronian supergroup and occur as undulating sills and dykes, conforming dykes, lopoliths and stocks, iii) Biscotasing dykes (2167 Ma, Buchan et al., 1993), iv) Post- SIC NW trending hornblende diabase dykes associated with the Murray fault set (trap dykes) (Cochrane, 1991), v), olivine diabase dykes (1238 Ma, Fahrig and West, 1986), intruded after the Sudbury event, that have been faulted and rotated about an axis perpendicular to the NE faults during the ca. 1 Ga Grenville orogeny (Zolnai et al., 1984; Tschirhart and Morris, 2012).

Geophysical maps reveal both contacts and lineaments. All geophysical sensors integrate signals in proximity of the sensor; some of these geological lineaments occur and are mappable on the surface, while some are buried at depth, especially within the Whitewater Series, or are under lakes, making it difficult to fully define their location. One major advantage of airborne

geophysical datasets is that they provide a synoptic view of the in-situ structures and contacts at varying depths. Although, the distribution of silicate and magnetic minerals are often not the same, qualitative interpretation of geophysical datasets can provide good ground control, especially in inaccessible and rugged terrains (Pilkington and Keating, 2004).

2.4 Geophysical data description

A combined helicopter-borne magnetic and electromagnetic survey of the Sudbury structure was acquired in 1987 for Falconbridge Limited (now Glencore) by Aerodat Limited. The helicopter was nominally flown at 60 m above the ground towing two geophysical sensors: i) a four frequency electromagnetic system and ii) a cesium vapour magnetometer sensor, each 30 m and 13 m below the aircraft respectively. Average nominal flight line spacing was 100 m and the flight line azimuth was from 150^0 to 330^0, depending on the prevailing strike direction of the major geological structures.

Additional aeromagnetic data incorporated in this study includes a multi-survey compilation completed by McMaster University for Wallbridge Mining. This compilation included data from over 31 individual magnetic surveys that covered segments of the footwall area of the North Range and East Range (Hernan Ugalde, personal communication, 2011). After individually microlevelling each survey, all the data were merged into a single master grid with a spatial resolution (grid cell) of 50 m. In order to fill in the gaps in between the surveys, and expand the coverage area, the Wanapitei Lake magnetic grid (100 m cell size, L'Heureux et al., 2003) and the Geological Survey of Canada (GSC) magnetic data (250 m cell size) were systematically re-gridded to 50 m, merged and microleveled with the footwall magnetic data.

For this study Glencore's Aerodat, GSC and the Wallbridge Mining magnetic grids (Table 1.1) were merged into a single composite grid and it is this data set that forms the basis of the interpretation presented herein.

Table 1.1: Description of airborne geophysical datasets used

S/No	Data type	Flight height	Flight line spacing	Cell size	Data provided courtesy
1	Magnetic	43m	100m	20m	Glencore
2	Magnetic	variable	200m	50m	GSC
3	Magnetic	variable	variable	10m	Wallbridge Mining
4	Frequency EM	30m	100m	20m	Glencore

2.5 Magnetic data processing method

A simple magnetic processing workflow was developed to prepare the magnetic dataset, eliminate non-geological noise and merge the datasets obtained from different sources. Grid enhancement and contact mapping techniques were applied afterwards, to enhance the shorter wavelength of the magnetic data which corresponds to near-surface magnetic contacts and lineaments.

The initial gridding of the line data was done to explore the dataset, assess the quality, and to have a pre-knowledge of the data attributes such as flight azimuth and spatial coverage of the dataset. Geosoft Oasis Montaj minimum curvature gridding algorithm (RANGRID) was used with a multiple of trial cell sizes of 20, 25 and 30 meters. RANGRID cell size should not be much less than half the nominal data point interval found in the areas of interest (Geosoft

technical workshop note). For the Sudbury dataset, the 20 m cell size grid had the best resolution and showed the highest continuity of subtle linear structures, so this cell size was selected for further processing. Several high-frequency data and non-geological features were observed in the directional derivatives of the higher derivatives of the gridded magnetic data, especially in the flight line direction (Figure 2.2a). The flight line artifacts are probably due to the aircraft heading effects or diurnal variations.

A rigorous Minty microleveling technique (Minty, 1985) was performed on the dataset in order to remove the artifacts along the flight lines. This procedure is very labour intensive, because of the multiple different flight directions involved. This required that the composite data set be divided into smaller data sets with a single flight line direction, so that each one could be individually microleveled. The Minty microleveling process was implemented in Oasis Montaj using the Butterworth and the directional cosine filters. The Minty method aims to generate an error grid, which consists of long wavelengths along and short wavelength across the flight lines. For each dataset with the same flight line direction, three filters were applied i) a filter with a cut-off wavelength of four times the flight line spacing using a high-pass Butterworth filter of sixth order across the flight lines, and ii) with a low-pass directional cosine filter (power of 1.0) along the flight lines. The output of this filter is the residual noise grid. iii) The second low pass filter was applied iteratively on the residual noise grid, until it was believed that only the non-geological long wavelength noises along the flight lines were isolated. The low passed error grid was then subtracted from the original grid to obtain the microleveled grid. If successfully applied, the first vertical derivative of the total magnetic intensity (TMI) should contain little evidence of any flight line striping apparent in the raw data (Figure 2.2b).

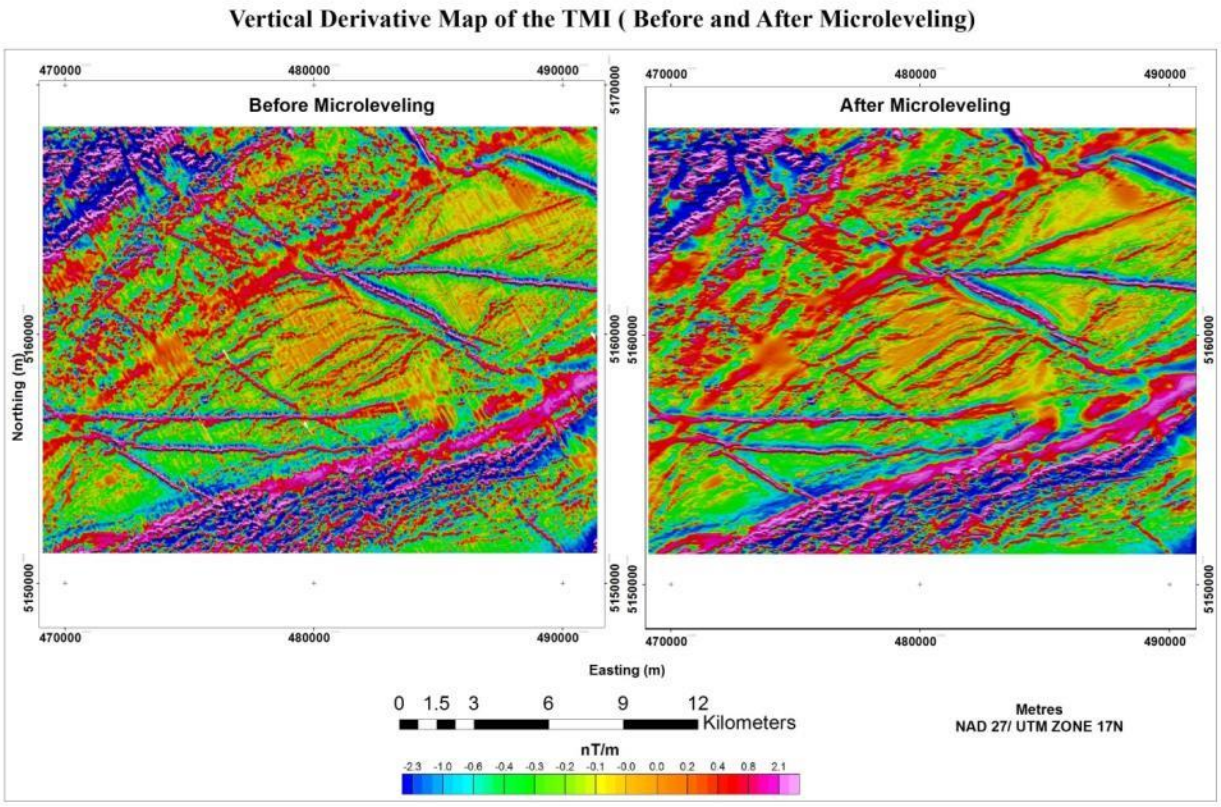

Figure 2.2: (a) First vertical derivative of the TMI before microleveling with geophysical acquisition noise features trend in the NW direction along the flight line. (b) First vertical derivative of the TMI after microleveling.

The microleveled grids of the magnetic data covering the SIC at 20m cell size was merged with the lower resolution 50m cell size dataset covering about 10 km of the footwall rocks from the SIC contact using the Boolean function 'OR' in the grid merging module of the Geosoft Oasis Montaj (Figure 2.3). Although, the merged dataset has lower resolution outside the SIC contact, some major linear magnetic anomalies were traceable from the higher resolution coverage into the lower resolution part. Figure 2.3 shows the merged total-magnetic-intensity field of the

Sudbury structure. The elliptical shape of the SIC is well defined by features with high magnetic intensity. In the North Range, Norite and Gneisses have the highest magnetic intensity especially in the western half of the North Range. Onaping, basal Onaping and the Norite exhibit high magnetic intensity in the South Range. Most dykes have a distinct high magnetic intensity while discontinuities and faults in the North Range have a low magnetic signature. A zone of discontinuity exists at the contact between North Range and East Range.

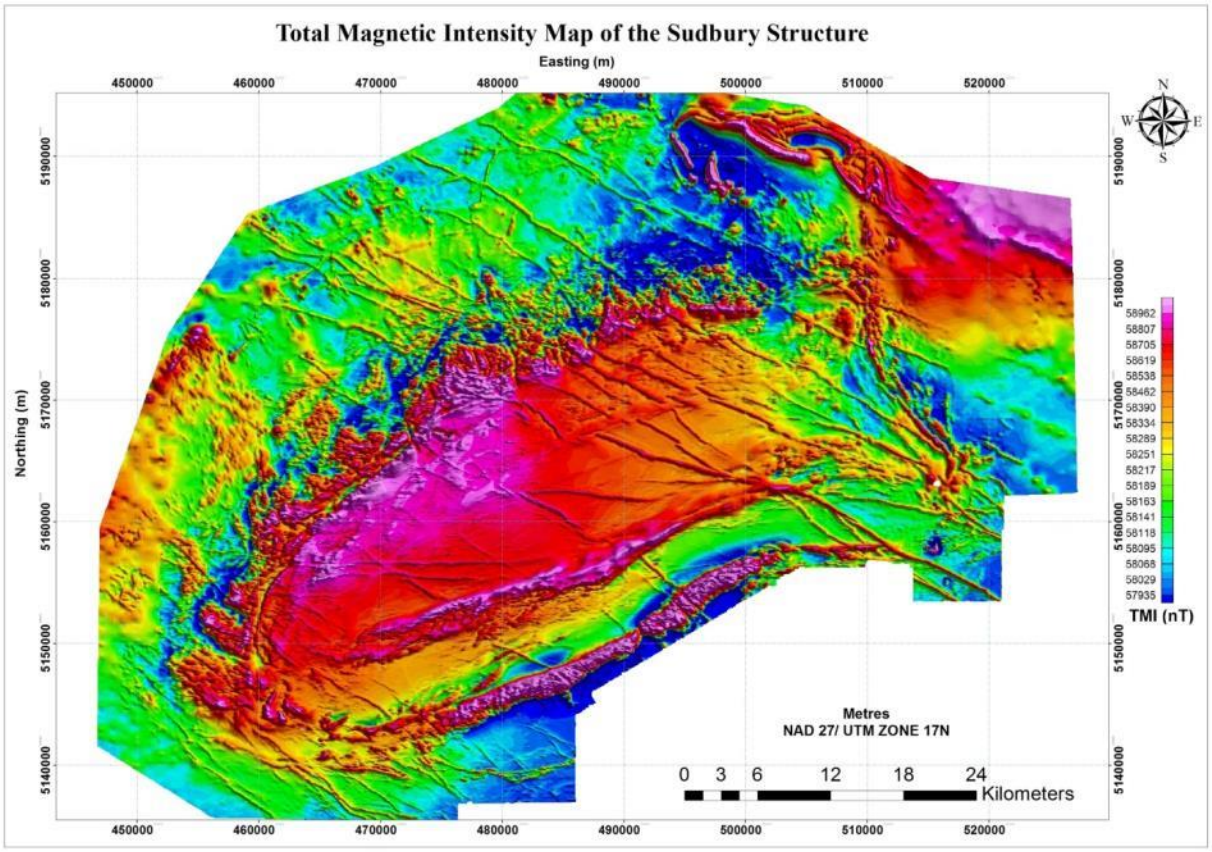

Figure 2.3: Merged total magnetic intensity field of the Sudbury structure. The SIC rocks, dense Levack gneisses and the NW trending dykes are characterised by high magnetic intensity, while the Huronian supergroup to the south and the Archean rocks in the north exhibits low to moderately high magnetic intensity

2.5.1 Magnetic data transformation and enhancement

Total magnetic intensity (TMI) data is a reflection of the spatial distribution of magnetic minerals. Depending on the rock type present the magnetic signal can be controlled by a small percentage of ferromagnetic minerals such as magnetite and pyrrhotite, or a large concentration of more weakly magnetic minerals such as chlorites, amphiboles and some clays. The magnetic signal does not represent standard geology, which is based on the concentration of silicate minerals. Amplitude and wavelength of the magnetic spectrum is dependent on the vertical separation between the magnetometer and the magnetic source (Reeves et al., 1997). The magnetic spectrum is made up of a wide range of short and long wavelength information, which depicts near and deeper sources (Spector and Grant, 1970). Although, shorter wavelength are not likely to be deep seated, long wavelength variations can be attributed to both deep and shallow sources. Subsurface geological evidence shows that the Sudbury igneous complex rocks that occur on the surface are continuous to more than 3 km depth. This configuration makes it difficult to isolate the residual due to near-surface sources from the regional field due to the deeper sources (Hearst and Morris, 2001). The distribution of magnetic minerals within a particular rock unit might not be homogenous due to alteration and metamorphism (Grant, 1985). A continuous rock unit can exhibit higher or lower magnetic intensity where there are altered or unaltered magnetic minerals. Caution and a good knowledge of the geology of the project area are important when processing and interpreting a magnetic dataset.

Traditional contact mapping techniques for gridded geophysical data have been developed over the years. Some contact mapping techniques exhibit maxima, while others highlight an inflection between positive and negative features over the magnetization contrast (Pilkington and Keating,

2010). Contact mapping and edge enhancement techniques on gridded data are accomplished using a convolution spatial filter or by multiplying the transformed data with the equivalent of the spatial filter in the frequency domain (Milligan and Gunn, 1997). Magnetic sources differ in shape, size, depth and geometry, therefore, a single enhancement method cannot provide accurate contact or edge information for all magnetic sources (Pilkington and Keating, 2010). Hence, a combination of contact mapping techniques was employed to delineate the magnetic contacts and lineaments in the Sudbury structure. Interpreting more than one magnetic derivative was helpful, because subtle features are more visible in some products than others.

Some derivatives are in specific directions such as the vertical derivative (VDR) (Hood 1965), total field horizontal derivative (THDR) (Grauch et al. 2001) or a combination of these (analytical signal amplitude) (Hsu et al., 1996). Lower or higher-order directional derivatives are sometimes normalized to amplify the weak, small amplitudes relative to the stronger, larger amplitude anomalies (Fairhead and Williams, 2006). Normalized derivatives such as the tilt angle (Miller and Singh, 1984), the theta derivative (Wijns et al., 2005), the TDX derivative (Cooper and Cowan, 2006) and the horizontal derivative of tilt, TI-HDR (Verduzco et al., 2004) have been implemented to enhance near-surface magnetic contacts and structures. Other higher-order functions such as 3-D local wavenumber (Smith et al., 1998) are based on second or third-order derivatives that require very high signal-to-noise ratios.

The accuracy of the directional and normalized contact mappers depends on the data quality as well as the geometry of the body. Edges of dipping contacts might not be accurately enhanced, as most of the techniques work best at highest gradient contrast. Some derivatives are excellent in mapping edges of vertical contacts while others are more suitable for lateral and textural variation. A recent evaluation of some of the contact enhancement techniques showed that most

of the recently introduced enhancements using higher derivatives are strongly related to the older enhancements, and are therefore redundant for contact mapping (Pilkington and Keating, 2010). This current work does not intend to re-evaluate the different techniques, for further reading, see Fairhead and Williams (2006), Pilkington and Keating (2004, 2010) and references therein.

Our approach was to map contacts and lineament using directional and normalized derivatives such as the vertical derivative (VDR) (Hood 1965), the total-field horizontal derivative (THDR) (Grauch et al. 2001), the tilt derivative (Miller and Singh, 1994), the TDX (Cooper and Cowan, 2006) and the analytical signal amplitude (Hsu et al., 1996). Directional derivatives, both vertical (VDR, Figure 2.4) and horizontal (THDR) were calculated to accentuate the shorter wavelength portion of the magnetic spectrum, which corresponds to the near-surface geological structure. The tilt derivative (Figure 2.5) and TDX of the TMI were calculated from the directional derivatives. Tilt angle values are restricted to lie between $-\pi/2$ and $+\pi/2$, regardless of the amplitude of the VDR or THDR (Miller and Singh, 1994). The Tilt and TDX derivatives enhanced subtle anomalies and form amplitude peaks over magnetic sources.

A combination of the RGB and greyscale of VDR image (Figure 2.4) enhances the magnetic fabrics of the different rock units, linear discontinuities and structural patterns within the highly heterogeneous Levack gneiss complex underlying the North Range and the East Range of the SIC. The filtered tilt derivative grid of values greater than 0, isolates peaks of highly magnetic lineaments, which are mostly NW trending dykes and contacts (Figure 2.5). Subtle SW trending features displaced by the NW trending dykes within the Chelmsford are also further enhanced in the tilt derivative.

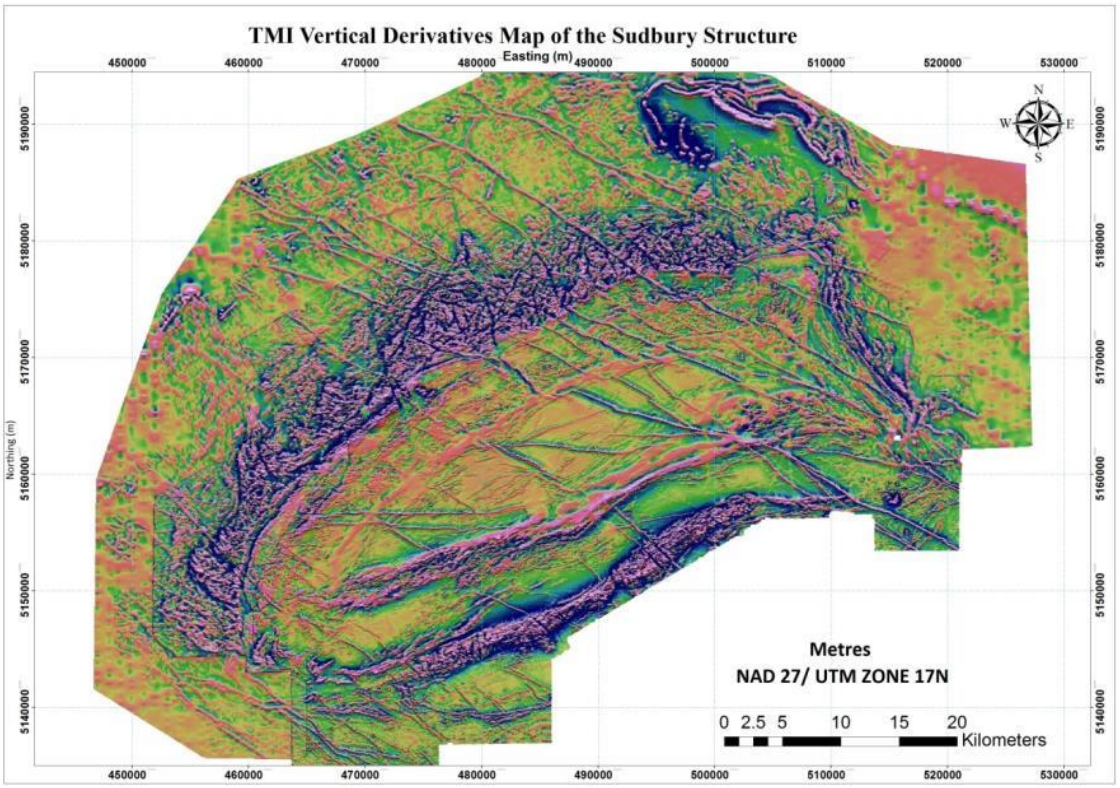

Figure 2.4: Composite map of transparent colored and grey scale images of the TMI vertical derivatives enhances different magnetic fabrics and lineaments in the magnetic data.

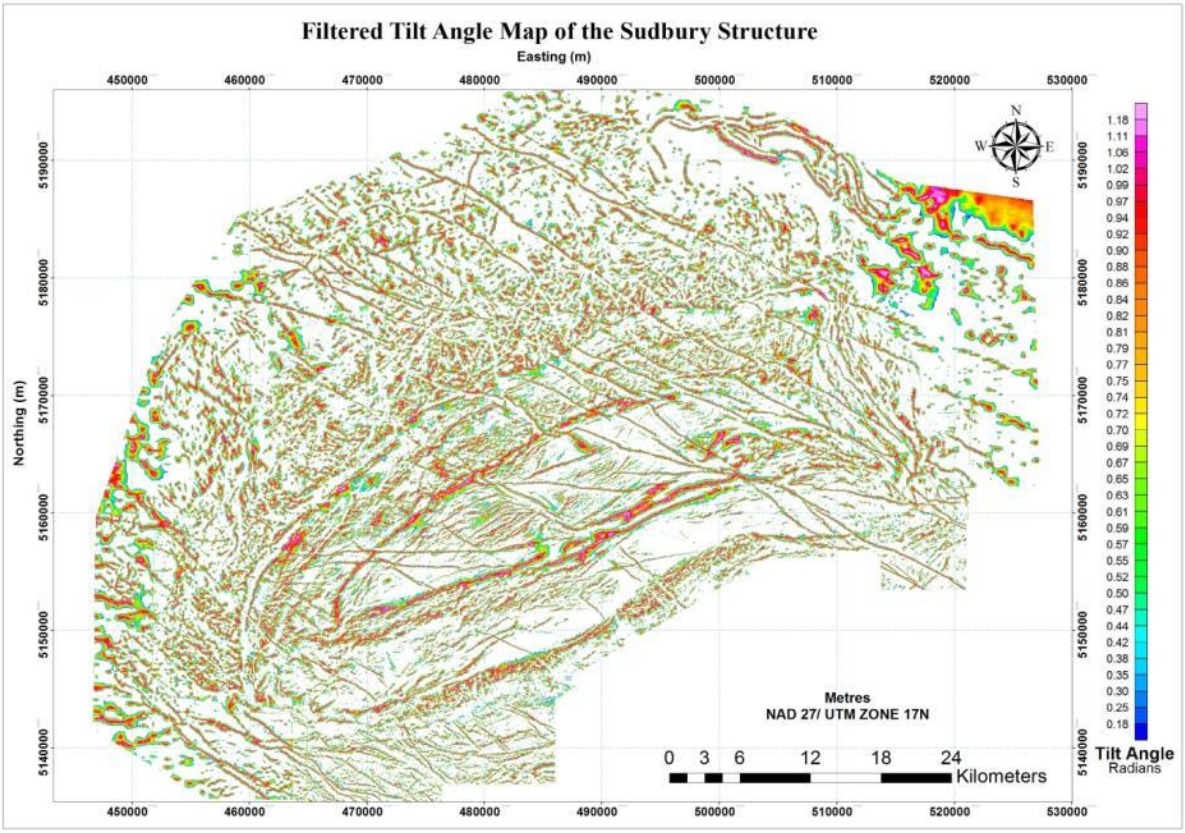

Figure 2.5: Filtered tilt angle derivative of the TMI further amplifies subtle signals and high magnetic lineaments

2.5.2 On-screen contact and lineament mapping

Information extraction was done in a geographic information system (GIS) using ESRI ARCMAP. All features on a map are represented in a GIS as points, lines and polygons. Point are discrete features with just XY e.g. peak of EM anomaly, borehole location, lines are series of discreet points X_1Y_1 X_2Y_2 $X_3Y_3 \ldots X_iY_i$ e.g. lineaments, roads, while polygons are series of discreet points which begin and end at same point X_1Y_1 X_2Y_2 $X_3Y_3 \ldots X_1Y_1$ e.g. lithological units, lakes etc. The scale of the map will influence which GIS object would be used to present a

feature. A lithological unit or dyke represented by a polygon at a large scale (1:2,000) will become a point or line respectively at smaller scale (1:100,000).

Part of the objective of this study was to compare the lineaments extracted from magnetic data with the published bedrock geological map (Ames et al., 2005). This was produced and published at 1:50,000, using UTM NAD 1927 coordinate system, so all the geophysical dataset were re-projected to NAD 27 and information extraction was concentrated on more regional features at a scale of 1: 75,000. Magnetic contacts and lineaments were first mapped as lines based on magnetic fabrics, magnetic peaks, contrasts and discontinuities

2.5.3 Magnetic interpretation map of the Sudbury structure

In addition to the different magnetic mineral content of rocks within the Sudbury structure, there are also different magnetic fabrics evident. This could be related to the grain shapes and preferred crystallographic orientation of the ferromagnetic and paramagnetic minerals in the rock units (Hrouda, 1982), or it could be a reflection of structural deformation, diagenesis, or the manner in which the rocks were deposited (e.g. turbidites). Magnetic stratigraphy contacts were solely differentiated based on qualitative classification of the magnetic fabrics. The differing magnetic textures were qualitatively classified and the point at which the magnetic fabrics changed to another is judged to be the contact of the two magnetic units. These contacts were digitized and polygonized to generate a magnetic stratigraphy map of the Sudbury structure.

The extracted linear information was thereafter classified either as a lithological contact, a fault, a dyke or some other lineament. When there was a close association or spatial relationship with

a known feature on the published geological map, that information was used in the classification. Major faults generally occur as discontinuities within the rocks and exhibit very low magnetic signature. This low magnetic signature exhibited by faults could be due to i) infilling of the fault zone with non-magnetic materials ii) oxidation of the magnetite at the fault plane due to exposure and iii) juxtaposition of displaced rocks against non-magnetic rocks. Mafic dykes, which dominate the Sudbury structure, contain abundant magnetic minerals (magnetite, pyrrhotite), and the dykes therefore exhibit very high magnetic signature relative to their host rocks. Most of the dykes occupying fault zones, e.g. olivine diabase dykes, display relatively low magnetic signature in the Sudbury region, particularly where they crosscut a more magnetic rock such as the SIC in the North Range. Integration of the magnetic stratigraphic map and lineaments generated a magnetic interpretation map of Sudbury structure, which is entirely based on the distribution of the magnetic minerals in the rocks and structures (Figure 2.6).

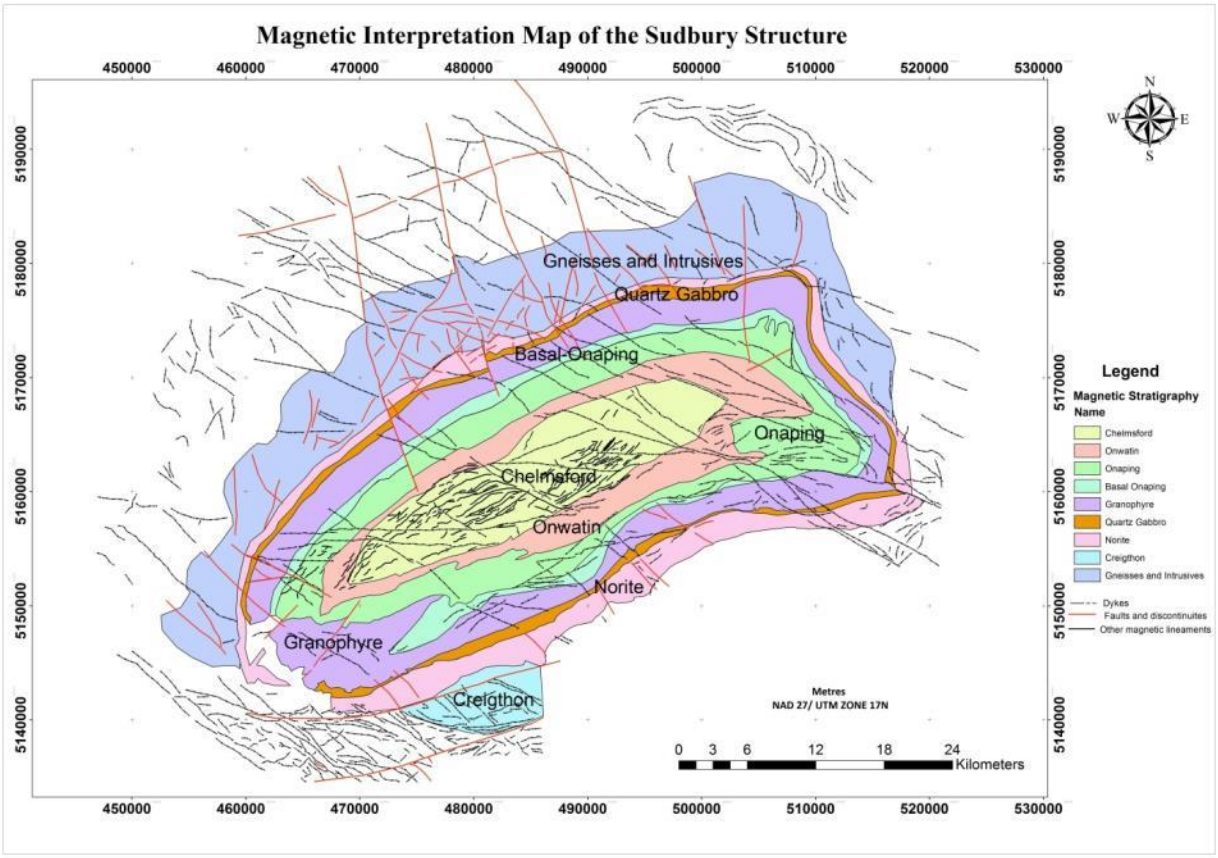

Figure 2.6: Geophysical interpretation map of the Sudbury structure. Magnetic stratigraphy is determined based on qualitative classification of magnetic fabrics representing different rock units. Magnetic discontinuities were mapped as fault, dykes and other magnetic lineaments.

2.6 Qualitative electromagnetic mapping

Electromagnetic surveys respond to conductivity variations in the subsurface. Using electromagnetic data for mapping entails identification of anomalous conductive zones or discrete locations along the traverse. The anomaly pattern varies and depends on the configuration of the transmitter-receiver (coaxial or coplanar) as well as the conductivity and geometry of the body. Frequency-domain electromagnetic data available for this project were

helicopter electromagnetic (HEM) data acquired with the Aerodat system using co-planar (32,000 Hz, 4175 Hz) and co-axial (4600Hz and 935 Hz) coil pairs. Figure 2.7 shows the theoretical HEM anomalies caused by simple conductors (Fraser, 1996).

Components of the secondary field at varying frequencies in the coplanar and coaxial modes were interpreted. The primary field of the coaxial transmitter is horizontal directly beneath the system, hence it couples well with steeply dipping bodies perpendicular to the flight line (Fraser, 1996). In coaxial mode, the EM responses mostly peak over the conductive bodies shown in Figure 2.7, and the exception is an extensive horizontal sheet with sharp edges. The coplanar response is more diagnostic of the geometry of this horizontal conductor (Fraser, 1996). The aim of the project was to interpret conductive structures, specifically faults or shear zones, therefore the EM response in coaxial mode at frequencies of 4600 Hz and 935 Hz were interpreted. The apparent resistivity grid at 32,000 Hz was also computed from the levelled inphase and quadrature components of the coplanar mode.

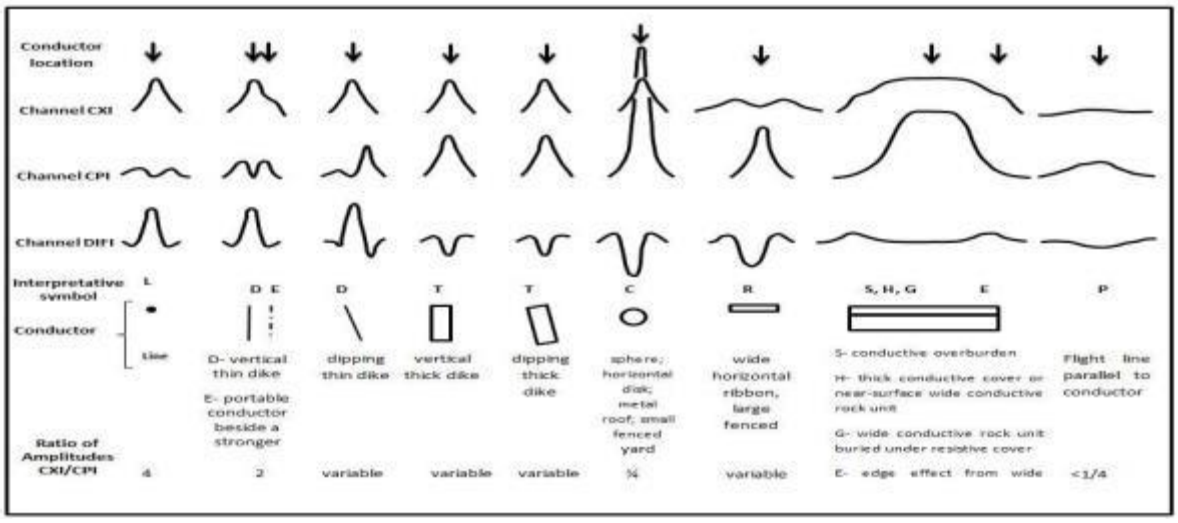

Figure 2.7: Shapes of theoretical HEM anomalies caused by simple conductors (after Fraser, 1996).

Quantitative interpretation of the conductive features was done interactively in geophysical software by displaying each of the EM profile data and manually selecting anomaly peaks. This process was very subjective, because it depends largely on the range between the highest and lowest amplitude values along each profile. A relatively small EM anomaly peak on a profile might disappear on the next profile, if it is superimposed on a broad large amplitude anomaly.

2.6.1 Electromagnetic map of the Sudbury structure

In the interpretation of the EM data, 7940 EM anomaly peaks were selected from the 1881 profile lines using the patterns in Figure 2.7. The peak locations were plotted as points and symbolized based on the conductivity; however, the large number of anomalies and the fact that the symbols are very small on images suitable for presentation in a scientific paper means that we have also included the gridded apparent resistivity derived from the 32,000 Hz data (Figure 2.8). In the resistivity image, the gneissic and granitic rocks in the Superior province, the Huronian sedimentary rocks and some human settlements (Chelmsford, Val Caron and Hammer) exhibit very high resistivity (greater than 1000 ohm.m). In order to isolate relatively low resistive zones and provide better visualisation, the highly resistive zones (greater than 1000 ohm.m) in the gridded apparent resistivity were not displayed.

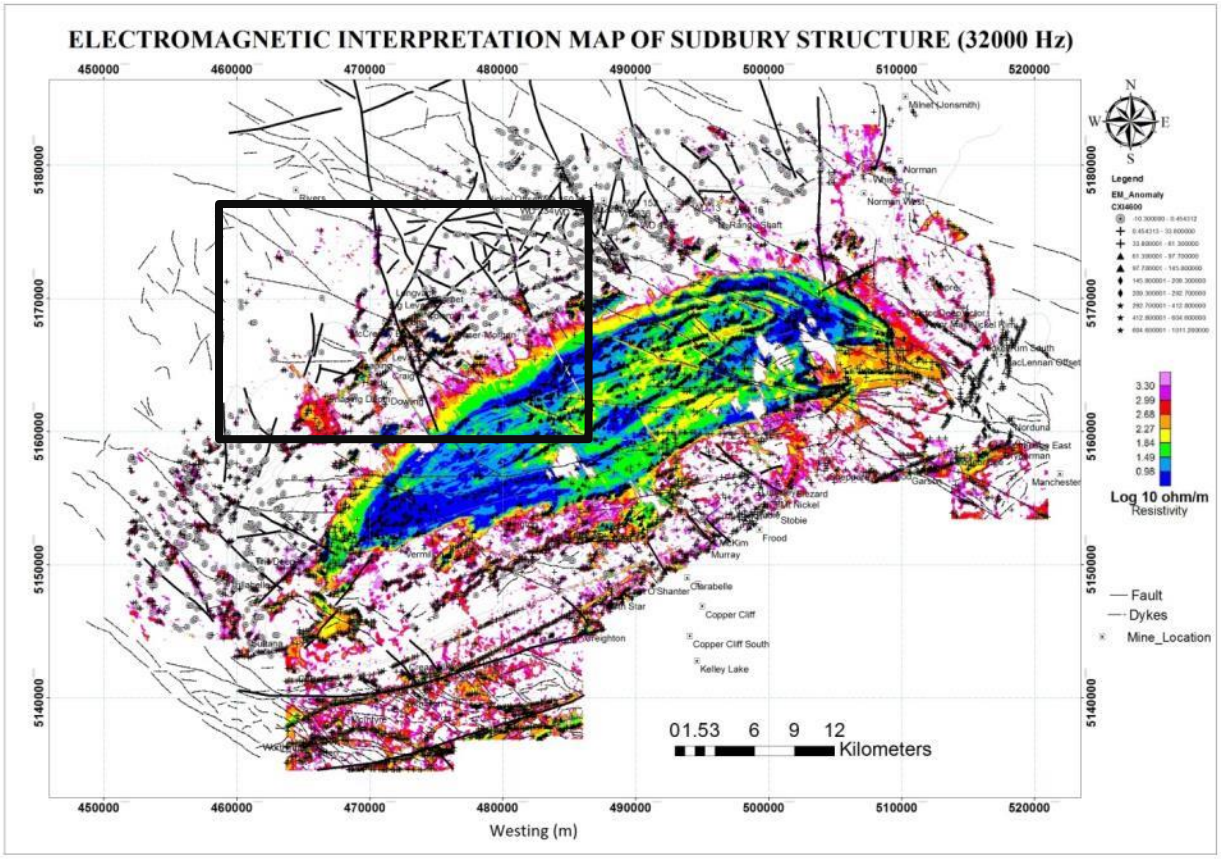

Figure 2.8: Electromagnetic anomaly map of the Sudbury structure with filtered resistivity grid as the coloured background. The Fecunis area is the black rectangular box that is enlarged and further discussed below. Blue colour indicates very low resistivity, orange and yellow are moderately low resistivity, while the pink and red are low resistivity.

There is a wealth of information on Figure 2.8 about the spatial distribution of conductive features related to metallic ore bodies, lithological contacts, faults, shear zone as well as man-made features like power lines, buildings and railways. Because it is difficult to see this information at the scale presented, we make use of enlargements for example the Fecunis area shown as a black rectangular box is enlarged in Figure 2.9.

In the main mass, sublayer and the footwall rocks numerous conductive zones, both linear and polygon shaped, are observed. The EM interpretation map shows that i) most of the known geological linear features - Fecunis, Creighton, Murray faults and mineralised offset dykes - the Foy and Worthington offsets are associated with linear and moderately high conductive anomalies, while the very highly conductive zones are more closely related to features associated with Whitewater group rocks; and ii) some of the non-linear and irregular shaped low resistive anomalies are due to water bodies (Windy, Nelson, Whitewater and Fairbank lakes), probably due to presence of organic-rich clay or silty materials at the bottom of the lakes or perhaps to ore bodies under the lakes – e.g. Joe Lake (Watts 1997).

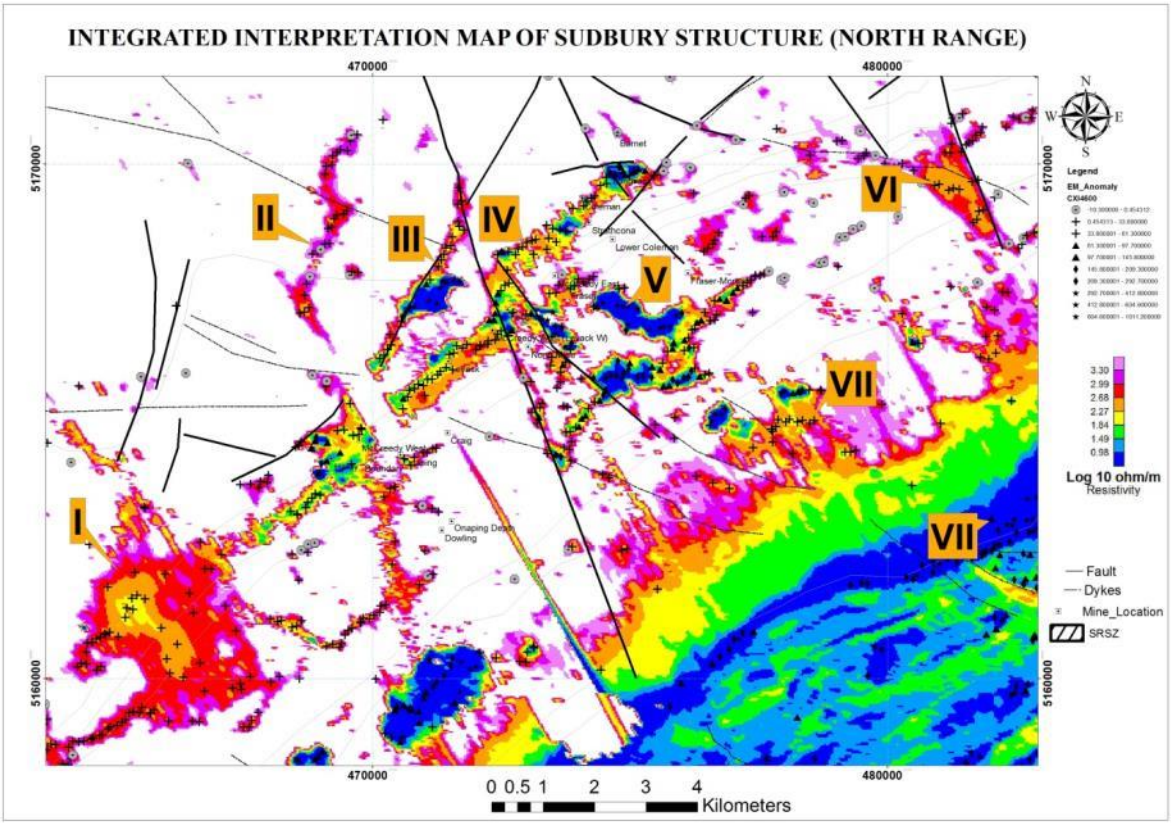

Figure 2.9: Electromagnetic anomaly map of the Fecunis area (North Range). Features I-VIII in the North Range are some of the electromagnetic anomalies discussed in the text.

The very low resistivity exhibited by most parts of the Whitewater Group sedimentary rocks, clearly differentiates them from the surrounding SIC rocks, allowing the contact between the Whitewater and the SIC to be qualitatively mapped. High conductivity zones within the sedimentary sequence appears to be due to i) the presence of carbon in the Dowling and Sandcherry members of the Onaping Formation, ii) the sulphide-rich carbonate of the Vermilion formation (containing Pb, Zn, Cu, Au and Ag) and iii) the pyritic and carbonaceous laminated mudstone of the Onwatin Formation. Carbon in Onwatin has been reportedly metamorphosed into anthraxolite veins (95% carbon, Burrow and Ricaby 1930). This could be responsible for some of the linear conductive features observable within the Whitewater Group (Figures 2.8 and 2.9).

Several moderately conductive anomalies dominate the boundary between the South Range Onaping and the Granophyre. This NE trending zone has been reversely sheared (Shanks and Schwerdtner 1991) and hosts sheared metallic ore type deposits within the Sudbury structure. Conductive anomalies within this South Range shear zone may be due to these ore bodies e.g. at Falconbridge and Garson mines. Lake bottom sediments - Whitewater, Whitson and Gorgon lakes within the zone - also exhibit high conductivities.

Figure 2.9 shows the EM anomaly, gridded resistivity data, magnetic lineament as well as locations of known deposits and mines. As well, a number of specific features have been labelled: I – Conductive Windy Lake anomaly; II- faulted conductive feature along Onaping River; III- very conductive anomaly due to structurally controlled Pine Lake; IV- A linear moderately conductive body in the Norite, contact Sublayer and Footwall breccia area. Some mines and known discoveries are associated with this feature. The linear anomaly is closely related to the access road to the mines; V- very conductive polygonal anomalies due to West

Morgan, Morgan and Moose Lakes. These could be due to mine tailing waste or lake bottom sediments; VI- very conductive and magnetic feature related to Sandcherry fault; VII-Moderately high conductivity in the Onwatin formation due the presence of carbon, Zn-Cu-Pb mineralisations and pyrite nodules; VIII- Conductive Onaping formation due to the presence of carbon in the Sandcherry and Dowling members.

2.7 Bedrock geological map versus geophysical interpretation map

Comparison of the published bedrock map and the magnetic interpretation was done by overlaying the established geological boundaries and structure on the interpreted magnetic contacts and lineaments. This was done in order to access the quality of the geophysical interpretation work done and identify the value added by the magnetic interpretation.

2.7.1 Geological contact versus Magnetic contact

The delineated magnetic contacts are mostly oriented in the same direction as the defined lithological boundaries in the bedrock map, but they are offset from the geological boundary at some places (Figure 2.10). These offsets could be related to the different degrees of alteration and destruction of magnetic minerals in the rocks at contacts or perhaps there were problems in the geologists identifying and mapping the contacts due to inaccessibility issues e.g. swamps, lakes etc., leading to extrapolations or interpolations on the geological map. Also, alteration of magnetic minerals may not change at geological contacts or may be hard to identify in the field and hence map. The black lines represent the geological contacts defined by field mapping, while the red lines represent locations where magnetic fabrics change to another depicting change in

rock unit. Chelmsford-Onwatin contact (Geological=A, Magnetic=A1), Onwatin-Onaping contact (Geological=B, Magnetic=B1), Onaping – Granophyre (Geological=C, Magnetic=C1).

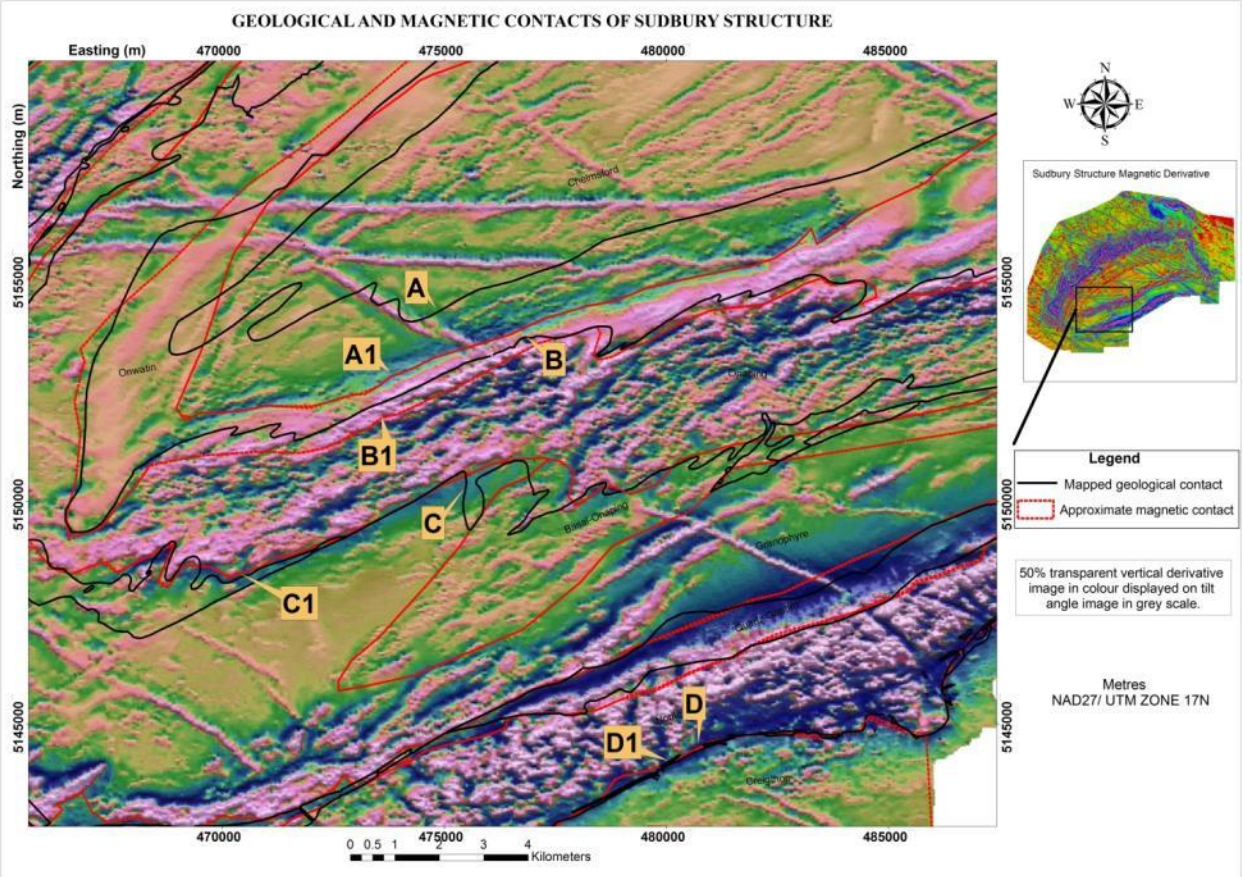

Figure 2.10: Comparison of the magnetic (red) and geological (black) contacts in the published map of the Sudbury structure displayed on VDR in greyscale.

The spatial resolution of the airborne data imposed a limit on the level of accuracy of the positions that can be ascertained from the image. Magnetic zones with dimensions below or close to the grid cell sizes (20 x 20 m within the SIC and 50 x 50 m in the footwall rock) are difficult to identify and approximate on the map. The first vertical derivative of the magnetics, shown in greyscale as the background to Figure 2.10, highlights the different magnetic fabrics of

different rocks of the Whitewater group and the SIC: Chelmsford (dark and moderately coarse), Onwatin (very bright and smooth), Onaping (bright and very coarse), Granophyre (relatively darker and less coarse than Onaping).

2.7.2 Sudbury Structure Geological and Magnetic lineaments

Mapped geological structures such as the North-South Fecunis Lake and Sandcherry faults (that displaced the rocks of the Sudbury structure in the North Range); the Murray and Creighton faults all coincide with the magnetic discontinuities in the vertical derivative, while some NE olivine diabase and offset dykes – Foy and Hess are delineated by magnetic peaks in the tilt derivative.

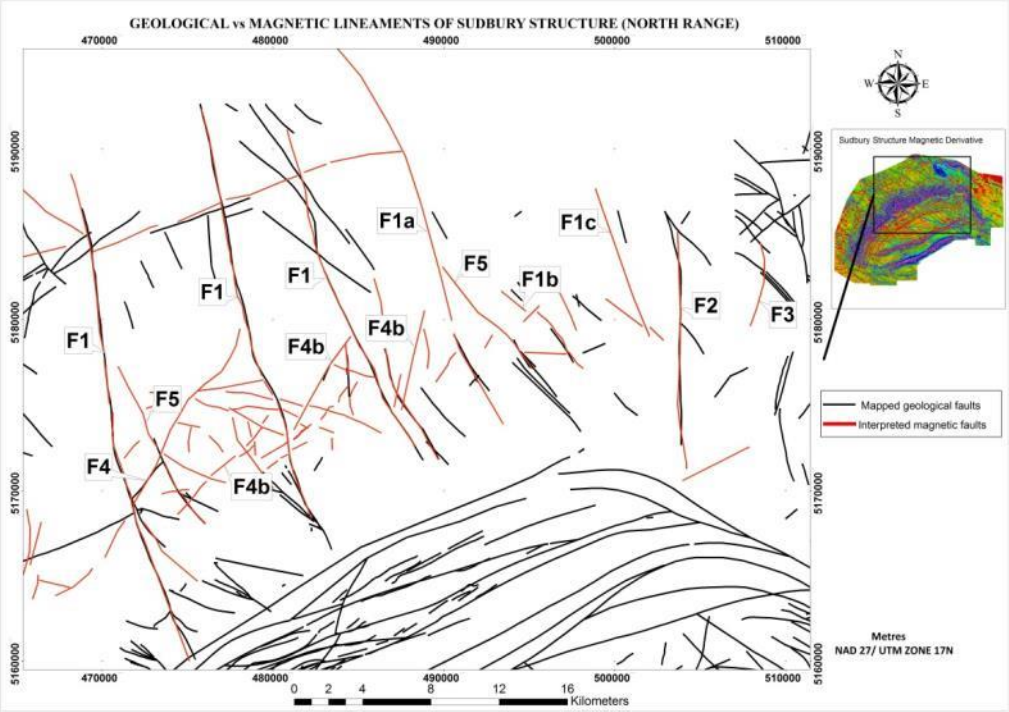

Figure 2.11: Map of the geological and magnetic fault sets in the North Range of SIC and footwall rocks. The black lines are the established faults, while the red lines represent the magnetic lineaments from derivatives.

Figure 2.11 shows the geological and magnetic fault sets in the North Range of the SIC and footwall rocks. The black lines are fault sets that have been established geologically, while the red lines represent the magnetic lineaments from derivatives. Although, the location of the magnetic feature deviates from the geological lineaments at some points along the drawn line, their overall location and orientation implies the geophysical feature is due to the geological structure. Similarly, some interpreted lineaments are further extensions of known geological structures while others are newly identified lineaments. Some known geological structures that were partially mapped in the bedrock map due to lack of exposures are more continuous in the magnetic derivative maps.

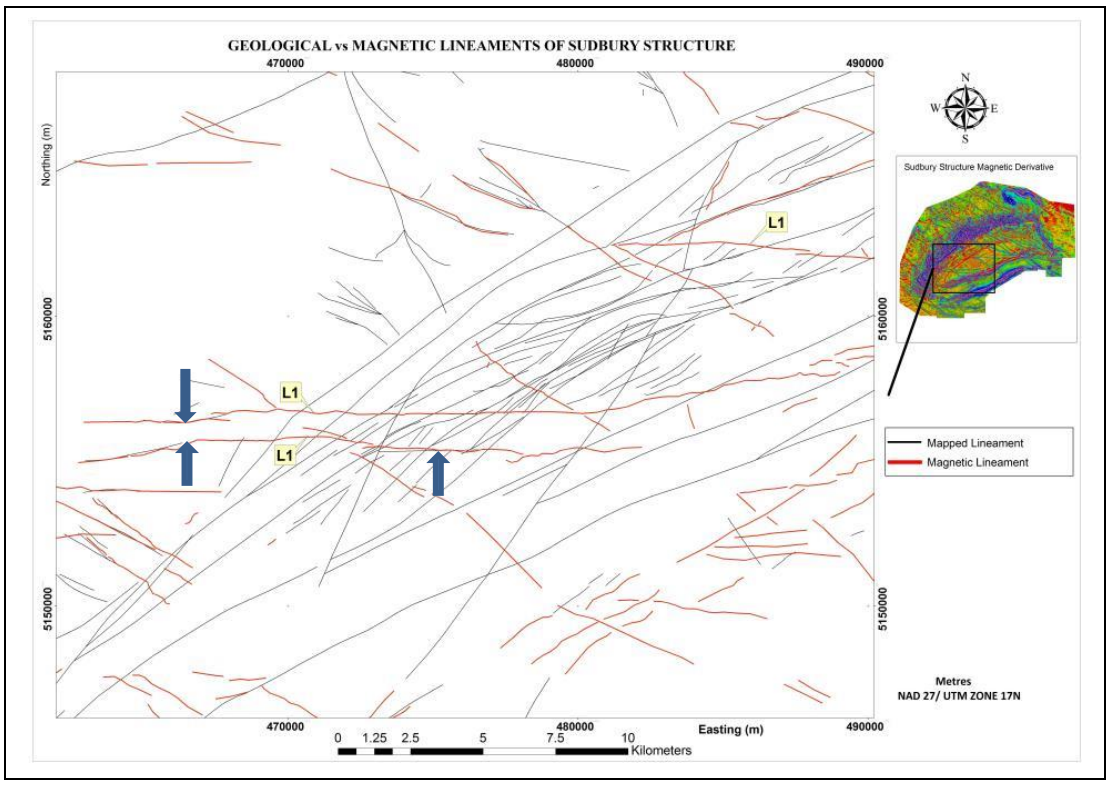

Figure 2.12: Map of the geological and magnetic fault sets in the western part of the SIC area. Three parallel E-W lineaments, possibly dykes, have been labelled L1. Where these have been more extensively mapped on the geophysics they are marked with blue arrows.

Figure 2.12 shows four parallel E-W lineaments (L1). Blue arrows indicate locations where they have been previously mapped in the field. The L1 features extend from the western part of the North Range into the South Range where they have been highly deformed and displaced. Some of the Sudbury swarm dykes were only partly mapped while some have not previously been mapped (Figure 2.13). These NW trending dykes are only partly mapped on the geological map, but a greater extent is evident on the geophysical interpretation (red lines) Also, the displacement patterns of the Sudbury swarm dykes is evident from the geophysics. Table 2.2 gives further details of the comparison of the geological and magnetic fault, dyke, and other lineaments seen in Figures 2.11 to 2.13.

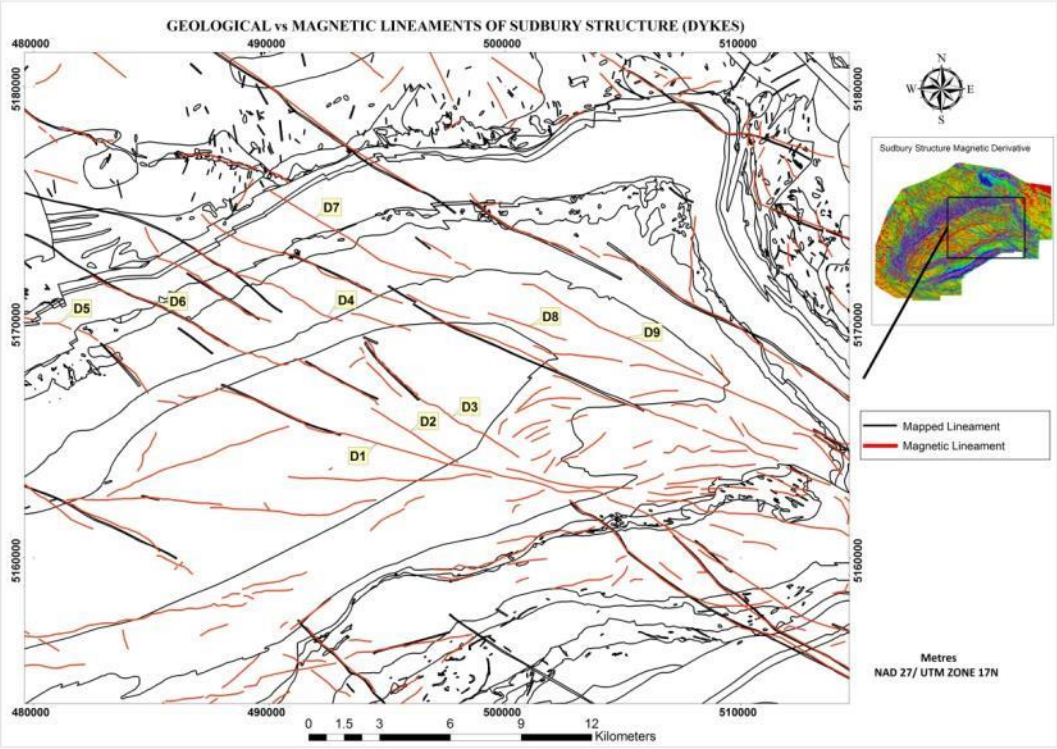

Figure 2.13: Map of the geological and magnetic fault sets in the NE part of the SIC. Partly mapped NW dykes are shown in black, while the red lines show the full extent and the displacement patterns of the Sudbury swarm dykes.

Table 2.2: Brief descriptions of some geological features and additional information from the magnetic interpretation

Label	Geological description	Remarks
F1	Fecunis fault set –Three NW striking lineaments, extends 20- 30km from the SIC contact into the North range.	Fully mapped, magnetics and geological interpretation correspond. Very small offsets from the geological and the magnetic interpretations where they have both been mapped.
F1a	Fecinus fault set? NW striking lineament, extends about 25km from the SIC contact into the North range footwall rocks	Lower part close to the SIC was partially mapped out by field mapping. The part of fault in the footwall rocks was interpreted from magnetic derivative.
	Fecinus fault set? NW striking lineament, extends about 6km from the SIC contact into the North range footwall rocks.	Partially mapped with little offset. The magnetic lineament is more extensive and displaced by a NE fault
F1c	Fecinus fault set? NW striking lineaments, extends 9.3km from the SIC contact into the North range footwall rocks	Not mapped before, new magnetic interpretation
F2	Almost NS striking lineament, extends 13km from the SIC near the contact of North and East range.	Partially mapped geologically in parts. The lineament continuity is interpreted from the magnetic derivatives.
F3	NE striking lineament, extend 5.1km into the footwall rock at the contact of North and East range	Not mapped before, new magnetic interpretation
F4	NE striking lineament, extend 19km through Fecunis to Sandcherry fault.	Partially mapped. Lineament is more extensive in the magnetic derivative
F4b	2 NE striking lineaments extend 6km from Sandcherry fault to the third NW fault and another one from the F1 fault to the F1a fault. They displaces the Foy offset dykes.	Not mapped before, new magnetic interpretation.
F5	2 NE trending lineament at an angle a little lesser than the Fecunis fault set	Partially mapped on the bedrock map.
L1	3 EW trending dykes, stretches from the western part of the Northrange into the Southrange and furthermore	Mapped in parts within the Chelmsford formation. New four EW magnetic dykes parallel to each other were interpreted from the magnetic derivatives.
D1-D9	9 NW dykes of varying length cutting across most rock of the Sudbury structure and have been faulted at some points.	All partially mapped. The magnetic derivatives showed that they continue from the Southrange, through the Whitewater group sediments into the Northrange and footwall rocks. NE trending faults have displaced some of the dykes.

2.8 Conclusions

Directional and normalized derivatives of the total magnetic intensity enhanced the mapping of the near-surface contacts and lineaments. The geophysical information interpreted shows that some lineaments were omitted from the geological map, while most are more extensive than previously indicated. The magnetic stratigraphy contacts defined based on qualitative classification of the magnetic texture showed that magnetic contacts do not always correspond to geological boundaries in the existing map. In some locales this difference translates into significantly different thickness estimates for some rock units. This discrepancy might warrant more detailed geological mapping and studies of the rocks to better understand the geological explanation for the differences between the published geological map and the geophysical interpretation.

Conductive locations identified from the EM profiles are probably due to responses from lake sediments, conductive ore bodies, faults, dykes, lithological contacts and geologic noise. The Onwatin formation is composed of conductive carbonaceous mudstones, and this has been mapped successfully with the EM data. Further investigations are required before drawing any definite conclusions about the low resistivity zones associated with known host rocks within Sudbury structures such as the contact Sublayer, offset dykes, Sudbury and footwall breccia and the SRSZ. The locations of faults and shears identified in the EM can be used to justify faults and other structures that are required in the inversion modelling we intend to undertake. The dykes identified from the magnetic data must also be incorporated in the magnetic modelling. In some cases these dykes appear to offset the stratigraphy, so they should also be interpreted as faults.

References

1. Ames, D. E., D. H. Watkinson, and R. R. Parrish, 1998, Dating of a regional hydrothermal system induced by the 1850Ma Sudbury impact event: Geology, **26**, 55-100.
2. Ames, D. E., A. Davidson, J. L. Buckle, and K. D. Card, 2005, Geology, Sudbury bedrock compilation, Ontario. Geological Survey of Canada, Open file 4570, Scale 1:50,000.
3. Bailey, J., B. Lafrance, A. M. McDonald, J. S. Fedorowich, S. Kamo, and D. A. Archibald, 2004, Mazatzale Labradorian-age (1.7e1.6 Ga) ductile deformation of the South Range Sudbury impact structure at the Thayer Lindsley mine, Ontario: Canadian Journal of Earth Sciences **41**, 1491-1505.
4. Bell, R., 1891, On the Sudbury Mining district, *in* Geological Survey of Canada, Annual Report, New Series, **5**, 5F-95F.
5. Buchan, K. L., J. K. Mortensen, and K. D. Card, 1993, Northeast-trending Early Proterozoic dykes of southern Superior Province: multiple episodes of emplacement recognized from integrated paleomagnetism and U-Pb geochronology: Canadian Journal of Earth Sciences, **30**, 1286-1296.
6. Blakely, R. J., and R. W. Simpson, 1986, Approximating the edges of source bodies from magnetic or gravity anomalies: Geophysics, **51**, 1494-1498.
7. Burrows, A. G., and H. C. Rickarby, 1930, Sudbury Basin area: 38th Annual report of the Ontario department of Mines, **38**(3), 55 p.
8. Card, K. D., 1964, Geology of Sudbury- Mautoulin area: Ontario Geological Survey, Report 166.

9. Card, K. D., 1978a, Metamorphism of the middle Precambrian (Aphebian) rocks of the eastern southern Province, *in* Metamorphism in the Canadian Shield: Geological Survey of Canada paper, **78**(10), 269-282.
10. Cochrane, L. B., 1991, Analysis of the structural and tectonic environment associated with rock mass failures in the mines of the Sudbury District, Unpublished PhD thesis, Queens University, Kingston, Ontario.
11. Collins, W. H., 1937, Life history of the Sudbury nickel irruptive (4): Mineralisation, Royal Society of Canadian, Transactions, Third series, **31**(4), 15-43
12. Cooper, G. R. J., and D. R. Cowan, 2006, Enhancing potential field data using filters based on the local phase: Computers & Geosciences, **32**, 1585-1591.
13. Corfu, F. and A. Andrews, 1986, A U-Pb age for mineralized Nipissing Diabase Gowganda, Ontario: Canadian Journal of Earth Sciences, **23**, 107-112.
14. Deutsch, A., R. A. F. Grieve, M. Avermann, L. Bischoff, B. Brockmeyer, D. Buhl, R. Lakoomy, R. Muller- Mohr, M. Ostermann, and D. Stoffer, 1995, The Sudbury structure (Ontario, Canada): a tectonically multi ring impact basin: Geologische Rundschau, **84**, 697-709.
15. Dietz, R.S. 1964. Sudbury structure as an astrobleme. Journal of Geology, **72**: 412-434
16. Dressler, B.O. 1984a. General Geology of the Sudbury area. *In* The Geology and Ore Deposit of the Sudbury structure, Ontario Geological Survey, Special Volume **1**: 57-82
17. Dressler, B.O., V.K. Gupta, and T.L. Muir. 1991. The Sudbury structure. *In* Geology of Ontario, Ontario Geological Survey, Special Volume **4**: 593-625.

18. Dreuse, R., D. Doman, T. Santimano, and R. Ulrich, 2010, Crater floor topography and impact melt sheet geometry of the Sudbury impact structure, Canada: Terra Nova, **22**, 463-469.
19. Fahrig, W. F., and T. D. West, 1986, Diabase dike swarms of the Canadian Shield. Geological Survey of Canada, Map 1627, Scale 1: 4 873 900.
20. Fairhead, J. D. and S. E. Williams, 2006, Evaluating normalized magnetic derivatives for structural mapping, SEG Expanded Abstracts.
21. Frarey, M. J., W. D. Loveridge, and R. W. Sillivian, 1982, A U-PB age for the Creighton granite, Ontario, *in* Rb-Sr and U-Pb isotope age studies, Report 5, Current Research, Part C, Geological Survey of Canada paper, **82**, 129-132.
22. Fraser, D. C., 1996, Geological application of airborne electromagnetics methods. Dighem frequency domain course note.
23. French, B. M., 1972, Shock metamorphism features in the Sudbury structure, Ontario, *in* new Developments in Sudbury Geology: Geological Association of Canada paper, **92**(1C), 179-187.
24. Giblin, P. E., 1984, History of exploration and development of geological studies and development of geological concept, *in* Geology and ore deposit of Sudbury structure, Ontario Geological Survey, Special Volume, **1**, 3-23.
25. Grauch, V. J. S., M. N. Hudson, and S. A. Minor, 2001, Aeromagnetic expression of faults that offset basin fill, Albuquerque basin, New Mexico: Geophysics, **66**, 707-720.
26. Gupta, V. K., F. S. Grant, and K. D. Card, Gravity and magnetic characteristics of the Sudbury structure, *in* E. G. Pye, A. J. Naldrett and P. E. Giblin eds.,The Geology and Ore

Deposits of the Sudbury structure: Ontario Geological Survey, Special Volume **1**, 381-410.

27. Grant, F. S., 1985, Aeromagnetic, geology and ore environments, 1, Magnetite in igneous, sedimentary and metamorphic rocks: An overview: Geoexploration, **23,** 303-333.
28. Grant, R. W., and A. Bite, 1984, Sudbury quartz diorite offset dykes, *in* The Geology and Ore Deposit of the Sudbury structure: Ontario geological Survey, Special volume **1**, 275-300.
29. Heaman, L. M., 1997, U-Pb dating of dyke swarms: what are the options?; abstract in International Association of Volcanology and chemistry of the Earth's interior, Continental Magnetism: New Mexico bureau of Mines and Mineral Resources, Bulletin **131**, 125.
30. Hearst, R. B. and W. A. Morris, 2001, Regional gravity setting of the Sudbury structure: Geophysics, **66**, 1680-1690.
31. Hearst, R. B., W. A. Morris, and M. D. Thomas, 1994, Magnetic interpretation along the Sudbury structure Lithoprobe Transect, in P.C. Lightfoot, and A. J. Naldrett eds., Proceedings of the Sudbury-Noril'sk Symposium: Ontario Geological Survey Special **5**, 33-43.
32. Hood, P. J., 1965, Gradient measurements in aeromagnetic surveying: Geophysics, **30**, 891-902.
33. Hrouda, F., 1982, Magnetic anisotropy of rocks and its application in geology and geophysics: Geophysical Survey, **5**, 37–82.

34. Krogh, T. E., D. W. Davis, and F. Corfu, 1984, Precise U-Pb zircon and baddeleyite ages for the Sudbury area, *in* the Geology and Ore Deposit of the Sudbury structure: Ontario Geological Survey, Special Volume **1**, 431-446.
35. Krogh, T. E., S. L. Kamo, and B. F. Bohor, 1996, Shocked metamorphosed zircons with correlated U-Pb discordance and melt rocks with concordant protolith ages indicate an impact origin for the Sudbury structures, *in* Earth processes, reading the isotope code, American Geophysical Union Monograph **95**, 343-352.
36. L'Heureux, E., H. Ugalde, B. Milkereit, N. Eyles, J. Boyce, and W. Morris, 2003, Magnetic, Gravity and Seismic Constraints on the nature of the Wanapitei Lake Impact Crater: 3rd International Conference on Large Meteorite Impacts, Germany August 2003.
37. Lightfoot, P. C., W. Doherty, K. P. Farrell, R. R. Keays, M. L., Moore, and D. Pekeski, 1997, Geochemistry of the main mass, Sublayer, offset and inclusions from the Sudbury Igneous Complex: Ontario Geological Survey, Open file report 5959.
38. Lochhead, D. R., 1995, The Falconbridge ore deposit, Canada: Economic Geology, 50, 42-50
39. McGrath, P. H., and H. J. Broome, 1994, A gravity model of the Sudbury structure along the Lithoprobe seismic line: Geophysical Research Letters, **21**(10), 955-958.
40. Minty, B. R. S., 1991, Simple micro-levelling for aeromagnetic data: Exploration Geophysics, **22**, 591-592.
41. Miller, H. G., and V. Singh, 1994, Potential field tilt - a new concept for location of potential field sources: Journal of Applied Geophysics, **32**, 213-217.
42. Milkereit, B., E. K. Berrer, A. R. King, A. H. Watts, B. Roberts, E. Adam, D.W. Eaton, J. Wu, and M. H., Salisbury, 2000, Development of 3-D seismic exploration technology

for deep nickel-copper deposit- A case history from the Sudbury basin, Canada: Geophysics, **65**(6), 1890-1899

43. Milkereit, B., A. Green, and Sudbury working group, 1992, Deep geometry of the Sudbury structure from seismic reflection profiling: Geology, **20**, 807-811.
44. Milkereit, B., Green, A., Wu, J., White, D., and Adam, E., 1994, Integrated seismic and borehole geophysical study of the Sudbury igneous complex, in D.E. Boerner, B. Milkereit, A.J. Naldrett eds., Lithoprobe Sudbury Project :Geophysical Research Letters, **21(**10), 931-934.
45. Milligan, P. R., and P. J. Gunn, 1997, Enhancement and presentation of airborne geophysical data: AGSO Journal of Australian Geology & Geophysics, **17**(2), 63-75.
46. Moon, W. M. and L. X. Jiao, 1998, Sudbury meteorite-impact structure modeling with Lithoprobe high resolution seismic refraction results, Geoscience Journal, **2** (1), 26- 36.
47. Mueller, E. L., and W. A. Morris, 1995, A 3-D model of the Sudbury igneous complex: 65th annual international meeting, Society of Exploration Geophysicists, Expanded Abstracts, **65**, 777-780.
48. Naldrett, A. J., 1984, Summary, discussion and synthesis, *in* E. G. Pye, A. J. Naldrett, and P. E. Giblin, eds., The geology and ore deposits of the Sudbury structure: Ontario Geological Survey, **1**, 533–570.
49. Naldrett, A. J and R. H. Hewlins, 1984, The main mass of the Sudbury structure; *in* The Geology and Ore Deposit of the Sudbury structure: Ontario Geological Survey, Special volume **1**, 231-251.

50. Noble, S. R. and P. C. Lightfoot, 1992, U-Pb baddeleyite ages for the Kerns and Triangle mountain intrusions, Nipissing diabase, Ontario: Canadian Journal of Earth Sciences, **29**, 1124-1129.
51. Paakki, J. J., 1992, The Errington Zn-Cu-Pb massive deposit, Sudbury, Ontario; its structural and stratigraphic setting and footwall alteration: Unpublished MSc thesis, Laurentian University, Sudbury Ontario.
52. Pattison, E. F., 1979, The Sudbury Sublayer: Canadian Mineralogist, **17**, 257-274.
53. Peredery, W. V., 1972, Chemistry of fluidal glasses and melt bodies in the Onaping formation; *in* New Development in Sudbury Geology: Geological Association of Canada, Special Paper Number **10**, 49-59.
54. Peredery, W. V., and G. G. Morrison, 1984, Discussion of the origin of the Sudbury structure: Ontario Department of Mines, Annual report for 1925, **34**(8), 1-61.
55. Pilkington, M., and P. Keating, 2004, Contact mapping from gridded magnetic data- a comparison of techniques: Exploration Geophysics, **35**, 306-311.
56. Pilkington, M., and P. Keating, 2010, Geologic application of magnetic data and using enhancement for contact mapping: 2010 EGM International Workshop, Expanded Abstract.
57. Popelar, J. 1972, Gravity Interpretation of the Sudbury Area, *in* J.V. Guy-Bray ed., New Developments in Sudbury Geology: Geological Association of Canada, Special Paper Number 11,103-115.
58. Reeves C. W., S. W. Reford and P. R. Milligan, 1997, Airborne geophysics: old methods, new images, Geophysics at the Millennium. *In* A. G. Gubins ed., Proceedings of Exploration 97, 4th Decennial International Conference on Mineral Exploration.

59. Riller, U., 2005 Structural characteristics of the Sudbury impact structure, Canada: impact induced and orogenic deformation: Meteoritics and Planetary Science, **40**, 1723-1740.

60. Rousell, D. H, 1984b, Onwatin and Chelmsford formations, *in* the Geology and Ore Deposit of the Sudbury structure: Ontario Geological Survey, Special volume **1**, 211-218.

61. Rousell, D. H., W. Meyer, and S. A. Prevec, 2002, Bedrock Geology and Mineral deposit, *in* the physical Environment of the city of Sudbury: Ontario Geological Survey, Special Volume 6, 21-55.

62. Sims, P. K., K. D. Card, G. B. Morey and Z. E. Peterman, 1980, The Great Lakes tectonic zone- a major crustal structure in the central North America, Geological society of America Bulletin, **91**, 690-698.

63. Spector, A., and F. S. Grant, 1970, Statistical models for interpreting aeromagnetic data: Geophysics, **35**, 293-302.

64. Thompson, J. E, 1957, Geology of the Sudbury basin: 65th Annual report of the Ontario Department of mines, **65**(3).

65. Thurston, J. B., and R. S. Smith, 1997, Automatic conversion of magnetic data to depth, dip, and susceptibility contrast using the SPI method: Geophysics, **62**, 807-813.

66. Tschirhart, P., and W. A. Morris, 2012, Grenville age deformation of the Sudbury impact structure: evidence from the magnetic modeling of the Sudbury diabase dykes swarm: Terra Nova, **00**, 1-8

67. Verduzco, B., J. D., Fairhead, C. M. Green, and C. Mackenzie, 2004, New insights to magnetic derivatives for structural mapping: Geophysics -The Leading Edge, **23**, 116-119.

68. Watts, A., 1997, Exploring for Nickel in the 90s, or 'til depth us do part', *in* A.G. Gubins ed., Proceedings of Exploration 97: Fourth Decennial International Conference on Mineral Exploration.
69. Wijns, C., C. Perez, and P. kowalczyk, 2005, Theta map: Edge detection in magnetic data, Geophysics, **70**, 39-43.
70. Zolnai, A. I., R. A. Price, and H. Helmstaedt, 1984, Regional Cross section of the southern province adjacent to Lake Huron, Ontario: implications for the tectonic significance of the Murray fault zone: Canadian Journal of Earth Sciences, **21**, 447-456.

CHAPTER 3: A constrained potential field data interpretation of the deep geometry of the Sudbury structure.

3.1 Abstract

Two coincident high-resolution airborne gravity and magnetic profiles of the Sudbury structure were forward modelled to better understand the geology of the structure at depth. A north-south profile was used to further investigate the deeper geological setting of the Sudbury Igneous Complex (SIC) along Lithoprobe seismic transect, while an east-west profile was selected to examine a discontinuity in the magnetic and gravity fields near the centre of the (SIC) in the North Range. Constraints imposed on the best-fit model were the location of surface magnetic contacts, interpreted seismic and geological sections, and petrophysical data acquired from surface and borehole data.

The constrained model computed for the north-south profile, elements of which are consistent with known Lithoprobe seismic reflectors, defines a north-verging fold in the deeper portion of the SIC. It may have developed during the modification of the initial geometry of the SIC by either a post-SIC thick-skinned basement shortening event, or by a compressive event of the SIC against tholeiitic basalts of the Elliot Lake Group during the Penokean Orogeny. The interpreted deep-seated basal folding explains the changes in dip of the seismic reflectors of the Archean basement and the SIC at about 4-8 km depth that were not fully accounted for in previous models of the Sudbury structure. This deformational event is interpreted to displace the base of the SIC rocks northwards to the depth of about 5 km, which is now reflected by a linear gravity high within the southern part of the Sudbury Basin. Lithological fence diagrams of the two interpreted sections across and along a magnetic anomaly located in the northwest portion of the SIC, show that features of the observed anomaly pattern can be explained by a series of closely spaced deep-seated growth faults trending north around the Sandcherry fault, which has been previously

interpreted as a reactivated pre-impact fault that affect the thickness and topography of both the SIC and highly magnetic Levack Gneiss Complex in that locality.

3.2 Introduction

Exploration and mining activities in the Sudbury structure has been on-going for over 100 years, to a depth of about 2.5 km, yet little is reported about the deep geometry of the centre of the structure. Most of the known mineral deposits are located in the offset dikes, SIC-basement contact, or footwall basement rocks below the Sudbury Igneous Complex (SIC). Numerous boreholes, most of which extend to a depth of less than 2 km, have been drilled at the margin of the SIC, or close to the contact, by mining companies, but the logs are largely inaccessible to the public. Detailed surface structural measurements indicate that the Sudbury structure has the shape of a flattened saucer or funnel shape, with the North Range gently dipping to the south and the South Range steeply dipping to the north (Pye et al., 1984). The dip of the SIC-basement contact is not constant: it has an average dip of ~30° in the North Range and it steepens to 41° closer to the centre and deeper part of the north range of the SIC (Dreuse et al., 2010).

Early gravity models (Gupta et al., 1984) attributed the gravity field measured over the Sudbury structure to be partly due to hidden sub-horizontal and highly dense mafic bodies occurring at about 5 km beneath the SIC. Using a different basement rock density of about 2.73 g/cm^3, McGrath and Broome (1984) modelled the data by introducing a slab of dense Levack gneiss under the SIC that extended to about 12 km depth to fit the measured Bouguer gravity field and challenge the hidden body hypothesis. In order to provide more insight into the deeper structural configuration of the SIC, the Canadian Lithoprobe program acquired 3 lines of regional deep

crustal seismic reflection data, and 2 lines of high resolution deep crustal seismic reflection data across the SIC and the Levack gneiss complex (LGC) (Milkereit et al., 1992). The inapplicability of standard sedimentary basin processing techniques used for seismic data, the weak acoustic impedance contrast between different rock types, and the high level of noise resulted in ambiguous interpretation of the Lithoprobe seismic sections (Boerner et al., 2000). Seismic reflection preferentially highlights shallowly dipping surfaces with differential acoustic impedance due to variation in rock densities and crystallographic preferred orientation in the crystalline environment (Fountain et al., 1994). As such seismic reflectors found underlying the North Range are well-defined and interpreted in the context of geological contacts. In contrast, on the South Range most of the lithological contacts are known to be sub-vertical, and the observed shallow dipping seismic reflectors more likely represent thrust faults and shear zones (Milkereit et al., 1994). Milkereit et al. (1994) suggested an asymmetric shape with the norite and granophyre units of the SIC on the North Range maintaining a dip to the south, reaching a depth of about 5 km below the centre of the Basin, and 12 km under the South Range. This Mikereit's model differs from Card and Jackson's (1995) interpretation, which portrays the layers of the SIC as exhibiting a saucer or broad fold geometry, with a northward translation of the South Range over the SIC on steep southerly dipping thrust surfaces not interpreted by Milkereit et al. (1994).

Subsequent attempts to model potential field variations colinear with the Lithoprobe seismic transect were based on the geometrical framework provided by the seismic interpretation (Milkereit et al., 1992; 1994) together with the available petrophysical data obtained from the Sudbury area (Hearst et al., 1994; McGrath and Broome, 1994). Regional scale aeromagnetic

data from the Geological Survey of Canada (GSC) database with ~500 m line spacing and mean terrain clearance of 300 m were interpreted along the Lithoprobe seismic section. Magnetic anomalies were attributed to three main sources; the LGC, the Onwatin-Onaping contact and the South Range Norite (Hearst et al., 1994). Hearst et al. (1994) used the Lithoprobe seismic section as a preliminary model template as well as available physical property measurement to constrain the models, but they were unable to obtain a good fit with the measured magnetic field data. They suggested that modelling the magnetic response of the Sudbury structure requires more detailed geologic data than that provided by the seismic interpretation of Milkereit et al. (1992).

This study uses recent high resolution airborne magnetic and gravity data together with more advanced geophysical modelling software, to produce a geological model that best explains the magnetic and gravity responses. The magnetic data used in this study was extracted from a new regional compilation (Olaniyan et al., 2013), which brings together data collected in over 40 different surveys in a single database (courtesy Sudbury Integrated Nickel Operations and Wallbridge Mining). Resolution of the gridded magnetic data varies from 20 m within the SIC to 50 m in a 10 km wide area to the north of the SIC. Airborne gravity data acquired at 90 m flight height and 200 m line spacing were provided by Vale for selected profiles. Regional gravity data used in this study include the low resolution GSC free air data of ~2000 m cell size. Free air gravity data are used in the interpretation so that topographic variation related to lithological boundaries can be resolved in the model. Interpreted magnetic contacts are based on the interpretation of Olaniyan et al. (2013). Geological and seismic sections together with physical property measurements (Hearst et al., 1994 and McGrath and Broome, 1994) were used to further constrain the subsurface geometry of the Sudbury structure.

3.3 Geological setting

The Sudbury structure formed 1850 Ma ago (Krogh et al. 1984) when a large extraterrestrial bolide impacted Paleoproterozoic Huronian supracrustal rocks of the Southern Province and underlying Archean rocks of the Superior Province (Pye et al., 1984). The Sudbury structure comprises the 58 km by 28 km elliptical Sudbury Igneous Complex (SIC), which consists of a lower magmatic breccia unit, called the sublayer, overlain by norite, quartz gabbro, and granophyre (Figure 3.1; Pye et al., 1984). The SIC formed by the differentiation of an impact melt sheet upon cooling (Grieve et al., 1991, Dickin et al., 1999, Lightfoot et al., 2001). The SIC and immediately adjacent basement rocks are geographically divided into the North Range, East Range and South Range. In the North Range, the SIC-basement contact dips on average 35^0 degrees south, dips ~ 75^0 south-west in the East Range, and generally dips 55^0 north in the South Range except in its eastern portion where it is overturned and south-dipping (Dreuse et al., 2010; Rousell, 1984b). Irregular bodies of Sudbury breccia within the basement rocks are present in the south and north, and have been mapped up to 80 km north of the SIC-basement contact along the North Range.

The SIC overlies the ca. 2711 Ma Levack Gneiss Complex (Krogh et al., 1984) and younger granitoids of the ca. 2642 Ma Cartier Batholith (Meldrum et al., 1997) in the North Range and metasedimentary and metavolcanic rocks of the ca. 2.4 Ga to 2.2 Ga Huronian Supergroup in the South Range. The Sudbury structure is folded into a doubly-plunging fold and the center of the structure, called the Sudbury Basin, is occupied by a ~3 km thick sequence of syn-impact breccias of the Onaping Formation (Peredery, 1972; Ames et al., 2002), and post-impact carbonaceous mudstone of the Onwatin Formation and turbiditic sandstone of the Chelmsford

Formation (Roussel, 1984b). These three formations constitute the Whitewater Group as shown in Figure 3.1.

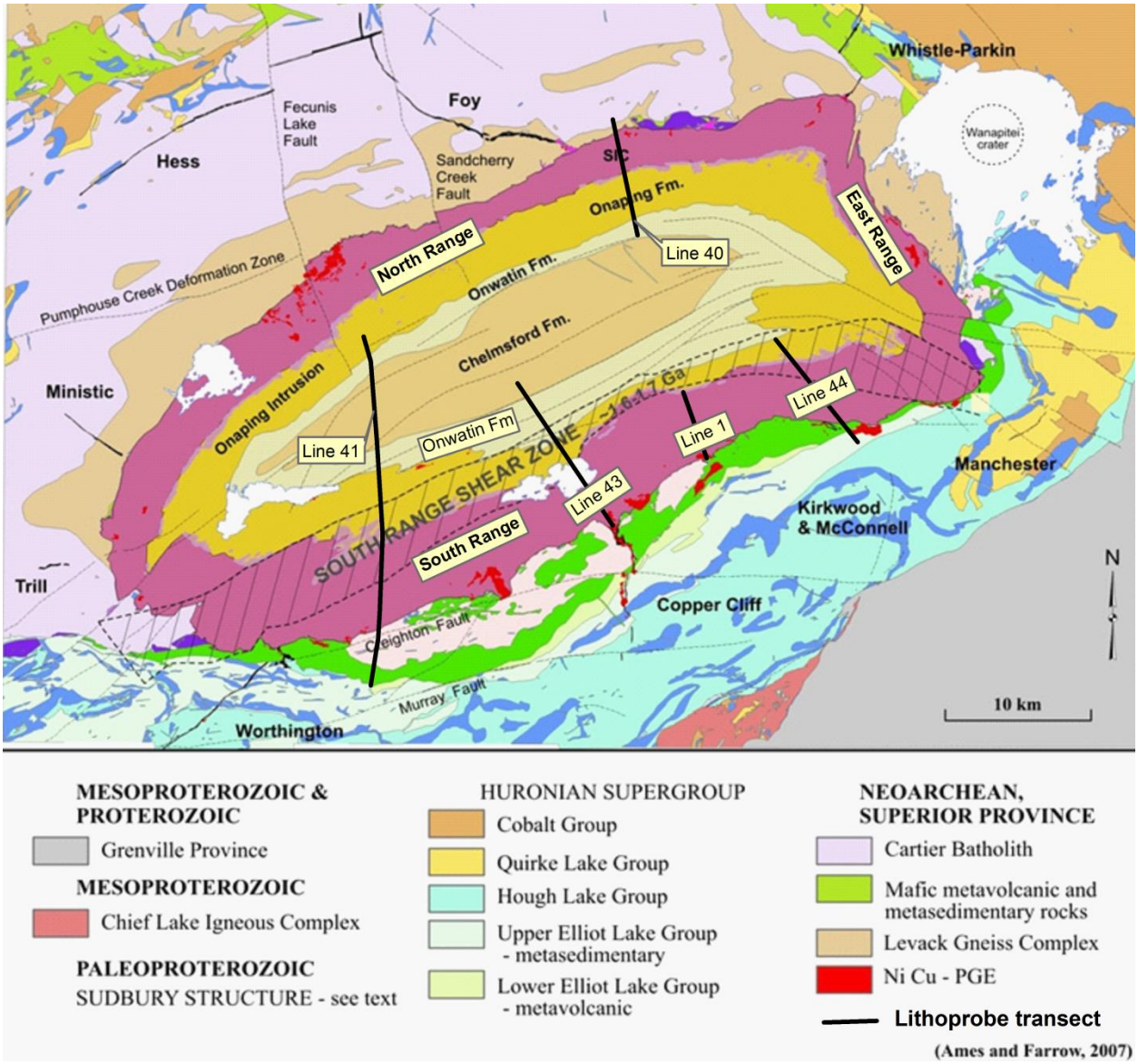

Figure 3.1: Regional geological setting of the Sudbury structure showing the locations of the Lithoprobe seismic profiles (modified from Ames and Farrow, 2007).

The current shape of the SIC is regarded to be an erosional relic of a highly deformed, multi-ring impact Basin (Butler, 1994; Thompson and Spray, 1994; Deutsch et al., 1995; Spray and

Thompson, 1995). After the impact, the SIC, Whitewater Group, and basement rocks were folded and cut by south-dipping reverse faults produced during the NW-directed, ca. 1.88 Ga – 1.82 Ga Penokean orogeny (Brocoum and Dalziel, 1974; Zolnai et al., 1984). This orogenic event modified the original geometry of the SIC and produced a Penokean mountain belt to the south that underwent erosion and shed sediments that were deposited as the turbidites of the Chelmsford Formation (Long, 2004).

A recent U-Pb titanite age in a shear zone at Garson Mine indicates that the Sudbury structure was deformed at 1849 Ma ± 6 Ma (Mukwakwami et al. 2014) shortly after cooling of the SIC. The Garson shear zones belong to the SE-dipping South Range Shear Zone system (SRSZ) which strongly affected the South Range of the SIC and Sudbury Basin (Shanks and Schwerdtner 1991). Other similar southeast-dipping shear zones at the South Range Thayer-Lindsey Mine and farther south in the Southern Province formed or were reactivated during the ca. 1.7 Ga – 1.6 Ga Yavapai and Mazatzal orogenies (Bailey et al., 2004; Raharimahefa et al. submitted). Finally, a major orogenic event, the ca. 1 Ga Grenvillian Orogeny, completely reworked the rocks south of the Sudbury structure. The Grenvillian had limited effects on the SIC and Sudbury Basin apart from minor reactivation of faults of the South Range Shear Zone system in the Sudbury Basin, as suggested by sinistral, scissor-type offsets of ca. 1238 Ma Sudbury olivine diabase dikes along the faults (Tschirhart and Morris, 2012).

Although much work still remains to be done to understand the surface geology of the Sudbury structure, its deep subsurface geology is even less well understood with many questions unanswered. Part of the issue is the magnitude and style of deformation of the deep part of the

SIC. The seismic sections of Milkereit et al. (1992) created by merging Lithoprobe lines 40 and 41 are herein qualitatively reinterpreted to investigate the deep subsurface geometry of the SIC and to provide more insight into the deformation history of the Sudbury structure.

3.4 Geophysical setting

The elliptical outer rim of the SIC is approximately 28 km wide, 58 km long and various magnetic and gravity anomalies are associated with the rim. Figure 3.2a and 3.2c show the high magnetic field and the gravity high respectively on part of the elliptical rim of the SIC. On a regional scale, the gravity and magnetic anomalies associated with the elliptical rim of the SIC are superimposed on a broader geophysical response of about 350 km in length that extends from Elliot Lake (to the west) through Sudbury to Englehart (Gupta et al., 1984). These gravity and magnetic regional anomalies are interpreted to be related to the paleo-continental margin between Archean rocks of the Superior Province and metamorphosed Huronian supracrustal rocks of the Southern Province (Gupta et al., 1984).

Within the Sudbury structure, local sources of high magnetic and gravity anomalies include the dense Levack Gneiss Complex in the North Range, the SIC norite and quartz gabbro, and the later NE-trending olivine diabase dykes. The norite and quartz gabbro have an average density of 2.81 g/cm^3 and 2.88 g/cm^3 (Table 1), respectively, and they are relatively dense compared to an average crustal density of 2.73 g/cm^3 (Gupta et al.,1994; McGrath and Broome, 1994), thus exhibiting a relatively high gravity field around the SIC (Figure 3.2c). These highly dense SIC rocks together with the sulfide-bearing sublayer-norite contribute to the local elliptical gravity high around the rim of the SIC. Granophyre rocks that form the uppermost layer in the SIC series have a relatively low average density value of 2.70 g/cm^3, thus the low gravity field over it.

The high magnetic susceptibilities of the Levack Gneiss Complex (0.068 SI), norite and quartz gabbro (0.035 SI) in the North Range contributes greatly to the high magnetic field in the northern rim and footwall of the SIC (Figure 3.2a). The lowest magnetic intensity in the study area is observable over the Huronian sediments in the South Range footwall. The area of low magnetic intensity is cross-cut by WNW trending positive magnetic lineaments related to mafic intrusions and Nipissing dykes and sills. These mafic intrusions within the Huronian sedimentary sequences also exhibit a relatively high gravity field. For more details on the general overview of the qualitative geophysical setting of the Sudbury structure, see Gupta et al. (1994); McGrath and Broome, (1994); Hearst and Morris, (2001); Olaniyan et al, (2013) and the references therein.

Underlying the elliptical magnetic and gravity anomalies produced by the SIC is a much broader anomaly pattern. It is readily apparent that the more north-western portion of the SIC is underlain by a high magnetic intensity anomaly, as the magnetic signatures over the granophyre unit and part of the Whitewater Group in this part of the North Range are enhanced as a result of being superimposed on a broader magnetic high (Figure 3.2a). This anomaly appears to change in character at the Sandcherry fault, narrowing fairly significantly as it crosses to the eastern side of the fault in the North Range, while the gradient of the flank of the anomaly reduces gradually towards the south. Profile B-B', which extends in an ENE direction sub-parallel to the long axis of the Sudbury structure, was modelled to investigate the source of this magnetic anomaly (Figures 3.2a - 3.2c).

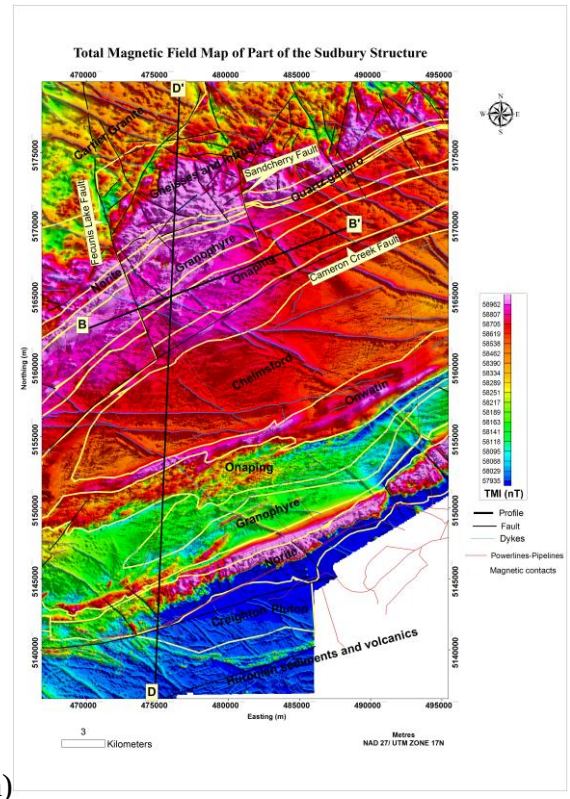

a)

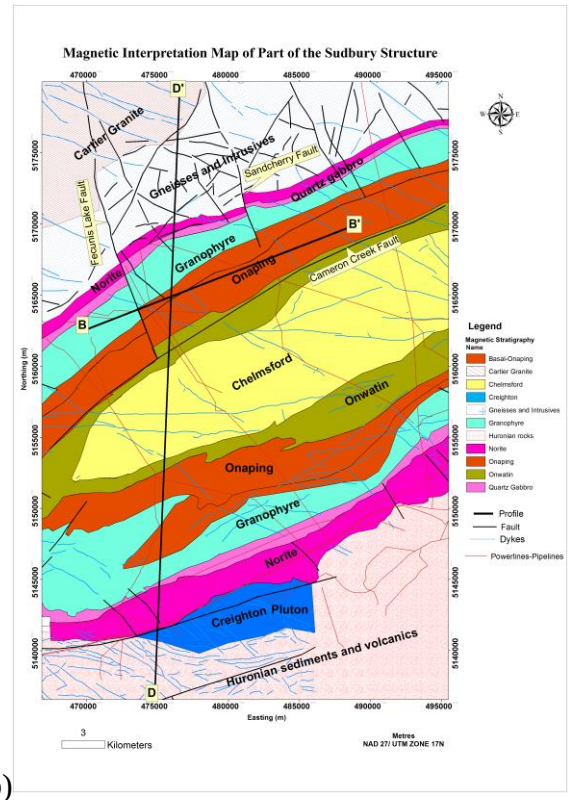

b)

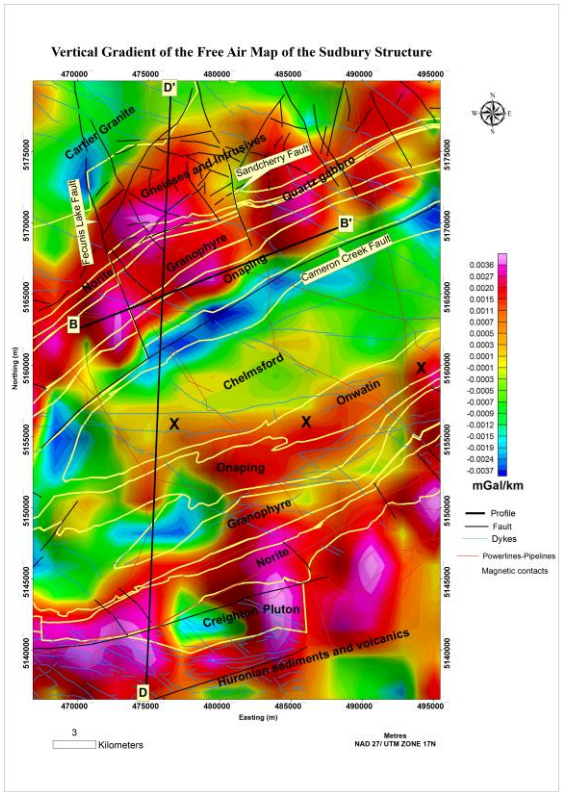

c)

Figure 3.2: Profile B-B’ and D-D’ displayed on the a) total magnetic intensity map compilation, b) magneto-stratigraphic map of the Sudbury structure (Olaniyan et al., 2013), and c) Free-air gravity (GSC dataset).

Profile D-D' (Figure 3.2a -3.2c) was modelled parallel to the NNE-trending Lithoprobe seismic transect to refine the geometrical configuration of the Sudbury structure at depth using the higher resolution aeromagnetic and ground gravity data, the processed seismic data, together with additional subsurface geological controls that were not available in the older gravity (McGrath and Broome, 1994) and magnetic studies (Hearst et al., 1994). The additional control data are discussed in the next section.

3.5 Forward modelling of gravity and magnetic data

Magnetic sensors are sensitive to variations in the Earth's ambient magnetic field: this can be used to infer the spatial distribution of magnetic minerals such as magnetite and pyrrhotite in the subsurface. High resolution magnetic field data are capable of detecting structural details that may be transparent to both seismic and gravity investigations (Hearst et al., 1994). Modelling of magnetic and gravity data can provide information about the subsurface distribution of magnetic material and the density of the rock. Geosoft GMSYS software was used to undertake 2.5-dimensional integrated forward modelling of the gravity and magnetic data along the two profiles B-B' and D-D' described above.

The Sudbury structure extends from surface to depths up to 12 km and local anomalies associated with the SIC are similar and orientated in the same direction as the more regional anomalies associated with the Superior-Southern Province boundary hosting the SIC (Hearst and Morris, 2001). Because it is difficult to isolate a residual field without introducing some bias into the potential field data of the Sudbury structure (Hearst and Morris, 2001), a geologically-related long wavelength component was not subtracted from the total magnetic field. Instead, the total

magnetic field was modeled by adjusting the shapes and physical properties of geological units until an appropriate match between the observed and modelled field was achieved.

The interpretative geological model comprises a series of polyhedral shapes with assigned physical property values with each polyhedron linked to a specific rock type. Although physical properties can vary considerably within a lithological unit, the computation of the calculated field is often simplified by assigning an average physical property value to each unit. Obtaining a perfect fit between the calculated and the measured field is difficult because: i) the model attempts to represent real world complex geological bodies and structures with simple bodies and shapes; ii) the high variability and multi-modal distribution of physical properties within lithological units due to the effect of secondary geological processes - alteration, metamorphism, faulting; iii) the presence of remanence magnetisation, and iv) the presence of magnetic cultural objects – railway, powerlines, pipes which represent noise in the observed data. Consequently detailed geological and topographical knowledge of the study area is essential in guiding variations in the geology and physical property distributions to mitigate ambiguity in the geophysical models and develop a reliable model.

3.6 Constraints on the 2.5-D model

The non-uniqueness of geophysical models is often demonstrated by fitting different models to the same geophysical data. In an effort to compute geophysical models that are geologically realistic, subsurface geological, geophysical and/or petrophysical information are used to geometrically and lithologically constrain models at depth. The 2.5-D models developed in this

study were constrained both on surface and in the subsurface: a description of the available geological and geophysical constraints follows.

3.6.1 Magneto-stratigraphic map: Previous geophysical models were constrained at surface using geological maps; however, recent studies have shown that the distribution of magnetic minerals in a rock is often not the same as that of the silicate minerals, especially in a highly altered geological environment like Sudbury. This is demonstrated in the comprehensive study of Morris (2006) on over 600 samples of norite. Morris (2006) used a paleomagnetic analysis approach to demonstrate the level of alteration and the existence of no less than five distinct remanence magnetisation directions in a rock that crystallized in about 400,000 years (Davis 2006) and that should therefore only have one remanence magnetisation direction. Therefore, magneto-stratigraphic contacts of the Sudbury structure (Figure 3.2b), which were interpreted from the airborne magnetic data (Olaniyan et al., 2013), only represent the approximate location of mapped geological contacts. They correspond well with the mapped surface bedrock contacts (Ames et al., 2005) especially in the North Range, where the magnetic contacts are well delineated by maximums in the magnetic field gradient. These magneto-stratigraphic contacts were used as surface controls for the models.

Also, additional information on lineaments (dikes and faults) obtained from the magnetic interpretation was used to update the available seismic and geological sections. In particular, Olaniyan et al. (2013) interpreted prominent EW lineaments cutting across the D-D' profile that were not included in the Vale's geological section. LIDAR elevation profile data acquired simultaneously with the airborne gravity data survey were used to constrain the surface

topography employed in the models. Bathymetry of lakes was treated as either void depressions or assumed to be infilled by recent sediments with relatively low density and magnetic susceptibility.

3.6.2 Geological section: A 3-D geological model of the Sudbury structure has been developed by Vale from borehole log data and other information including geophysical data acquired around the Sudbury structure. A geological section (Figure 3.3) extracted from this 3-D model along the Lithoprobe transect was made available for this study by Vale. Vale's geological section is well constrained by borehole data up to 2 km depth, after which geological contact and structures were projected further down to about 5 km supported by geophysical data. Information presented below 2 km in the geological section is treated as an interpretative constraint with a lower degree of confidence during the modelling and was not strictly adhere too.

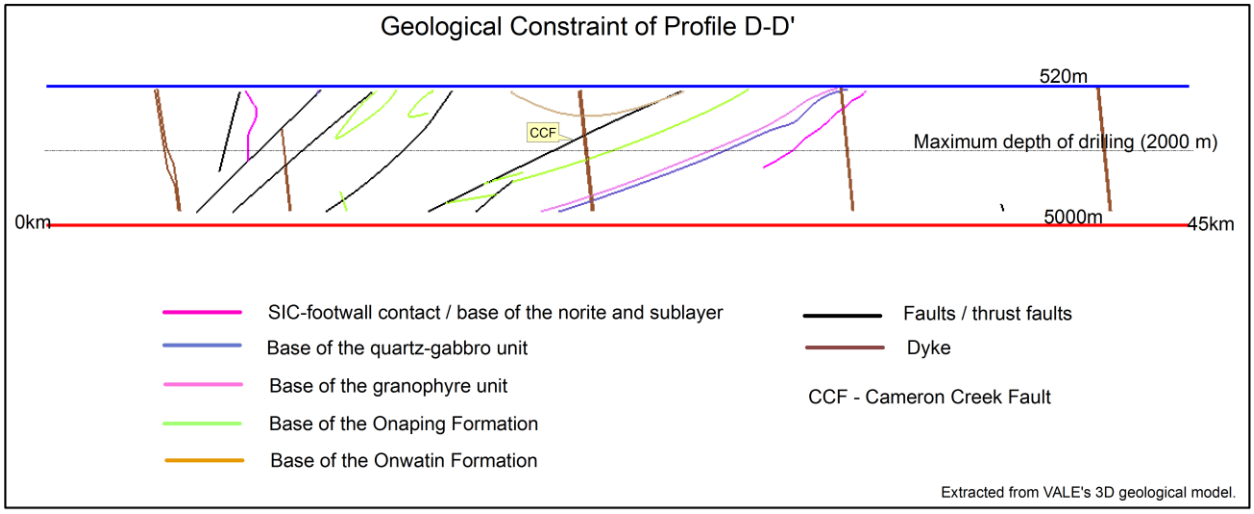

Figure 3.3: The geological section along profile D-D' extracted from the 3-D geological model developed from borehole logs and other geological and geophysical data by Vale. The colored lines are the base of lithological units within the SIC, black and brown lines are faults and olivine

diabase dykes respectively. The upper limit of the Vale model delineated (blue) is at 520 m below sea level while the lower limit (red) is 5000 m below sea level. The maximum depth of drilling is an approximate value for the whole section and could be up to 3 km in places.

This geological section shows well-constrained SIC-basement contacts and SIC internal contacts in the North Range. These contacts are displaced by the south dipping Cameron Creek fault (CCF) beneath the Sudbury Basin. In the South Range, NW-directed reverse faults truncate the Onaping Formation and the SIC-basement contact.

3.6.3 Lithoprobe seismic section: Section 41 of the Lithoprobe program is close to section D-D' in the South Range; however, section 40, which traverses the eastern part of the North Range is displaced about 20 km to the east of profile D-D' (Figure 3.1). Milkereit et al. (1992) assumed that there was little change in the structure of the SIC in the North Range between sections 40 and 41, and they therefore combined the two sections into a single continuous seismic section. The merged litho-seismic section 40 and 41 exhibits reflector patterns, orientation styles and concentration, which reflect the differing petrophysical attributes of rocks in the Sudbury structure (Figure 3.4a). For example, the high reflector density between the norite and granophyre units is due to the relative high density of quartz gabbro (2.88 g/cm^3).

Wu et al. (1995) re-processed the ambiguous Lithoprobe seismic sections using pseudo three-dimensional seismic processing technique to further enhance the seismic data. The enhanced seismic sections they produced show more continuous reflectors and they were structurally re-interpreted (Wu et al., 1995), but their reinterpretation did not include some of the reflectors that are likely to be fault offsets. They also did not adequately explain the implications of some

well-defined patterns of reflectors, as for example, the distinct curved band of reflectors labelled B in Figure 3.4a.

Therefore, as part of this study the seismic section was qualitatively re-interpreted to delineate contacts and sub-surface structures (Figure 3.4b). Typical compositional layering in gneissic rocks creates a high reflectivity contrast where such rocks are in contact with noritic rocks at the base of the SIC (Green et al., 1990). This contact is therefore well delineated in the seismic profile and it dips southwards from surface in the North Range to a depth of 7 km, where it exhibits a "kink" below the Sudbury Basin (Figure 3.4a and 3.4b) (Milkereit et al., 1992). The contact then continues to dip to the south to a depth of about 12 km. In the merged seismic section, granophyre is seismically transparent, but the transition zone between the norite and granophyre is marked by a reflective zone traceable to a depth of about 6 km before it changes in dip direction (Boerner et al., 1994).

On Figure 3.4b, a south dipping reflective block (A) occurs between the highly reflective Archean basement and the transparent norite in the South Range at about 6 km depth. Some scattered reflectors (B) in the Southern Province correspond to the boundary of the SIC and the Creighton pluton as defined in Vale's geological section. South dipping reflectors labelled SRSZ in the South Range truncate the contacts of the north-dipping transitional zone Figure 3.4a (features previously identified by Milkereit et al., 1994). A post-depositional normal fault appears to have offset the Onwatin Formation by about 1 km near the centre of the Whitewater Group series. This interpreted fault is apparently evident in the processed seismic section, but there is no geological or geophysical evidence to support its existence, so it is not included in the modelling process.

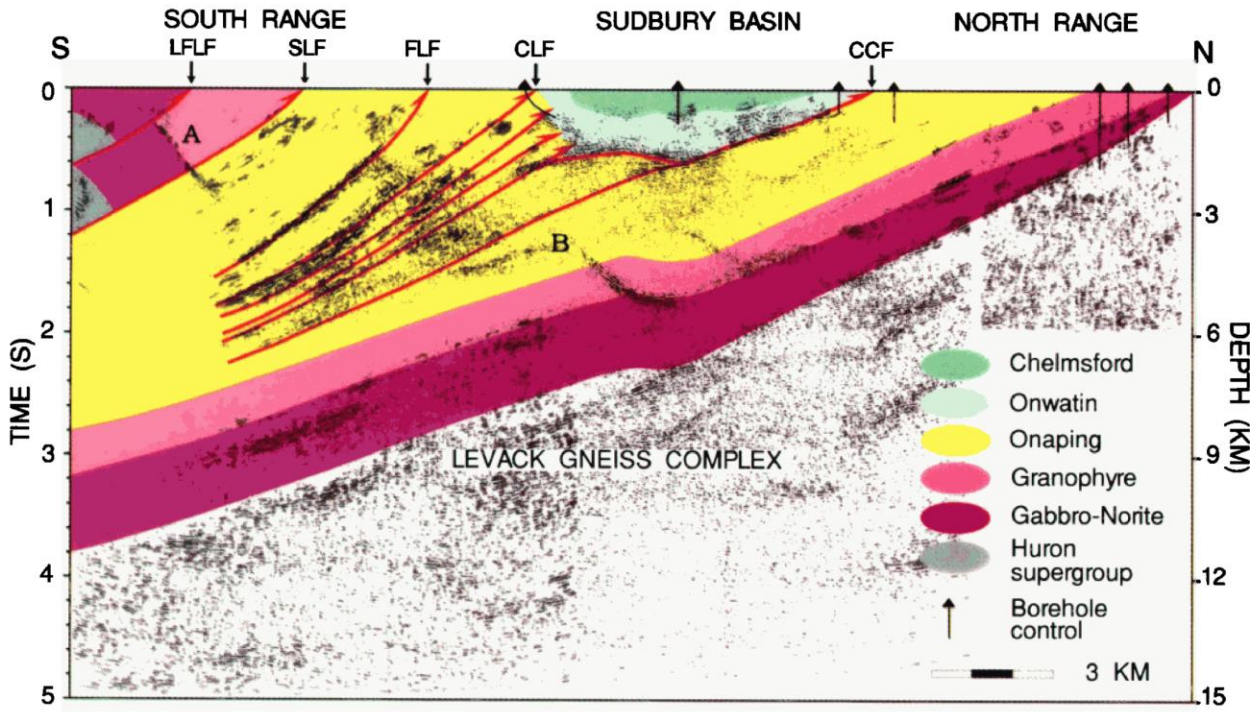

Figure 3.4a: Lithoprobe seismic section interpretation from Wu et al. (1995).

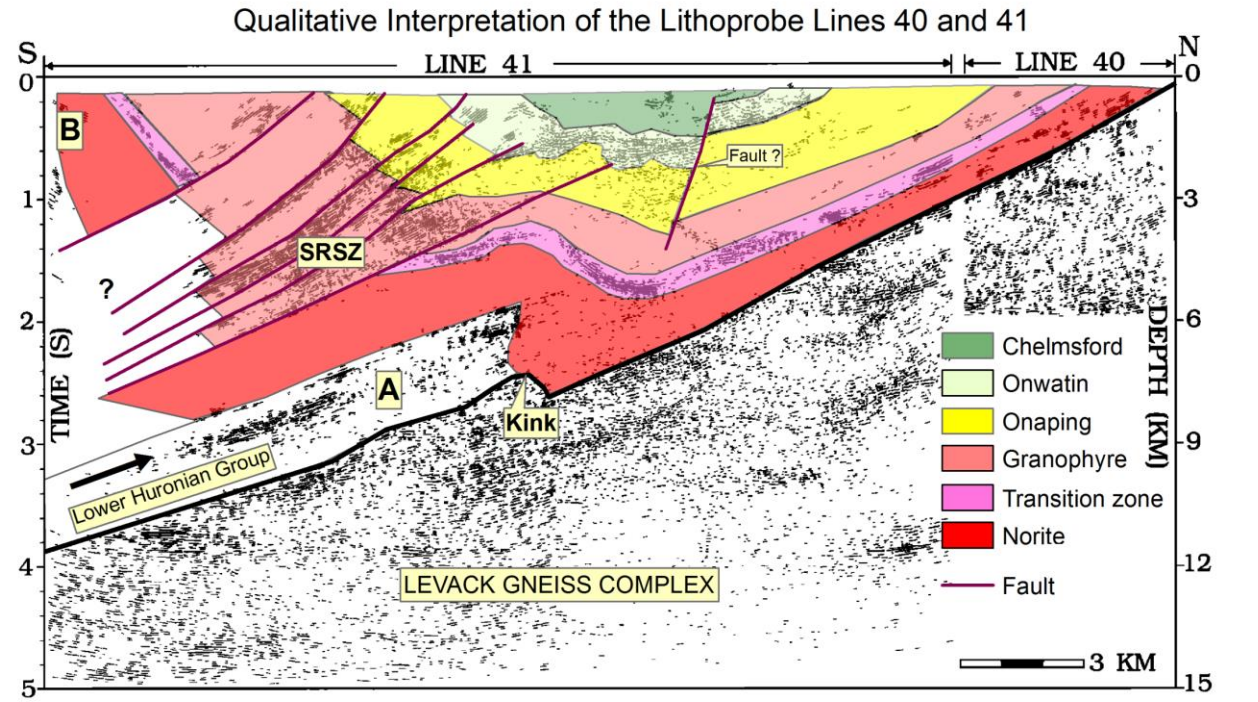

Figure 3.4b: Quantitatively re-interpreted Lithoprobe seismic section of this study.

The merged Lithoprobe lines 40 and 41 (Figure 3.4a) presents a full seismic section across the SIC, but defining the surface contacts of rocks in the western part of the SIC North Range (where the Profile DD' crosses the North Range) with the seismic line from the eastern portion (where the Lithoprobe seismic line 40 was acquired), introduces some inconsistencies in the lithological units (Figure 3.1). This is because the long axis of the SIC regionally trends in the northeast, so in the North Range lithological contacts in the eastern part are further north than their respective contacts in the western part. For example, the Onwatin-Onaping contact in the eastern part of the North Range is at the same latitude as the SIC-basement contact on the western side. Our model relied more on the inferred magnetic contacts across the profile to locate the rock boundaries on the surface and consequently produced a different location of the contacts compared to the previous interpretations of the Lithoprobe data (Milkereit et al., 1992, 1994; Card and Jackson, 1995).

3.6.4 Physical properties: The physical properties of the different lithological unit in the models presented here are from published average magnetic susceptibility, natural remanent magnetisation, and density values (Table 3.1) obtained from surface and borehole samples within the Sudbury structure (McGrath and Broome, 1994; Hearst et al., 1994). Due to the level of alteration and deformation, the distribution of magnetic minerals is not uniform within similar rocks in the Sudbury structure (Hearst et al., 1994), so the susceptibility values were allowed to vary from the estimated values by about +/-0.005 SI. The direction of the natural remanence was kept constant, while the magnitude was also allowed to vary (Hearst et al., 1994). Similarly, the density values of some rocks were varied up to ±0.05 g/cm^3 in order to achieve a good fit.

When developing the 2.5-D models, the average physical property values is initially assigned to a polygon representing a lithological unit. The polygon is further fragmented into smaller polygons and the physical properties of the some the fragmented polygons are varied within the accepted limit to reduce the misfit of the measured and the calculated fields. In reality, this simulates the differential alteration or unequal distribution of magnetic minerals within a rock unit.

Table 3.1: Average physical properties of rocks used to compute the calculated field in the models. Density contrast values from McGrath and Broome (1994). Magnetic susceptibility and natural remanence values (magnetic inclination, declination and intensity) are modified from Hearst et al. (1994). The magnetic susceptibility values were allowed to deviate by ±0.005 SI from the actual, while the density contrast in varied up to ±0.05 g/cm^3 at some instances.

Rock unit	**Magnetic susceptibility (SI)**	**Natural Remanence Magnetisation (NRM)**			**Density (g/cm^3)**
SIC North Range		Declination (degree)	Inclination (degree)	Intensity (SI)	
Norite	0.035	316	69	varied	2.81
Quartz gabbro	0.035	329	68	varied	2.88
Granophyre	0.025	329	68	varied	2.70
SIC South Range					
Norite	0.004	189	64	varied	2.81
Quartz gabbro	0.035	189	64	varied	2.88
Granophyre	0.001	116	84	varied	2.70
Whitewater group					
Onaping	0.025	130	21	varied	2.77
Onwatin	0.010	291	75	varied	2.68
Chelmsford	0.010	291	75	varied	2.75
Dense Levack gneiss	0.068				2.88
Levack gneiss	0.047				2.73
Cartier granite	0.012				2.65
Dykes	0.024				2.85
Huronian sediment	0.014				2.70
Huronian mafic	0.029				2.88
Creighton	0.025				2.76

3.7 2.5-D model approach

The selected profiles are not exactly orthogonal to the strike of the major geological units of the Sudbury structure, so finite strike lengths of 5 km and 2 km were assigned on either sides of profile D-D' and B-B' respectively to compute the two-and a-half dimensional (2.5-D) forward models. Our procedure for joint forward modelling of gravity and magnetics data was as follows: i) we defined the magneto-stratigraphic contacts (Olaniyan et al. 2013) across the profile as surface controls; ii) The subsurface lithological models of various shapes were constructed using the geological and seismic sections for D-D' as guide; iii) we associated the surface magnetic contacts with the lithological contacts of the subsurface geometrical constraints; iv) the subsurface distribution of rock masses was first computed by assigning the average density contrast values to each lithological unit; vi) the shape and position of the geological bodies were adjusted to fit the calculated gravity field to the measured response as closely as possible; vii) lineaments and structures often transparent to the gravity field were then modelled from the Vale's geological section and the interpreted magnetic data, while average magnetic susceptibility and NRM values were assigned to each geological units; viii) the calculated fields were simultaneously modified by varying the magnetic and the density parameters within the acceptable variance and the shapes of the lithological units until the misfit between the calculated and the measured fields was reduced as much as possible.

3.7.1 Profile D-D'

Profile D-D' along the Lithoprobe transect is approximately 45 km long. From south to north, it includes the Huronian mafic volcanic and sedimentary rocks, the Creighton pluton, the SIC in the South Range, the Whitewater Group, the SIC in the North Range, the underlying Levack

Gneiss Complex, and the Cartier Batholith (Figure 3.5). Along the profile, the Huronian rocks exhibit very low magnetic intensity relative to the SIC. In the South Range, a prominent short wavelength magnetic high is coincident with roughly the southern two-thirds of the Onaping Formation, and another magnetic high is coincident with roughly the southern two-third of the Onwatin Formation. North of these two peaks the magnetic field increases gradually across the Sudbury structure up to the contact between norite and the dense basement Levack gneisses and it then starts decreasing to the north across the basement rocks. Highly magnetic NW-trending olivine diabase dykes, EW faults infilled by magnetic dykes, and some mafic intrusions also occur along the profile.

The measured free air gravity data exhibits a relative gravity high over the Huronian mafics in the south, the SIC, and the Levack gneisses in the north. The gravity high over the South Range footwall is attributed to the thrusting of the basal Huronian volcanic rocks and mafic intrusions in the middle and upper Huronian sequences. This gravity high due to the South Range footwall rocks together with the SIC noritic-gabbro rocks decreases from 4 mGal to -3 mGal at 14 km along the profile in the middle of the granophyre (2.70 g/cm^3) (Figure 3.5). The gravity high observed about mid-way of the granophyre is interpreted to be due to the basal Onaping intrusions occurring at the near-surface at this location. Onaping Formation (2.77 g/cm^3) exhibits a local gravity high at about 19 km along the profile, whereas a moderate gravity low is observed over the Onwatin and Chelmsford formations of the Whitewater Group. The gravity field over the Onwatin Formation (2.6 g/cm^3) differs from the North Range to the South Range (Figure 3.5). This might imply that the gravity field related to the South Range Onwatin Formation is being influenced by gravity field due to other deep-seated dense bodies. At 29 km, a gravity low coincides with the Fecunis fault, though it is not apparent in the magnetic field (Figure 3.5). This

fault has down thrown the SIC to the south, resulting in a higher gravity response to the north of the fault within the Onaping Formation. Alternatively, the likelihood of a river valley in this fault zone might have also resulted into the observed gravity low. A splay of Fecunis fault also transects the SIC rocks at about 32 km along the profile, resulting in a sudden low field in the observed gravity.

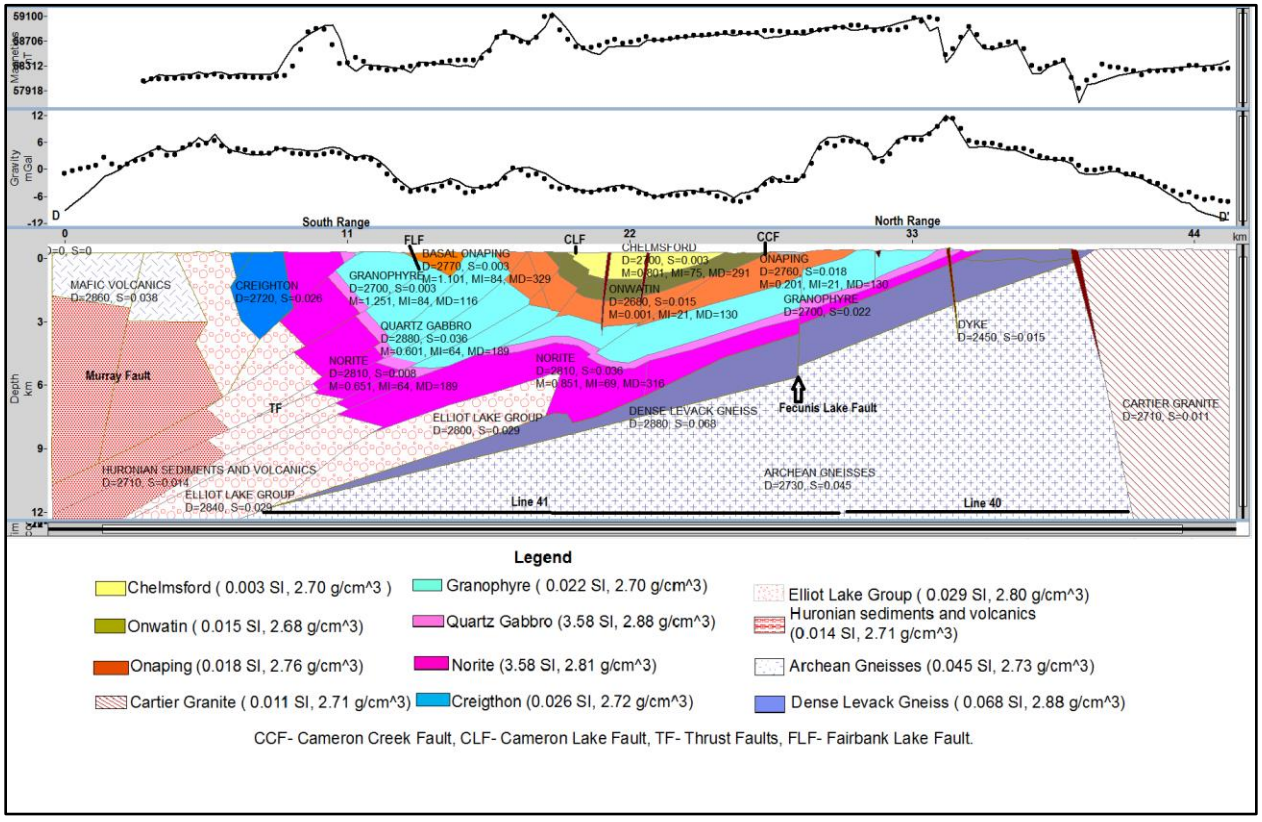

Figure 3.5: 2.5-dimensional geological model for profile D-D' (bottom) and the corresponding magnetic (top) and gravity (middle) data from the compilation of Olaniyan et al., 2013 and the airborne gravity data provided by Vale. The measured data is the thick dotted line and the forward model data is the thin solid line. The vertical exaggeration of this geological model is 0.70. D-density (kg/m^3), S-susceptibility (SI), M- remanent magnetization (A/M), MI-

inclination of remanent magnetization (degrees) and MD- declination of remanent magnetization (degrees).

The 2.5-D model of the D-D' profile (Figure 3.5) defined the Archean basement topography based on the seismic section (Milkereit et al., 1992). The Huronian rocks (2450 Ma) rest uncomformably on the Archean basement gneisses in the South Range (Card, 1994), whereas the Cartier Batholith intrudes the Archean gneisses with a steeply north dipping contact in the North Range (Boerner et al., 1994). The dip of the SIC-basement contact in the North Range was modelled to be consistent with the geologic and seismic evidence. Although the contact between the Levack Gneiss Complex and the Archean gneisses is not well differentiated in the Lithoprobe seismic section, surface geological contact and orientation parameters (Ames et al., 2005) were employed to model a slab of highly dense Levack gneiss complex (2.88 g/cm^3) into our model to fit the observed free air gravity. This dense slab is about 4 km wide at the surface, gently dipping (~30^0) to the south and gradually thins out at a depth of about 12 km below the South Range. The south dipping norite – granophyre contact can be interpreted from the seismic section to a depth of about 6 km, where it exhibits a dramatic change of dip. This is seen at a similar depth on all the seismic lines (1, 43 and 44) crossing the South Range (Boerner and Milkereit, 1999). The deformational event that resulted in the change in dip exhibited by the Archean basement, also affected the SIC. Folding of the transition zone between the norite and granophyre under the Sudbury Basin (Figure 3.4b) indicates that the deformation event is post-impact.

Below the tectonically induced reflections in the south, the zone of high reflectivity marked (A) in Figure 3.4b, occurs above the south dipping basement contact and below the transparent norite

in the South Range at about 6 -7 km depth. This deformational structure "A" could have resulted from a thick-skinned deformation, which displaced a portion of the Archean basement gneisses (block A) up slope, thereby folding the base of the SIC northwards. Alternatively, the displaced block A in the interpreted geological section could be the iron-enriched massive and pillowed tholeiitic basaltic flows and intrusions of the Elliot Lake Group at the base of the Huronian Supergroup (Long and Lloyd, 1983). These mafic rocks might have been displaced up-slope over the Archean basement in the South Range during compressive deformation related to the Penokean orogeny that also resulted in north-verging folding of the basal portion of the SIC. Whereas, the nature of the highly reflective rock unit (A) at the base of the SIC remains debatable until further investigated, it occurs above the south dipping Archean basement and clearly shows different seismic reflection properties compared with those of the norite unit (Figure 3.4b).

3.7.2 Profile B-B'

Profile B-B' (Figure 3.2a-c) typically does not represent an ideal two-dimensional section, because of its orientation and location. When viewed downhole, the section cuts through the lithological units dipping ~ 30^0 to the south, which represent only the apparent thickness of the rock units in strike direction. Nonetheless, profile B-B' seems to be the most appropriate location and orientation to investigate the EW change in the character of the magnetic and gravity signatures near the centre of the SIC in the North Range. The interpretation is also broadly non-unique, because it was simply guided by the variation in the thicknesses of lithological units in the magnetic interpretation map (Figure 3.2b). On the interpretation map (Figure 3.2b), the thicknesses of the Archean gneisses and Onaping Formation increase, the

granophyre reduces, while the norite-gabbro rocks remain relatively constant from the west to the east along the 21 km profile.

On the surface, the profile B-B' traverses the granophyre and the Onaping Formation across a zone where the magnetic values decrease gradually from the WSW to the ENE (Figure 3.6). Between the southwest end of the profile and about 11 km along the profile the measured magnetic data exhibit a relatively high intensity (59165 nT -58948 nT), but thereafter decreases to about 58661 nT at the ENE end of the profile. North-south powerlines and pipelines cut across the profile D-D' at 4.5 km adding cultural noise to the magnetic field (Figure 3.2b, 3.6). Two prominent short wavelength magnetic highs are observed superposed on this eastward-decreasing trend in this section of the profile. The gravity field between 0 and 11 km distance along the profile is characterized by a series of sinusoidal highs and lows with peak to trough differences ranging generally from about 2 to 4 mGal. The gravity field decreases from a level of about 7 mgal to about 0 mgal between 11 km and 14 km as it defines the western flank of a relatively long wavelength gravity low: the eastern flank is defined by a gradual increase in the field between 14 km and 18 km along the profile.

A series of closely spaced, east-dipping normal and reverse faults, located between 11 km and 18 km along the profile, is interpreted to have influenced the stepwise gradient in the measured magnetic and gravity fields. The basement topography of the highly magnetic and dense Levack gneisses remain constant at about 1.5 km depth along the profile from 4km up to 11 km, east of which it is steeply downthrown by a series of block faults to about 6 km. Within the fault zone, the deepest part of the basement topography is at 7.2 km depth and sub-parallel to the

Sandcherry fault (Figure 3.2b) that displaced the North Range and footwall rocks. At 15 km, a fault zone that has been infilled with mafic material creates a local anomaly. The local low magnetic and gravity anomalies at about 4 km along the profile coincide with the Fecunis Lake fault, which has been interpreted earlier on D-D' profile to be due to the river valley in the fault zone. Overburden of approximately 1.00 g/cm^3 density value and an average thickness of about 100m is interpreted to have filled the upper part of blocks of SIC and basement rocks that have been displaced by series of faults between 11 km and 18 km of the profile (Figure 3.6).

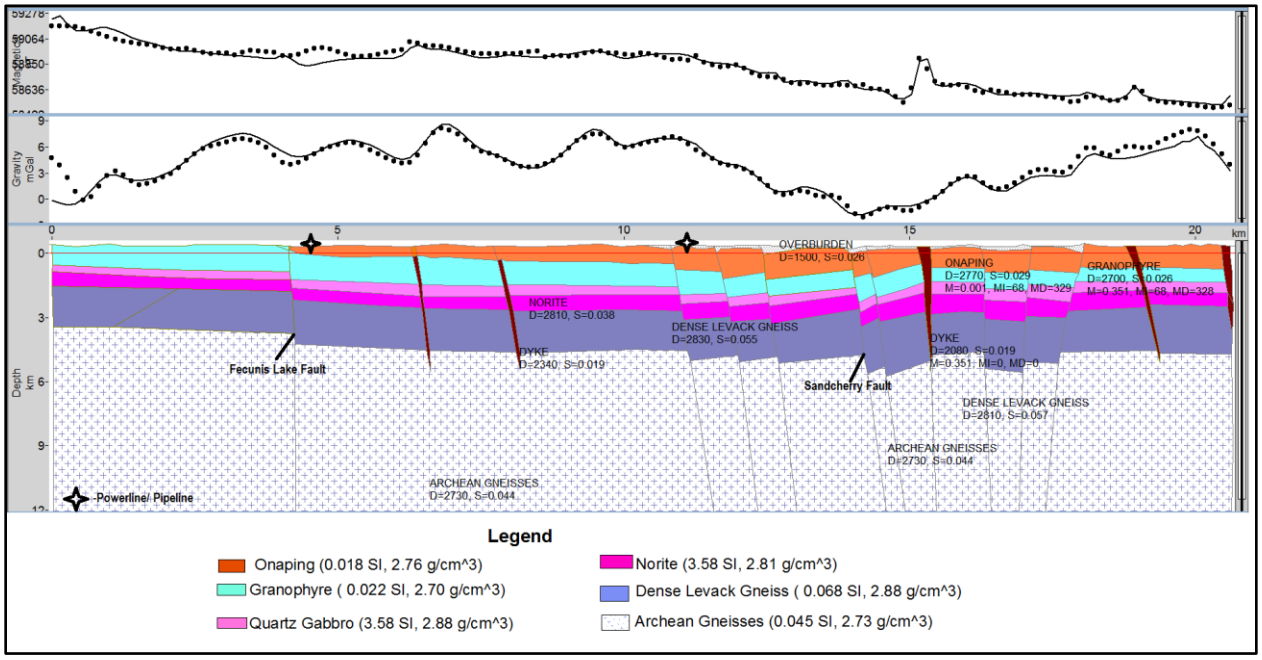

Figure 3.6: Profile B-B'. The 2.5-D geological model is shown in the bottom panel. The modelled magnetic data (top) and gravity data (middle) is shown with a thin solid line, while the measured data is shown with a thick dotted line. Note the gradual change between 11 and 18 km in both the magnetics and gravity fields. D-density (kg/m^3), S-susceptibility (SI), M- remanent magnetization (A/M), MI- inclination of remanent magnetization (degrees) and MD- declination of remanent magnetization (degrees).

3.8 Discussion

3.8.1 Thrust block under the SIC?

The existence of dense bodies below or within the SIC have been suggested by past workers (Gupta et al., 1984; King, 2007) due to the linear positive gravity high (XXX) observed in the SIC (Figure 3.7). Geologically-constrained three-dimensional inversions of the GSC gravity data of the Sudbury structure isolated a linear and dense body below the southern portion of the Sudbury Basin, away from the SIC rim (Figure 24, King, 2007), suggesting that the dense bodies are not related to the norite-gabbro at the SIC rim. The displaced block (A) (Figure 3.4b) interpreted at the basal part of the norite provides a good fit to the measured gravity and magnetic data, when average density and susceptibility values of 2.80 g/cm^3 and 0.029 SI values are assigned respectively. This block's density value is less than the average density and susceptibilty of norite (2.83 g/cm^3, 0.036 SI), but higher than the density of the Archean gneisses (2.73 g/cm^3, 0.045 SI). The model fitness error in GMSYS software is reduced from 25% to 3%, when the petrophysical values used to model the lower part of the Huronian Supergroup (Elliot Lake Group) are assigned to the displaced block (A), rather than of the Archean gneisses. When the south dipping reflective zone (A) in Figure 3.4 is considered to be a thick thrust-stacked norite the gravity response increases and the calculated magnetic field decreases thereby slightly increasing the model misfit. Thus, the former model that assigned the Elliot Lake Group's petrophysical values is more likely and is consistent with deformation of a SIC that originally had a flat saucer or sill geometry and that was deformed by reverse thrust faults in the South Range (Card and Jackson, 1995). This interpretation is also supported by the presence of thrust units of the Elsie Mountain Formation of the Lower Huronian Supergroup at the South Range footwall adjacent the norite and Sublayer units (Figure 1, Ames et al., 2007)

3.8.2 Linear gravity high in Whitewater Group

Sedimentary basins generally exhibit low gravity response when filled with very porous sedimentary sequences. The occurrence of a linear gravity high (labelled XXX, Figure 3.7) in the Onwatin and Chelmsford Formations of the Sudbury Basin is unusual considering their relative low densities of 2.68 g/cm^3 and 2.75 g/cm^3 respectively (McGrath and Broome, 1994). The linear gravity high aligns somewhat with the South Range Onaping Formation, but further extends to the centre of the Chemford Formation in the western part and over the Granophyre to the eastern part of the SIC (Figure 3.7). In 1999, Boerner and Milkereit hinted that the change in dip of the basement rock at 6 km depth (labelled B) in the merged Lithoprobe seismic section 40 and 41 (Figure 3.4a) is inconclusively observable in the other seismic lines (1, 43 and 44) of the South Range and the causative structure laterally extends through most of the SIC.

The coincidence of the linear gravity high with the north-verging fold in the two dimensional interpretation (Figure 4), suggests that the two aforementioned interpretations are consistent and might be related to deformation at the base of the SIC. The presence of a north-directed fold at the base of the SIC rocks together with the thrust-related mafic bodies of the Elliot Lake Group at the depth of 4 km to 10 km in the South Range explains the cause of the linear gravity high observed in the Sudbury Basin (Figure 7). Hidden mafic bodies had been suggested to exist at about 4 km depth under the SIC (Gupta et al., 1984). The fold at the base of the SIC and regional folding of the SIC into a doubly-plunging fold likely occurred during the Penokean orogeny and the folds were then transected by shear zones of the SRSZ system that formed during the same orogenic event (Shanks and Schwerdtner 1991; Cowan and Schwerdtner 1994; Mukwakwami et al., 2014).

3.8.3 Growth faults in the North Range?

A series of fractures created by the impact event might have allowed relative vertical movement of basement rocks during the formation of the SIC and deposition of the Onaping formation (Ames et al., 2008), which resulted in the gradual changes in the magnetic and gravity data at 11 km to 18 km along the profile B-B' (Figure 6). These gradual changes in the potential field dataset appears to be related to a series closely-spaced fault system, displacing the Sudbury structure and basement rocks in the North Range. This event resulted in a paleotopographic high and low, as well as a variation in the thickness of debris flows in the upper contact Sandcherry member of the Onaping Formation (Ames et al., 2008).

Visual inspection of the low resolution GSC gravity grids (Figure 3.2c) indicates that the low gravity field observed along this profile extends further to the north around the Sandcherry Creek fault. This observation is in contrast to the gravity field observed around the similar Fecunis Lake fault, 9 km west of the Sandcherry Creek fault (Figure 3.2c) suggesting a likely difference in the geological setting of these two similar faults. The gravity low over the Fecunis Lake fault zone is more likely to be due to river valley that has been filled with overburden or less dense materials.

3.8.4 Deep prospective zone?

The deformed base of the SIC in the South Range occurs at about 5 km depth and may be shallower near the central portion considering the increased gravity intensity in this region (Figure 3.7). This inferred shallowness could also be related to the more northwards indentation of the South Range observed near its central portion, indicating that the north-west directed

Penokean orogenic regime likely had more effect along that portion. A north-verging fold at the base of the SIC in the South Range would imply that the highly Cu-Ni-PGE-rich sublayer and norite at the base of the SIC is shallower at depth under the Sudbury Basin. The southern portion of the Sudbury Basin is a potential prospective zone for mineral exploration in the future, when cheaper and safe technology is developed for deeper mining beyond the present profitable benchmark of 2.5 km in the Sudbury camp. In subsequent work we intend to undertake constrained 3-D modelling to better image the Sudbury structure.

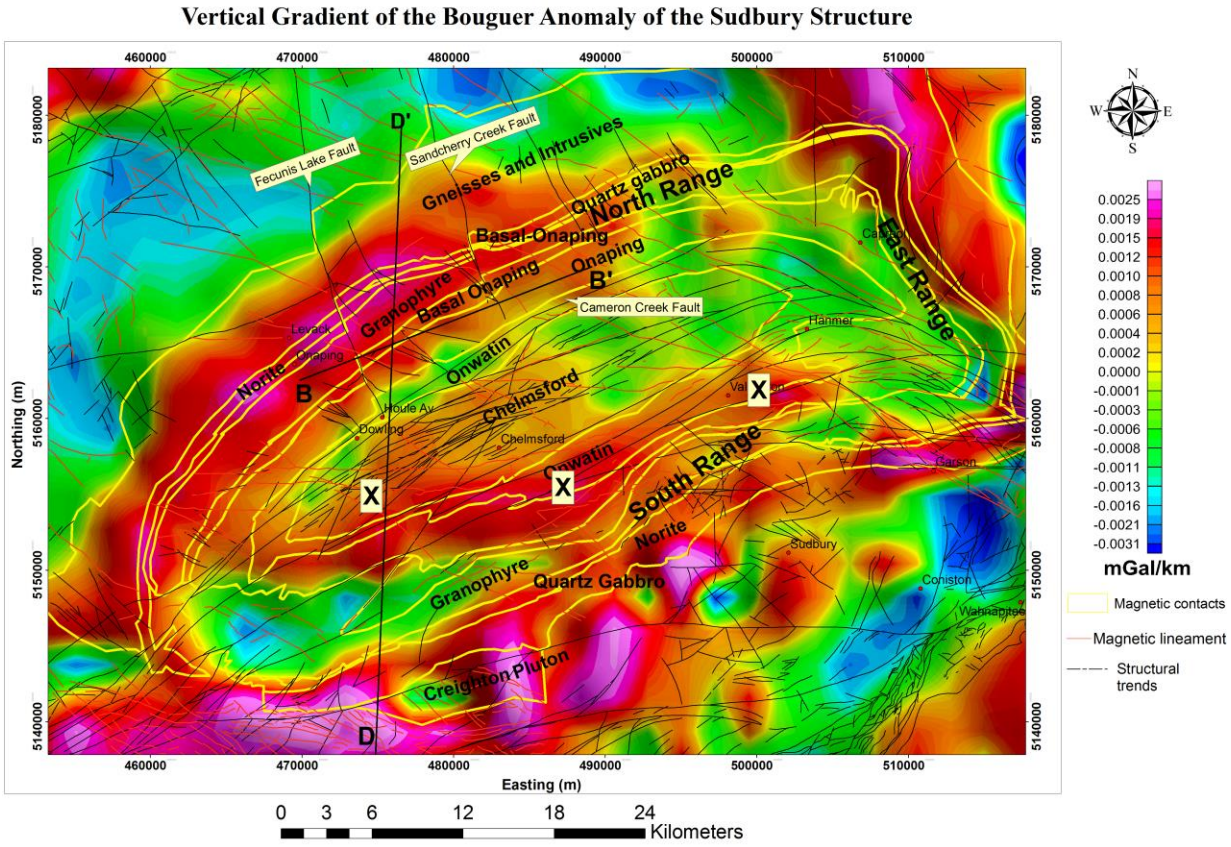

Figure 3.7: Map of the vertical gradient of the gravity Bouguer anomaly of the Sudbury structure. A linear local gravity high within the Sudbury sedimentary Basin marked (XXX) coincides with the location of the basal deformation of the SIC in the 2.5-D section. Major structures (thin black lines) were extracted from the Published bedrock map (Ames et al., 2005).

3.8.5 3-D lithofence diagram

The interpretation of the fence lithological diagram (Figure 3.8) of profiles B-B' and D-D' presents the variation in thickness and depth of lithological units along the ENE and NNE of the Sudbury structure. Specifically the modelling indicates that: i) the Levack gneiss complex is about 2 km thick in the western part of the SIC as observed also in the surface geological map; ii) the depth to the top of the magnetic LGC is shallower (~2 km) in the west (see Figure 3.6) and gets deeper southwards as it dips under the Whitewater Group. The increasing depth to the magnetic basement southwards from ~2 km to ~7.5 km under the SIC and the Whitewater sedimentary series is responsible for the gradual reduction of the magnetic intensity southwards, iii) the gradual reduction in the magnetic intensity towards the east appears to be controlled by a series of NS deep-seated normal and reverse faults, which have downthrown both the SIC and the Archean basement rock near the centre of the SIC in the North Range.

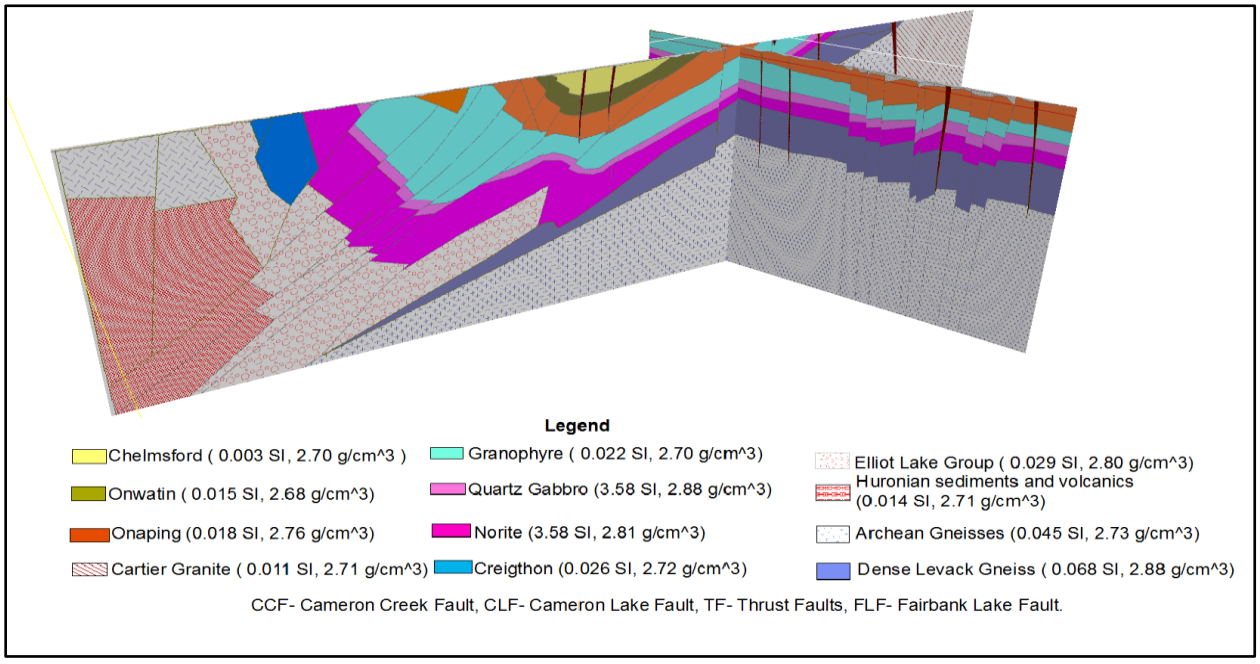

Figure 3.8: Two-dimensional lithological fence diagrams of profiles B-B' and D-D' show the geological configuration and continuity of the basement and the over-lying SIC rocks.

The northwards decreasing thickness of the lower norite unit and the non-parallel geometry of the internal unit contacts within the SIC are significant. If the upper surface of the melt sheet is used to infer the paleo horizontal during different stages of cooling and crystallisation of the SIC, then we conclude that the SIC was not a flat sheet with parallel lower and upper limits, but had a slight lopolithic shape with a flat upper surface and a non-parallel gently south-dipping lower surface. This also implies that the melt either occupied a wide saucer-shaped crater or that the melt occupied the interior of the peak ring cavity of a multi-ring impact basin as suggested by Spray et al. (2004).

Further work in this study will include development of four other 2.5-D models across the SIC. The six 2.5-D profiles will then be incorporated into a 3-D geological model. In this next stage we intend to use 3-D forward and possibly inversion modelling to extrapolate features between the profiles to investigate the continuity as well as depth of the deformation of the SIC in the South Range, and the variation in the thickness of the dense Levack gneiss in the North Range. If a deep hole were to be drilled as previously proposed in the International Continental Drilling Program proposal (Mungall et al., 2003), then an interesting location would be a hole to about 5-6 km depth in the southern part of the Sudbury Basin to provide more insight into the tectonic evolution of the Sudbury structure. The precise location of this deep hole might be better determined by the 3-D inversion modelling.

The airborne data analyzed in this study were acquired using flight lines flown in the NW direction across the SIC, which is sub parallel to the interpreted growth fault zones in the North Range. Ideally, geophysical surveys better resolves geological structures that are perpendicular

or almost perpendicular to the survey directions. This might have contributed to the very subtle anomalies observed in the magnetic and gravity data. Ground or airborne gravity and magnetic surveys with EW lines should be acquired and interpreted in this region to further validate this interpretation. The coincidence of the formation of the growth faults with the known Ni-Cu-Co mineralisation occurrences around this interpreted fault zone (Figure 8, Ames et al., 2008) could be used as a guide to further exploration around the other faults identified in the modelling.

3.9 Conclusions

The study uses a constrained forward modeling technique to interpret potential field data and explain regional discontinuities and anomalies observed across the Sudbury structure. Surface magnetic contacts and interpreted geological and seismic sections are used to constrain the lithological units in the North Range, whereas modelling of the South Range relies on qualitative interpretation of the south-dipping seismic reflectors and on the few contacts shown on Vale's geological section. The interpretation of the constrained integrated model suggests that the SIC includes a north-verging fold that affects the norite and the transition zone beneath the Sudbury Basin at about 6 km. The fold is located to the north of a block of material interpreted to be thrust-displaced Elsie Mountain Formation. An elongate gravity high feature on the regional gravity map may be the expression of the interpreted fold.

A prospective sub-layer norite could lie above the basal deformation zone below the norite, so could be prospective for mineralization. However, the depth of the prospective zone is too deep for current mining methods, but it might be an interesting target should a deep hole be drilled in the Sudbury structure. Modelling of the gravity and magnetic data along profile B-B' supports previous interpretations for series of closely-spaced fault system inferred to be growth faults

oriented perpendicular to strike of the SIC, such as the Sandcherry fault. If this fault zone is pre- or syn-impact event, it might have controlled and trap the migration of sulfide-rich hydrothermal fluids, and might also be prospective.

References

Ames, D.E., Davidson, A.J., Buckle, L., and Card, K.D. 2005. Geology, Sudbury bedrock compilation, Ontario, Geological Survey of Canada, Open file 4570, Scale 1:50,000.

Ames, D.E., Davidson, A.J., and Wodicka, N. 2008. Geology of the Giant Sudbury Polymetallic Mining Camp, Ontario, Canada. Economic Geology, **103**: 1057-1077.

Ames, D.E., Goligthly, J.P., Lightfoot, P.C., and Gibson, H.L. 2002. Vitric composition in the Onaping Formation and their relationship to the Sudbury Igneous Complex, Sudbury structure. Economic Geology and the Bulletin of the Society of Economic Geologists, **97**: 1541-1562.

Bailey, J., Lafrance, B., McDonald, A.M., Fedorowich, J.S., Kamo, S., and Archibald, D. A. 2004. Mazatzal Labradorian-age (1.7-1.6 Ga) ductile deformation of the South Range Sudbury impact structure at the Thayer Lindsley mine, Ontario. Canadian Journal of Earth Sciences, **41**: 1491-1505.

Boerner, D.E., Milkereit, B., and Naldrett, A.J. 1994. Introduction to the special session on Lithoprobe Sudbury Project. Geophysical Research Letters, **21**: 943-946.

Boerner, D.E., Milkereit, B. 1999. Structural evolution of the Sudbury Impact structure in the light of seismic reflection data. *In* Impact cratering and Planetary Evolution II, Boulder Colorado. *Edited by* B. Dressler, and V.L. Sharpton. Geological Society of America, Special Paper 339, pp. 419-430.

Boerner, D.E., Milkereit, B. and Davidson, A. 2000. Geoscience impact: a synthesis of studies of the Sudbury structure. Canadian Journal of Earth Sciences, **37**: 477-501.

Brocoum, S.J., and Dalziel, I.W.D. 1974. The Sudbury Basin, the Southern Province, the Grenville Front, and the Penokean Orogeny. Geological Society of America Bulletin, **85**: 1571–1580.

Butler, K.L. 1984. Lineament analysis of the Sudbury multi-ring impact structure. *In* Large Meteorite Impacts and Planetary Evolution, Geological Society of America, Special Paper 293, pp. 319-329.

Card, K.D. 1994. Geology of the Levack gneiss complex, the northern footwall of the Sudbury structure, Ontario. *In* Current research 119-C, Geological Survey of Canada, pp. 269-278.

Card, K.D., and Jackson, S.L. 1995. Tectonics and Metallogeny of the Early Proterozoic Huronian foldbelt and the Sudbury structure of the Canadian Shield, Field Trip Guide Book, Geological Survey of Canada, Open File 3139.

Cowan, E.J., and Schwerdtner, W.M. 1994. Fold origin of the Sudbury Basin. *In* Proceeding of the Sudbury-Noril'sk symposium. *Edited by* P.C. Ligthfoot and A. Naldrett. Ontario Geological Survey, Canada, Special Volume 5, pp. 45 – 55.

Deutsch, A., Grieve, R.A.F., Avermann, M., Bischoff, L., Brockmeyer, B., Buhl, D., Lakoomy, R., Muller-Mohr, R., Ostermann, M., and Stoffer, D. 1995. The Sudbury structure (Ontario, Canada): a tectonically multi ring impact Basin. Geologische Rundschau, **84**: 697-709.

Dickin, A.P., Nguyen, T., and Crocket, J. H. 1999. Isotopic evidence for a single impact melt origin of the Sudbury Igneous Complex. Geological Society of America, Special Paper 339: 361-372.

Dreuse, R., Doman, D., Santimano, T., and Ulrich, R. 2010. Crater floor topography and impact melt sheet geometry of the Sudbury impact structure, Canada. Terra Nova, **22**: 463-469.

Fedorowich, J.S., Parrish, R.R., and Sager-Kinsman, A. 2006. U-Pb dating of a diabase dike resolves the problem of mutually crosscutting relationships within the Fraser-Strathcona Deep Copper vein system, Sudbury Basin. Economic Geology, **101**: 1595–1603.

Fountain, D.M., Boundy, T.M, Austrheim, H., and Rey, P. 1994. Eclogite- facies shear zones-deep crustal reflectors? Tectonophysics, **232**: 411-424.

Green A., and 10 others. 1990. Origin of deep crustal reflections: Seismic profiling across high-grade metamorphic terranes in Canada. Tectonophysics, **173**: 627-638.

Grieve, R.A.F., Stoffler, D., and Deutsch, A. 1991. The Sudbury structure: controversial and misunderstood? Journal of Geophysical Research, **96**: 22753-22764.

Gupta, V.K., Grant, F.S., and Card, K.D. 1984. Gravity and magnetic characteristics of the Sudbury structure. *In* The Geology and Ore Deposits of the Sudbury structure: Ontario Geological Survey. *Edited by* E.G. Pye, A. J. Naldrett and P. E. Giblin. Special Volume 1, pp. 381-410.

Hearst, R.B., Morris, W.A., and Thomas, M.D. 1994. Magnetic interpretation along the Sudbury structure Lithoprobe Transect. *In* Proceedings of the Sudbury-Noril'sk Symposium Ontario Geological Survey. *Edited by* P.C. Lightfoot, and A. J. Naldrett. Special Volume 5, pp. 33-43.

Hearst, R.B., and Morris, W.A. 2001. Regional gravity setting of the Sudbury structure. Geophysics, **66**: 1680-1690.

Ivanov B.A., and Deutsch, A. 1999. Sudbury impact event: cratering mechanism and thermal history. *In* Large Meteorite Impact and Planetary Evolution II, Geological Society of America, Special Paper 339, pp 389- 398.

King, A. 2007. Review of geophysical technology for Ni-Cu-PGE deposits. *In* Proceedings of Exploration'07, Fifth Decennial International Conference on Geophysics and Geochemical Exploration for Minerals. *Edited by* B. Milkereit. pp. 647-665.

Krogh, T.E., Davis, D.W., and Corfu, F. 1984. Precise U-Pb zircon and baddeleyite ages for the Sudbury area. *In* The Geology and Ore Deposit of the Sudbury structure, Ontario Geological Survey, Special Volume 1, pp. 431-446.

Lafrance, B., and Kamber, B.S. 2010. Geochemical and microstructural evidence for in situ formation of pseudotachylitic Sudbury breccia by shock-induced compression and cataclasis. Precambrian Research, **180**: 237-250.

Lightfoot, P.C., Keays, R.R., and Doherty, W. 2001. Chemical evolution and origin of nickel sulfide mineralization in the Sudbury igneous complex, Ontario, Canada. Economic Geology, **96**: 1855-1875.

Long, D.G.F. 2004. The tectonostatigraphic evolution of the Huronian basement and the subsequent Basin fill: geological constraints on impact models of the Sudbury Event. Precambrian Research, **129**: 203-223.

Long, D.G.F., and Lloyd, T.R. 1983, Placer gold potential of basal Huronian of the Elliot Lake Group in the Sudbury Area, Ontario. Ontario Geological Survey Miscellaneous Paper **126**: 256-258.

McGrath, P.H., and Broome, H. J. 1994. A gravity model of the Sudbury structure along the Lithoprobe seismic line. Geophysical Research Letters, **21**: 955-958.

Meldrum, A., Abdel-Rahman, A. M., Martin, R.F., and Wodicka, N. 1997. The nature, age and petrogenesis of the Cartier Batholith, northern flank of the Sudbury structure, Ontario, Canada. Precambrian Research, **82**: 265-285.

Milkereit, B., Green, A., and Sudbury working group 1992. Deep geometry of the Sudbury structure from seismic reflection profiling. Geology, **20**: 807-811.

Milkereit, B., Green, A., Wu, J., White, D., and Adam, E. 1994. Integrated seismic and borehole geophysical study of the Sudbury igneous complex. *In* Lithoprobe Sudbury Project. *Edited by* D.E. Boerner, B. Milkereit, and A.J. Naldrett. Geophysical Research Letters,
21: 931-934.

Morris, W.A. 1981. Intrusive and tectonic history of the Sudbury micropegmatite; the evidence from paleomagnetism. Economic Geology, **76**: 791-804.

Mukwakwami, J., Lafrance, B., Lesher, C.M., Tinkham, D.K., Rayner, N.M., Ames, D.E. 2014. Deformation, metamorphism and mobilisation of Ni-Cu-PGE sulfides ores at Garson Mine, Sudbury. Mineralium Deposita, **49**: 175-198.

Olaniyan, O.F., Smith R.S., and Morris, W.M. 2013. Qualitative interpretation of the Sudbury structure. Interpretation, **1**: 25-43.

Peredery, W.V. 1972. The origin of rocks at the base of the Onaping Formation, Sudbury, Ontario. Ph.D. thesis, University of Toronto, Canada.

Pye, E.G., Naldrett, A.J., and Giblin, P.G. 1984. The Geology and Ore Deposits of the Sudbury structure. Ontario Geological Survey, Special Volume 1: 603p.

Raharimahefa, T., Lafrance, B., and Tinkham, D.K. (Submitted). Structural, metamorphic and U-Pb geochronological evolution of the Southern Province, Sudbury, Canada. Precambrian Research.

Riller, U., and Schwerdtner, W.M. 1997. Mid-crustal deformation of the southern flank of the Sudbury Basin, central Ontario, Canada. Geological Society of America Bulletin, **109**: 841-854.

Rousell, D.H. 1984b. Onwatin and Chelmsford formations. *In* the Geology and Ore Deposits of the Sudbury structure. Ontario Geological Survey, Special volume 1: 211-218.

Shanks, W.S., and Schwerdtner, W.M. 1991. Structural analysis of the central and southwestern Sudbury structure, Southern Province, Canadian Shield. Canadian Journal of Earth Sciences, **28**: 411-430.

Spray, J.G., Butler, H.R., and Thompson, L.M. 2004. Tectonic influences on the morphometry of the Sudbury impact Structure: implication for terrestrial cratering and modeling. Meteoritics and Planetary Science, **39**: 287-301.

Spray, J.G., and Thompson, L.M. 1995. Friction melt distribution in a multi-ring impact Basin. Nature, **373**: 130-132.

Stockwell, C.H. 1982. Proposal for the time classification and correlation of Precambrian rocks and events in Canada and adjacent areas of the Canadian Shield. Geological Survey of Canada, Special Paper, 80-19, 135p.

Thompson, L.M., and Spray, J.G. 1994. Pseudotachylitic rock distribution and genesis within the Sudbury impact structure. *In* Large Meteorite Impacts and Planetary Evolution. *Edited by* B.O. Dressler, R.A.F. Grieve, and V.L. Sharpton. Geological Society of America, Special Paper 293, pp. 275-288.

Tschirhart, P., and Morris, W.A. 2012. Grenville age deformation of the Sudbury impact structure: evidence from the magnetic modeling of the Sudbury diabase dykes swarm. Terra Nova, **24**: 213-220.

Wu, J., Milkereit, B., and Boerner, D. 1995. Seismic Imaging of the enigmatic Sudbury structure. Journal of Geophysical Research, **100**: 4117-4130.

Zolnai, A.I., Price, R.A., and Helmstaedt, H. 1984. Regional Cross section of the Southern Province adjacent to Lake Huron, Ontario: implications for the tectonic significance of the Murray fault zone. Canadian Journal of Earth Sciences, **21**: 447-456.

CHAPTER 4: Developing a geological 3-D model of the Sudbury structure in Geomodeller

4.1 Abstract

Understanding the subsurface geology of the Sudbury structure requires predicting its geological and structural setting everywhere: data from surface and shallow subsurface points must be extrapolated to the deeper subsurface. Multiple deformational episodes, together with limited subsurface geological and geophysical information in most parts of the Sudbury structure, make this task especially difficult. Mapped bedrock geological contacts and six geological sections interpreted from 2.5-D modelling of high-resolution airborne magnetic and gravity data were used to construct a 3-D geological model of the Sudbury structure using the 3-D Geomodeller software. Unlike other CAD-based 3-D software, Geomodeller utilizes the field interpolator method, whereby contacts of rock units are assumed to be equipotential surfaces, wheras orientation data determine the gradient and direction of the surfaces. Contacts and orientation variables are co-kriged to generate three-dimensional continuous surfaces for each geological unit. The derived 3-D geological model is qualitatively evaluated by forward computing of the predicted gravity response at 1 m above topography and by comparing this response to the measured gravity field. Large scale structures within the Onaping Formation and Archean basement, which overlie and underlie the Sudbury Igneous Complex (SIC) respectively, are not the cause of the linear gravity high in the centre of the Sudbury structure. We suggest that the deformation of the initial circular SIC may have commenced under the Sudbury Basin due to the reversal of the normal faults related to the Huronian rift system during the Penokean orogeny . This new interpretation is consistent with the magnetic and gravity data and honours most of the significant seismic reflectors in the Lithoprobe section.

4.2 Introduction

Exploration and mining of nickel and copper in offset dikes and embayments at the base of the Sudbury Igneous Complex (SIC) have been on-going for more than a century, with the deepest producing mine now at a depth of about 2 km. Exploration for ore bodies close to surface is gradually becoming less rewarding and more difficult. High-grade sulfide mineralisation is indubitably present at greater depths, where it is likely controlled by pre-existing and syn-impact structures and impact-brecciated footwall rocks. However, exploration beyond depths of 500 m is very challenging as few geophysical exploration methods can see that deep. Seismic surveys and borehole geophysical tools in deep boreholes could be used to detect ore zones, but these techniques are very expensive (Polzer, 2000; Milkereit et al., 1992)

Recent advances in 3-D modeling, such as GOCAD, Geomodeller, and Encom Model Vision and inversion codes such as the University British Colombia (UBC) inversion codes, to mention a few, have enhanced the capability to develop an intuitive model that projects the known 2-D surface geological information to depth, or to develop a subsurface physical property distribution map that is consistent with the geophysical data. These advancements, together with seismic and potential field datasets, have been incorporated in the subsurface bedrock investigation of large impact structures around the world, such as the Chicxulub structure in Mexico and the Vredefort dome in South Africa (Veermeesch and Morgan, 2008; Galdeno et al., 2008). The Sudbury structure, first proposed by Dietz (1964) and now broadly accepted as an impact structure (Pye et al., 1984), has been largely eroded leaving only relics of an interpreted central peak-ring crater (Deutsch et al., 1995; Spray et al. 2004), buried under a thick pile of sedimentary rocks of the Whitewater Group. A better understanding of the subsurface geology at depth using new 3-D modeling and inversion codes will further assist in the prediction of pre-existing structures that

might act as controls or traps for mineralization, thereby defining deeper prospective zones for future exploration.

A Lithoprobe seismic transect was completed across the Sudbury structure in 1992. Two seismic lines, Lines 40 and 41, were merged to provide a full section across the SIC (Milkereit et al., 1992). Interpretations of the section differ because some reflectors were ill-defined due to seismic noise, a lack of impedance contrast between units, and their sub vertical dips (Milkereit et al 1992; Card and Jackson, 1995; Wu et al.,1995; Olaniyan et al., 2013b). The interpreted subsurface geometry of the merged Lithoprobe section has been used to further constrain magnetic and gravity sections across the SIC (Hearst et al., 1994; McGrath and Broome., 1994). Olaniyan et al. (2013b) highlighted the major challenges in the merging of these two lines as modelling along an east-west line shows changes in depth and thickness of lithological units and in the spatial location of the SIC-footwall contact.

Past work (Gupta et al., 1994; Hearst et al., 1994; McGrath and Broome., 1994) and recent qualitative geophysical interpretation of high-resolution geophysical data (Olaniyan et al., 2013a) have not provided an adequate explanation of some extensive geophysical anomalies observed within the SIC (Figures 4.1a and 4.2b). These include i) the abrupt discontinuity of the high magnetic intensity in the North Range around the Sandcherry fault, ii) the low magnetic intensity zone that extends from the North Range to the South Range at their junction with the East Range, and iii) the linear gravity high observed in the center of the Sudbury structure. The latter trends east-southeast from the western part of the North Range to the south part of the East Range. Gupta et al. (1984) investigated this gravity high and concluded that it is not related to the any of the SIC rocks, but is more likely due to deeper mafic intrusions. However, their study did not

consider the possibility of northward-directed thrusting and folding at the base of the SIC (Olaniyan et al., 2013b).

Explaining these anomalies requires understanding the deep subsurface geological architecture of the Sudbury structure. In this study, a 3-D geological model is constructed from six interpreted sections inferred from 2.5-D modelling of high-resolution airborne gravity and magnetic NNW profiles including two modelled by Olaniyan et al. (2013b), and an additional ENE profile across the SIC.

4.3 Geophysical setting of the Sudbury structure

The Sudbury structure straddles the Archean Superior craton and the overlying Southern Province in Ontario, Canada. It comprises i) the Sudbury Igneous Complex (SIC) – a differentiated igneous complex consisting, from bottom to top, of sublayer, norite, quartz gabbro and granophyre; ii) an overlying 2900 m thick sedimentary and breccia sequence of the Whitewater Group comprising from bottom to top the Onaping, Onwatin, and Chelmsford Formations; iii) the impact-brecciated footwall rocks below the SIC. A more detailed description of the geological setting of the Sudbury structure has been summarized in previous papers by Pye et al (1984); Dressler (1984); Naldrett et al. (1970); and Rousell et al. (1984); Spray et al. (2004); Riller 2005; Ames and Farrow (2007) and the references therein.

The SIC has an elliptical shape with a long axis of 60 km and a short axis of 28 km. Several magnetic and gravity anomalies are associated with the rim of the SIC (Figure 4.1a and 4.1b). On a regional scale, these elliptical geophysical anomalies are superimposed on a broader geophysical response of about 350 km in length, which extends from Elliot Lake to the west, through Sudbury, then to Englehart to the east (Gupta et al., 1984). This regional anomaly is

interpreted to be related to a paleo-continental margin of the Archean Superior Province overlain by deformed and metamorphosed Huronian supracrustal rocks of the Southern Province. There is a zone of high magnetic intensity about 10 km NE of the SIC which is also related to the Superior-Southern Province boundary, but may also be enhanced by banded iron formation. Other sources of high magnetic intensity in the Sudbury structure include the basement Levack Gneiss Complex in the North Range, SIC norite and quartz gabbro and younger NE trending olivine diabase dykes. The SIC's norite and quartz gabbro layers are relatively dense and have an average density of 2.81 g/cm^3 and 2.88g/cm^3 (Gupta et al.,1994; McGrath and Broome, 1994). These rocks together with the dense Levack Gneiss Complex and the sulfide-bearing sublayer contribute to the local elliptical gravity high around the rim of the SIC.

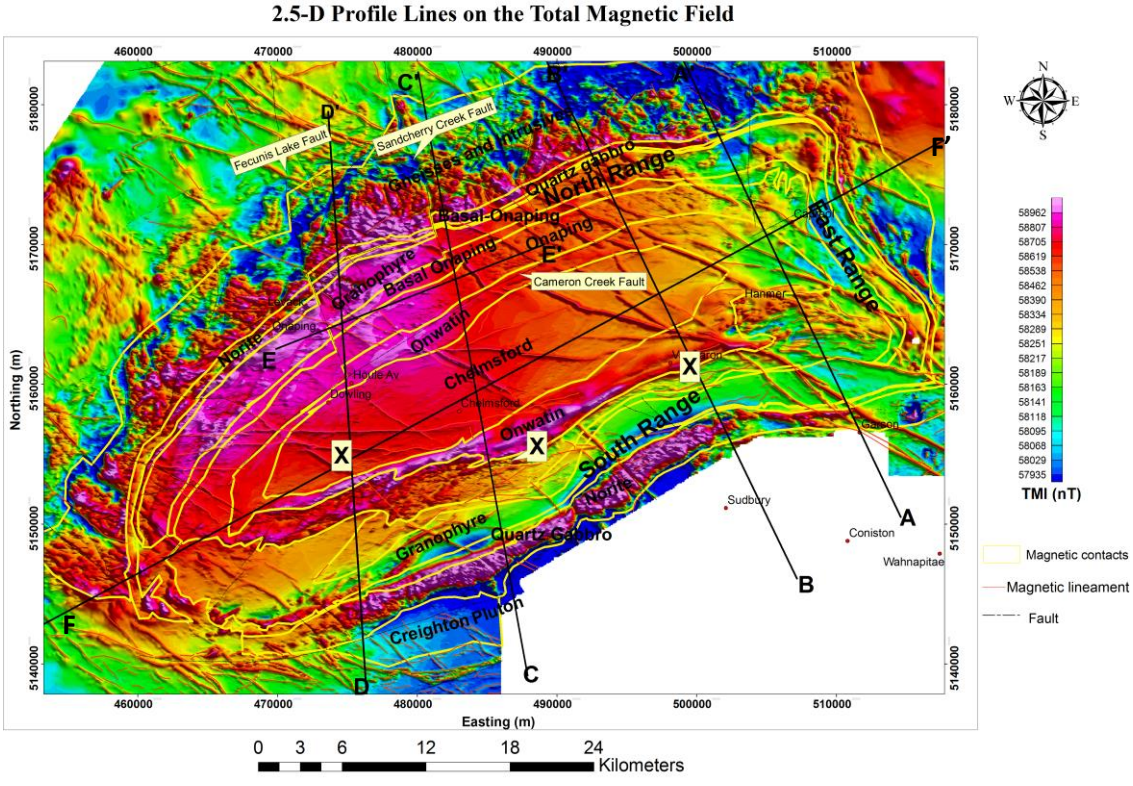

(A)

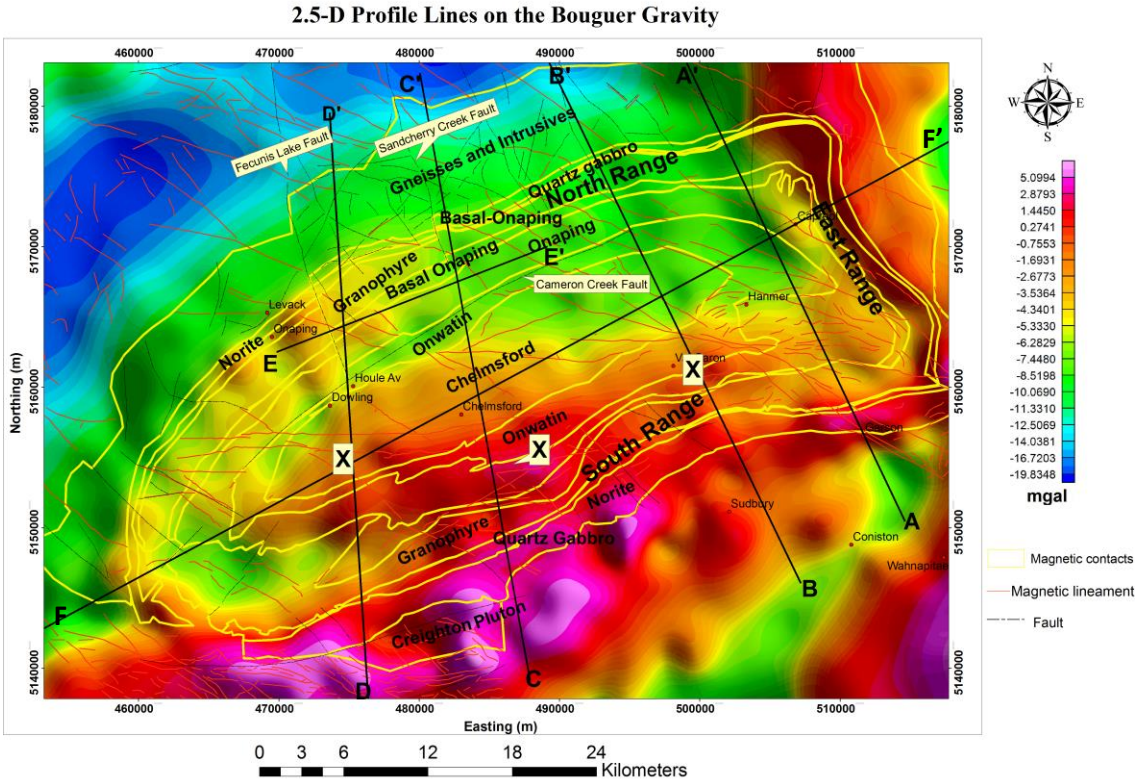

(B)

Figure 4.1: (a) Total magnetic intensity and (b) Bouguer gravity fields of the Sudbury structure showing the high gravity and magnetic responses delineating the elliptical rim of the SIC and location of sections A through F. A linear gravity high trend extending from the Sudbury Basin to the East Range is marked XXX.

4.4 Outline of methodology

4.4.1 Two and half- dimensional modelling and assumptions

Olaniyan et al. (2013b) modelled one NNW profile and one ENE profile. In this paper, we model three additional NNW profiles and one additional ENE profile using the same high-resolution airborne geophysical datasets. We assume that the seismically delineated south-dipping topography of the Archean basement rocks from the Lithoprobe section (Milkereit et al.,

1992) is continuous under the SIC, and is essentially replicated on all the sections. Vale's two-dimensional geological sections that show their interpretation of the base of the different rock units of the Sudbury structure along the selected sections were used to constrain the subsurface geometry between 520 m and 5000 m depth Figure (4.2a– d). Vale's geological section is well constrained by borehole data up to 2 km depth, after which geological contact and structures were projected further down to about 5 km supported by geological data. Information presented below 2 km in the geological section is treated as an interpretative constraint with a lower degree of confidence during the modelling and was not strictly adhere too.

The continuity of the linear gravity high under the Sudbury basin into the eastern part of the South Range could imply that the source of anomaly also extends likewise to the east. To investigate this assertion, the interpreted north-verging fold at the basal part of the SIC in the South Range is modelled in all the NNW profiles. No numerical filtering or regional-residual separation is applied to the measured geophysical dataset because the deeper geological setting of the Sudbury structure is interpreted from the longer wavelength responses. The modelling is done using the GMSYS software.

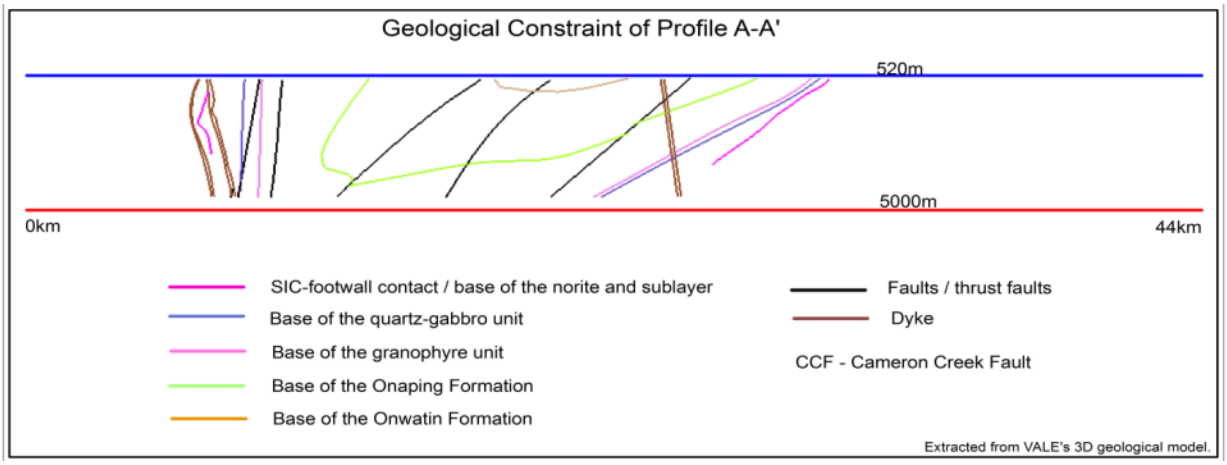

Figure 4.2a: Geological section of the profile A-A' extracted from the Vale's 3-D geological model. The various coloured lines indicate the approximate interpreted contacts of the different rock units of the Sudbury structure based on drilled holes and other geological data, black south-dipping lines are faults, while the brown double lines are dykes. SIC rocks in the South Range were overturned after the thrusting.

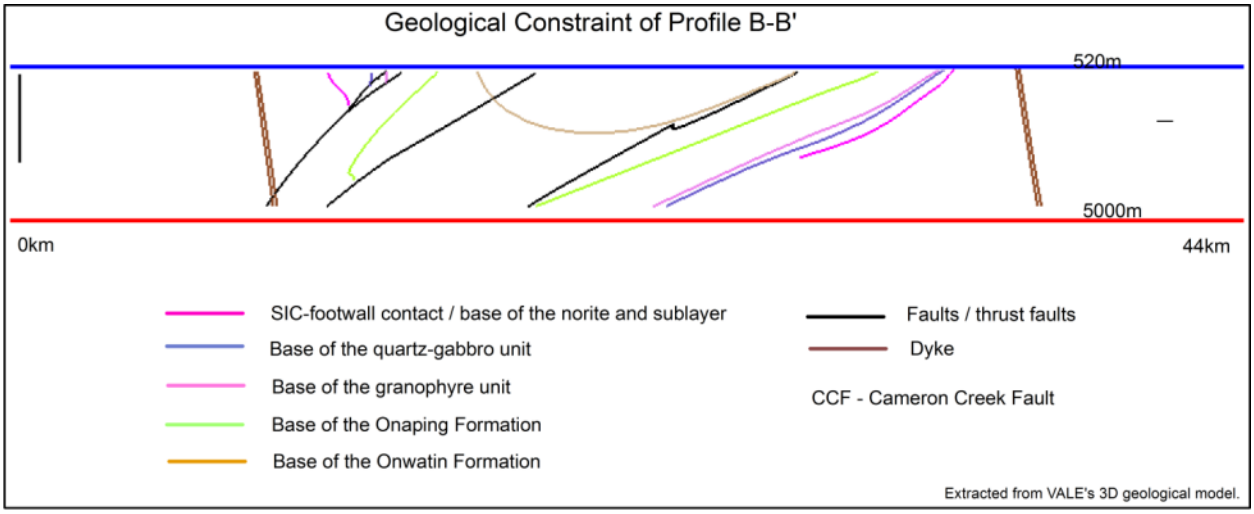

Figure 4.2b: Geological section of the profile B-B' extracted from the Vale's 3-D geological model. The various coloured lines indicate the approximate interpreted contacts of the different

rock units of the Sudbury structure based on drilled holes and other geological data, black south-dipping lines are faults, while the brown double lines are dykes.

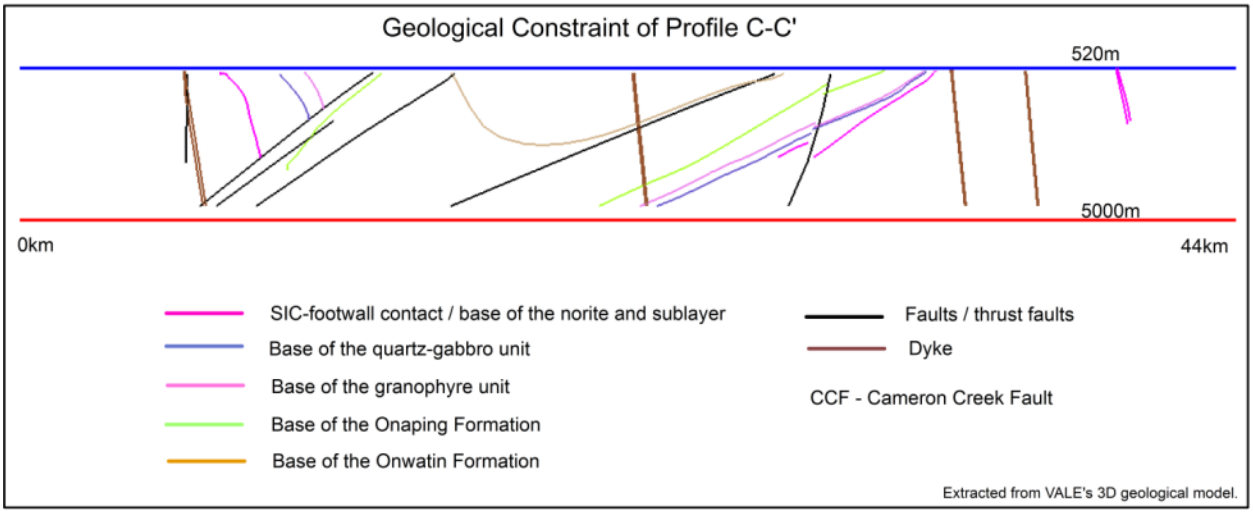

Figure 4.2c: Geological section of the profile C-C' extracted from the Vale's 3-D geological model. The various coloured lines indicate the approximate interpreted contacts of the different rock units of the Sudbury structure based on drilled holes and other geological data, black south-dipping lines are faults, while the brown double lines are dykes.

The magnetic field strength data reflects the spatial distribution of magnetic minerals: typically magnetite and/or pyrrhotite in the source rock. This magnetic field strength can be interpreted to estimate the contact locations, depth and orientation of the source body. However, alteration, mineralization and deformational events tend to either create or destroy magnetic minerals in the rock, introducing complexities into the interpretation process. This can be a disadvantage, but it can also be used to map alteration zones. The gravity field on the other hand is indicative of the distribution of the density and volumetric distribution of rock in the subsurface. The density of a rock unit appears to be relatively more consistent and less complicated than magnetic

susceptibility, although it tends to increase with depth due to increased pressure from burial and subsequent closures of pores especially in the sedimentary successions. Simultaneous interpretation of magnetic and gravity data along the selected profiles in GMSYS aid in interpretations of the geometrical configuration of lithological units, faults orientations, dykes and shear zones of the Sudbury structure. The 2.5-D sections that formed the basis for the modelling are discussed below.

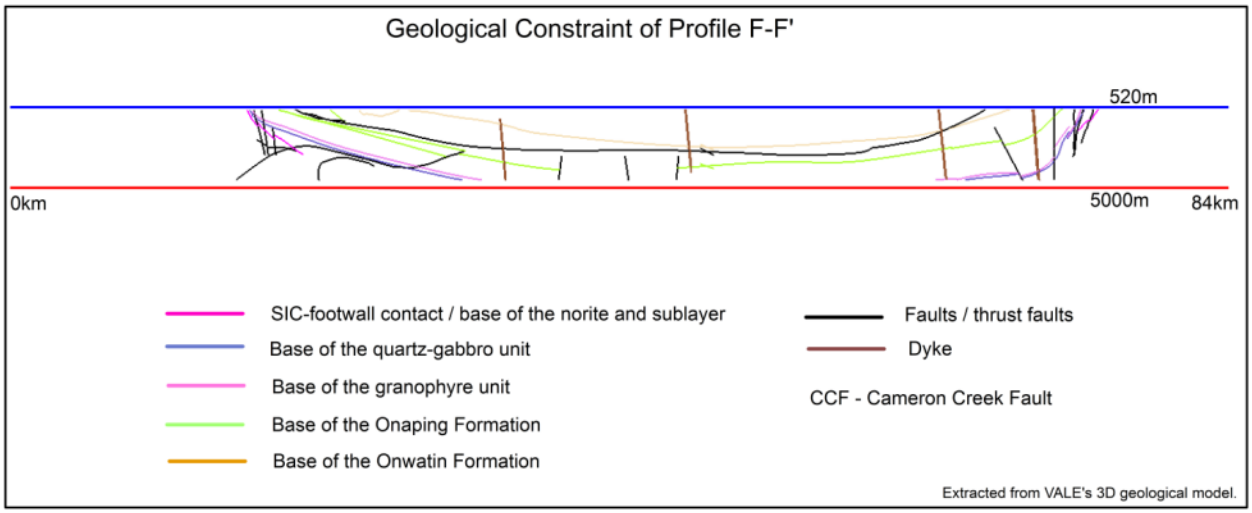

Figure 4.2d: Longitudinal geological section along profile F-F' extracted from the Vale's 3-D geological model. The various coloured lines indicate the approximate interpreted contacts of the different rock units of the Sudbury structure based on drilled holes and other geological data, black lines are faults, while the brown double lines are dykes.

4.4.2 Three-dimensional geological modelling

When there is limited subsurface geological data such as borehole logs and seismic data, a representation of the subsurface geometry can be approximated from potential field data, which is a function of the 3-D distribution of the source (Lane and Guillen, 2005). Magnetic and gravity

sources are interpreted along the 2.5-D sections and then the latter are interpolated and extrapolated to construct an initial 3-D geological model that is broadly representative of the subsurface geometry. This 3-D geological model, generated directly from observed field measurements, can be revised as more geological data becomes available and quickly recomputed in 3D Geomodeller.

A workspace covering the minimum and maximum longitude and latitude of the study area was defined to a depth of 15 km and 1 km above the topographical surface. The six interpreted 2.5-D sections were imported into Geomodeller in an image file format (.png), because of the lack of good data exchange format between GMSYS and the 3D Geomodeller. One of the difficulties of using an image file format is that an average topographic surface has to be assumed for each section, which introduced elevation issues into the 3-D forward modelling and inversion processes.

Contacts and orientation data of the geological units in both the surface geological map and the interpreted 2.5-D sections are digitised and attributed in 3D Geomodeller. This geological modelling package is developed based on potential field theory (McInerney et al., 2005) and it defines known contacts of a geological unit as an iso-potential surface, while the orientation data determine the gradient and direction of the iso-surfaces. Using a co-kriging interpolation technique (McInerney et al., 2005) and obeying the defined chrono-stratigraphic order of the geological sequence, defined contacts and orientation data in both the geological map and the 2.5-D litho-fence are interpolated to generate coherent 3-D geological curvilinear surfaces, which approximate the defined contacts of the rock units (Lajaunie et al., 1997).

4.4.3 Three-dimensional geophysical modelling

The 3-D geological model of the Sudbury structure is forward modelled to compute the predicted geophysical response on a grid. This is compared to the measured data to iteratively estimate the misfit and modify the 3-D geological model. The forward modelling algorithm assumes petrophysical attributes for each geological unit and uses the same parameters to characterize the ambient earth's magnetic field.

The forward modelling algorithm in Geomodeller requires that an observation point be defined at a given height above the topography. The 3-D volume is converted into geological voxels the size of which is selected by the user. The attributes at the centre of each voxel is assumed to be representative of the entire cell size. Therefore, the smaller the cell size, the better the apparent resolution, but more computing power and time is required. Geomodeller allows for the vertical height of the cells to be variable, so the cell resolution close to surface to a specified depth can be made finer to fit the topography better than the deeper cells, which are larger.

Our derived 3-D geological model is converted into 1000 m x 1000 m voxel sizes in the X and Y directions. In the Z direction, the cell size is 1m from surface topography to -200 m depth, while the cell size from -200 m to -15 km is a 1000 m. The predicted gravity and magnetic response are computed at 1 m above the surface. Computation of the gravity response uses published densities values (Gupta et al., 1994; McGrath and Broome, 1994; Hearst and Morris, 2001). The average density value of the Levack Gneiss Complex (2.73 g/cm^3) background was assumed to be the reference background density value.

4.5 Results and Discussion

4.5.1 Two-and-a-half dimensional geological models

The 2.5-D sections across the SIC all have an Archean basement dipping gently (~30^0) to the south (Milkereit et al., 1992). The Archean basement rocks are in steep, north-dipping, contact with the Cartier Batholith and they are overlain by Huronian supracrustal rocks to the south. NW trending olivine diabase dykes were emplaced along faults cutting across the Sudbury structure and they regionally contribute to the observed magnetic and gravity fields in the region. Figures 4.3 – 4.6 shows the interpreted geometry of the SIC along four interpreted sections A-A', B-B', C-C', and F-F' below. Profiles D-D' and E-E' have been previously described (Olaniyan et al., 2013b). The NNW profiles are all viewed facing west (South Range to the North Range), while the longitudinal profile is viewed facing north (west on the left; east on the right).

4.5.1.1 *Profile A-A'*

The most easterly profile A-A' is 44 km in length and parallel to the East Range (Figure 4.3a) where the magnetic and gravity field are generally low. This low magnetic field zone was interpreted along the longitudinal section (see F-F' below) and shows that a series of east-dipping, N-S faults parallel to the East Range has downthrown the basement and the SIC rock. On profile A-A', moving from the left to right, there is no data coverage over the Huronian sedimeantary rocks; the high magnetic and gravity response at about 8 km along the profile corresponds to the Elliot Lake mafic volcanic rocks, South Range norite and quartz gabbro, while granophyre exhibits a relatively lower magnetic and gravity responses (Figure 4.3). The rocks of the SIC and Huronian strata in this part have been overturned, and are almost vertical or steeply dipping to the south (Card, 1965). In the South Range, a local gravity high due to the

Onaping formation at about 13 km on the profile sits on a much broader and more subtle magnetic and gravity high, which terminates abruptly around 18 km by the Cameron Lake fault (CLF) along the profile. This subtle gravity high appears to have originated from a deeper source and is interpreted to be a product of thrusting of the SIC and the Elliot Lake mafic volcanic rocks along the Fairbank Lake (FLF) and the Cameron Lake faults to about 4-6 km depth.

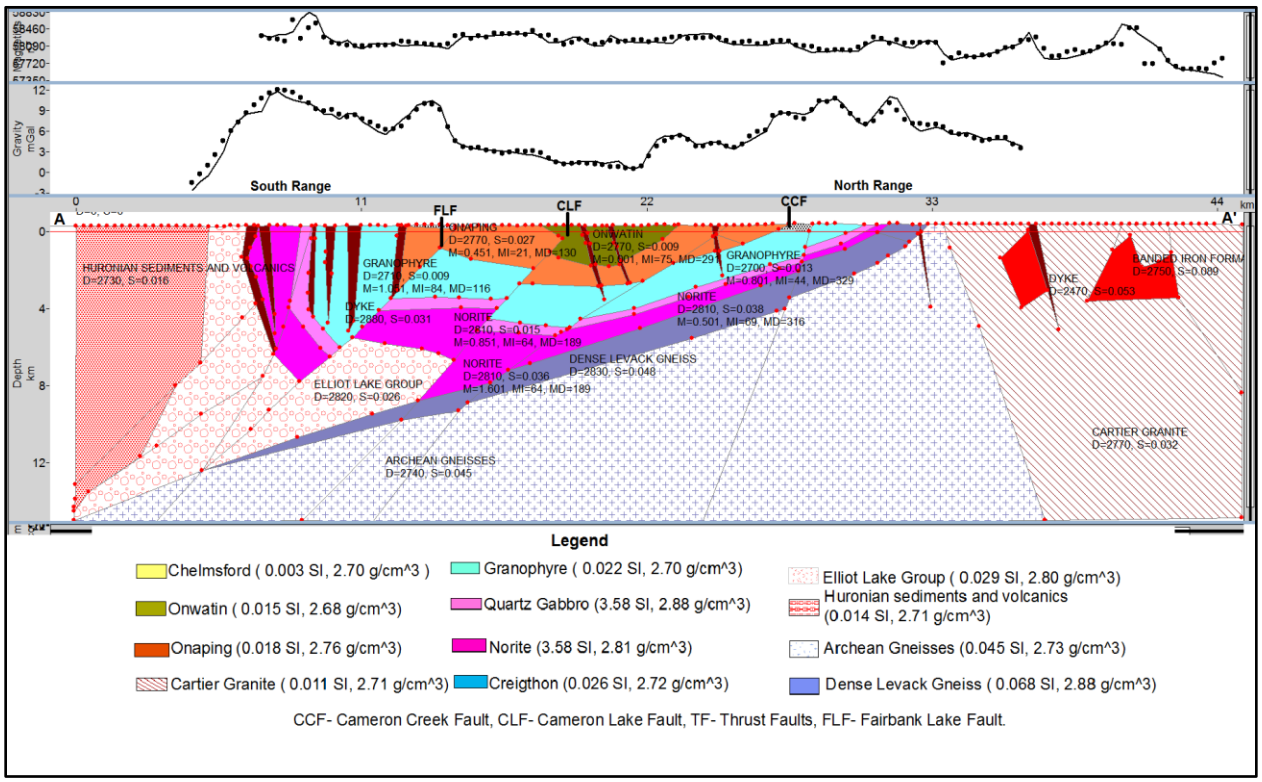

Figure 4.3: 2.5-dimensional geological model for profile A-A' (bottom) and the corresponding magnetic (top) from the compilation of Olaniyan et al., 2013a and airborne gravity data (middle) provided by Vale. The measured data is the thick dotted line and the forward model data is the thin solid line. FLF- Fairbank Lake fault, CLF- Cameron Lake Fault and CCF- Cameron Creek Fault.

At 30 km, a normal fault displaces the SIC in the North Range down to the south resulting into a discontinuity and low magnetic and gravity fields. The high gravity and fairly high magnetic field observed in the North Range to the north of this fault is due to dense Levack gneisses, norite and quartz gabbro. The contact between the gently south-dipping LGC and the Cartier Batholith dips to the North (Milkereit et al., 1992) and exhibits a sharp discontinuity in both the magnetic and gravity fields. Banded Iron formations further north near the boundary of the Cartier Batholith and Huronian supracrustal rocks exhibits relatively high magnetic signature (Figure 4.1a).

4.5.1.2 *Profile B-B'*

Profile B-B' (Figure 4.4) is 44 km long and is located 8.5 km west of profile A-A'. The magnetic field across this profile is relatively stronger than on profile A-A' and ranges from 57,910 nT to 59,152 nT with highest magnetic and gravity peaks over the SIC and dense Levack gneiss complex rocks and lowest over the Whitewater sedimentary series. At about 10 km in the South Range, a broad double peak gravity anomaly is observed, this is interpreted to be part of the thrust rocks of the SIC and the Elsie Mountain Formation that were later overturned at about 3-6 km depth. The local gravity anomaly over the Onaping at 16 km and broader subtle gravity high ascribed to the proposed SIC basal deformation on A-A' is also evident B-B' and gradually reduces till about 22 km along the profile. On profile B-B' the basal deformation is controlled by the Cameron Creek fault in the north, and Cameron Creek fault in the south. The Onwatin formation (2.68 g/cm^3) exhibits relatively low gravity field in the North Range in comparison to the South Range, which also signifies the presence of a denser and probably deeper source of the gravity anomaly in the South Range. The north-dipping contact of the Archean basement rocks and the Cartier granite shows a very steep magnetic gradient.

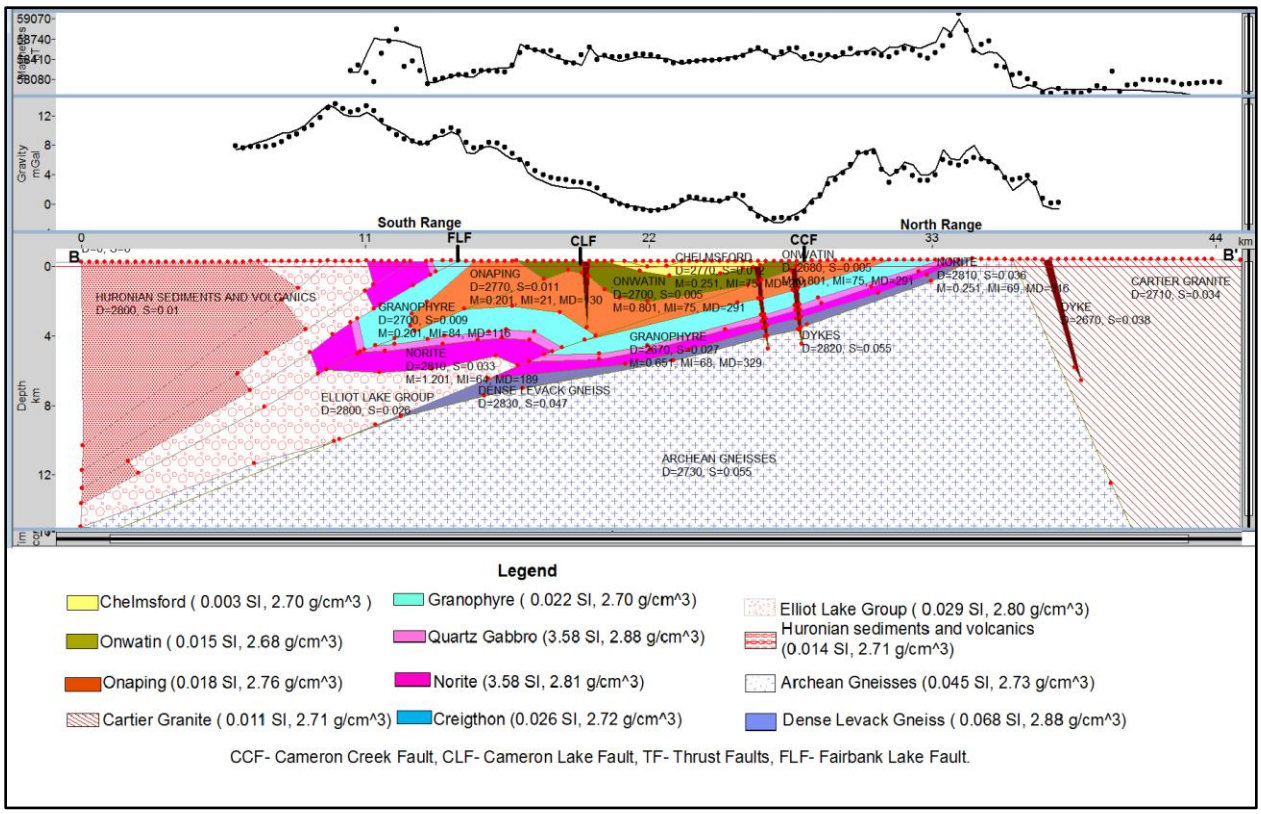

Figure 4.4: 2.5-dimensional geological model for profile B-B' (bottom) and the corresponding magnetic (top) from the compilation of Olaniyan et al., 2013a and airborne gravity data (middle) provided by Vale. The measured data is the thick dotted line and the forward model data is the thin solid line. Note the difference in the gravity response over the Onwatin formation in the South Range and North Range. FLF- Fairbank Lake fault, CLF- Cameron Lake Fault and CCF- Cameron Creek Fault.

4.5.1.3 Profile C-C'

Profile C-C' (Figure 4.5) is located 14 km west of profile BB. It is 44 km in length and from south to north transects Huronian supracrustal rocks, the Creighton pluton, the SIC, the LGC and the Cartier Batholith. The Huronian rocks and the Creighton pluton exhibit low magnetic intensity south of the high magnetic field caused by the norite and quartz gabbro. Although the

magnetic field is relatively smooth, the gravity data shows variation in the distribution of the subsurface masses.

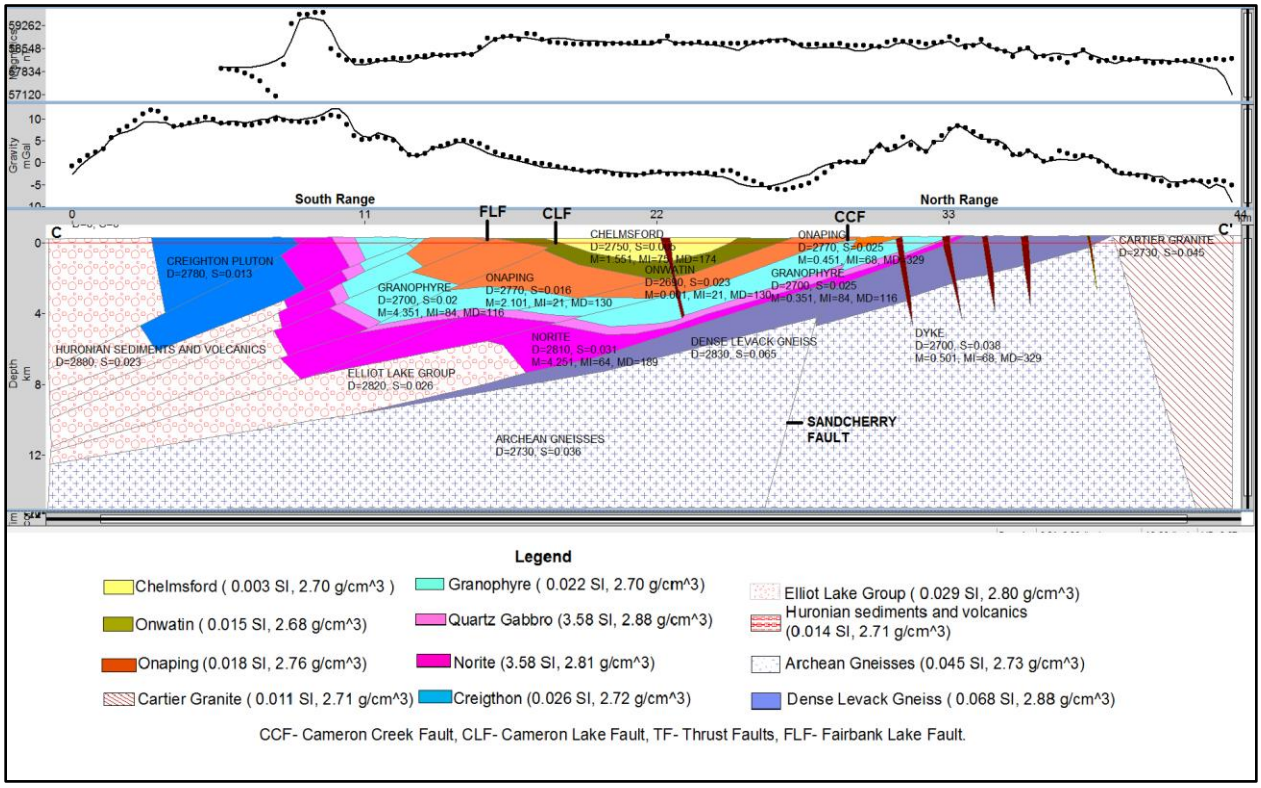

Figure 4.5: 2.5-dimensional geological model for profile C-C' (bottom) and the corresponding magnetic (top) from the compilation of Olaniyan et al., 2013a and airborne gravity data (middle) provided by Vale. The measured data is the thick dotted line and the forward model data is the thin solid line. The measured data in thick dotted line broadly fits the calculated field in the thin solid line. FLF- Fairbank Lake fault, CLF- Cameron Lake Fault and CCF- Cameron Creek Fault.

A fairly high gravity anomaly of about 10 mgal between 3 and 10 km along the section corresponds to South Range SIC, Creighton pluton and the basal Huronian mafic intrusions that occur at the footwall. The extensive high gravity observed over the Creighton Pluton can be explained by the presence of dense mafic volcanic rocks of the Elliot Lake Group. A realtively low gravity field is observed over the granophyre, while the local gravity high due to the

Onaping Formation continues from previous parallel profiles. The subtle broader gravity anomaly, which gradually fades northwards, corresponds to the location of the change in dip of the North Range as observed in the Lithoprobe seismic section (Milkereit et al., 1992). The northern extension of the Onwatin formation (0.68 g/cm^3) exhibits a very low gravity field. The high gravity field in the North Range is related to the norite-gabbro rocks, Levack gneiss as well as mafic dykes (2.70 g/cm^3) in that portion.

4.5.1.4 Profile F-F'

Profile F-F' is 84 km long and traverses the longitudinal axis of the SIC. Regionally, the measured magnetic and the gravity response are shaped like a dome, with a low response at the either ends, while the central part of the profile have a relatively high response. However there is a pronounced gravity high associated with dense levack gneiss at the west and east ends of the traverse. At this scale, the focus was to model the regional mass distribution of rocks at the subsurface and major structures such faults and dykes in-filling fault zones causing the dome shape of the measured fields, with less attention to minor lineaments along the longitudinal section. On the western flank, normal faults have displaced the south western portion of the SIC downwards. These faults are interpreted to be post-SIC and near-surface they do not affect the Archean basement (Figure 4.2d), but likely resulted into a relative low gravity field from 10 km to about 23 km along the profile due to the down throw of the SIC rocks and presence of about 100 m of overburden . Vermilion Lake, Fairbank Lake and Gordon Lake occur around this region and could have occupied the depression created by the displacement. The proposed basal deformation of the SIC by the Huronian mafic rocks occur along the profile up to about 43 km,

then verges southwards away from the profile. This part of the SIC is uplifted relative to the eastern flank and is controlled by a fault zone in-filled by a dyke. It is not clear at this point, if this in-filled fault is related to the growth faults interpreted in the North Range along the E-E' profile discussed in Olaniyan et al. (2013b). This uplifted western part of the SIC might have also contributed to the high magnetic field observed in the western half of the SIC (Figure 4.1a). The low magnetic and gravity field parallel to the East Range at around 63 km is explained by series of closely packed NS trending east-dipping normal fault system (Figure 4.6).

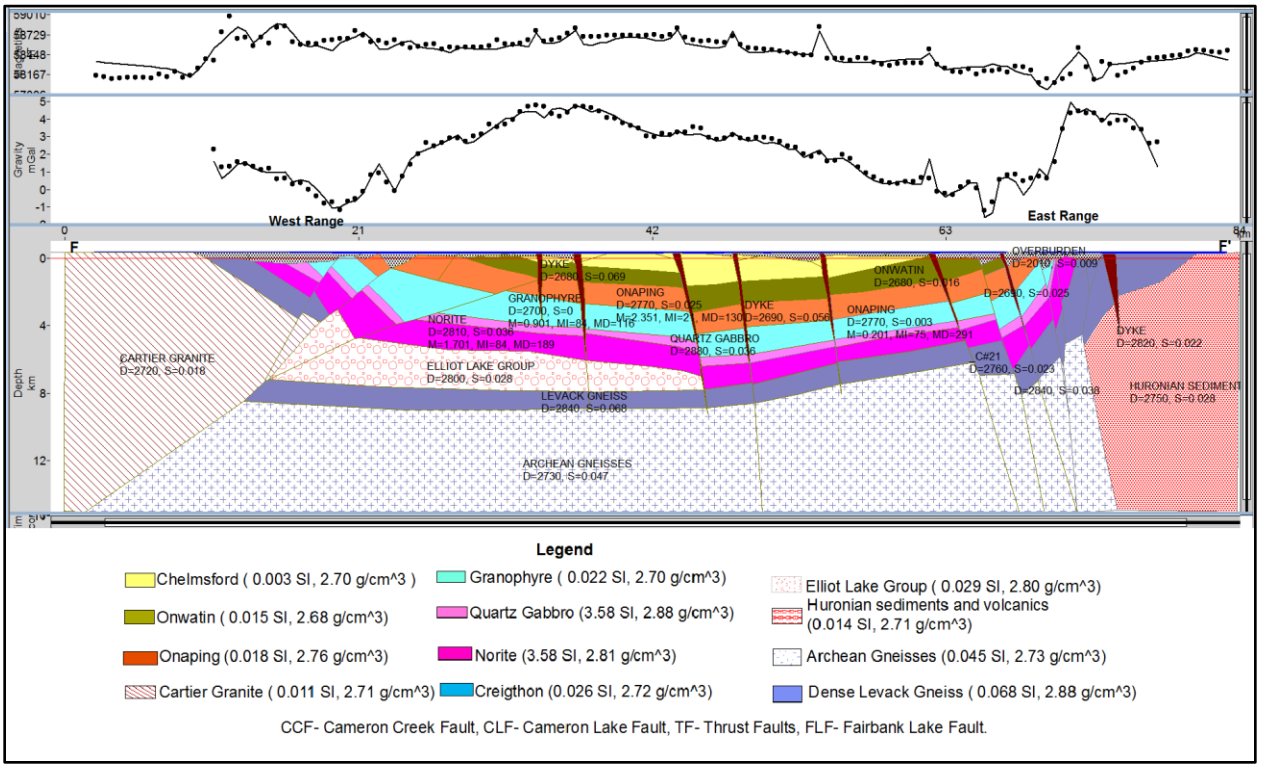

Figure 4.6: 2.5-dimensional geological interpretation along the longitudinal section F-F' (bottom) and the corresponding magnetic (top) and gravity (middle) data from the compilation of Olaniyan et al., 2013 and the airborne gravity data provided by Vale. The measured data in thick dotted line broadly forms a dome shape and have higher intensities in the western part of the SIC. The calculated field is the thin solid line.

In the gridded data (Figure 4.1a), the low magnetic field zone extends from the North Range footwall to the South Range, suggesting the pre-existence of a NNW fault / shear system in the Archean basement before the emplacement of the SIC. This basement fault must have been re-activated to deform the SIC. Rocks of the SIC, Levack Gneiss Complex, and the Archean gneisses have been down thrown to the east, allowing for about 100-150 m thick overburden cover near the East Range. This linear fault zone contains Joe Lake in the North Range and the Joe Lake mafic intrusion in the footwall. Joe Lake is elongated in shape and aligned with this NNW fault zone, so might also be structurally controlled. Ames et al. (2013) described the Joe Lake mafic intrusion fabric as penetrative and preliminary U-Pb geochronology of Joe Lake mafic intrusion also indicates that it was metamorphosed in the Archean (2657 ± 9 Ma, Ames et al., 2013). This indicates that the Joe mafic intrusion might have been localized along the NNW fault zone during the Archean, an interpretation which is consistent with the presence of the fault pre-emplacement of the SIC. Considering the geological setting and the occurrence of sulfides in the base of the Joe Lake (Watts 1997), the NNW fault zone might have controlled sulfide mineralisations associated with the SIC, therefore very prospective.

4.5.2 Three-dimensional geologically constrained model

The imported 2.5-D geological images were modified and aligned to ensure continuities among lithological units and structures in the 3-D Geomodeller software Figure 4.7 (a-b). This litho-fence diagram of the interpreted geological features in combination with the surface geology map forms the inner framework of the 3-D geological volume, from which the geology of unknown areas were inferred by extrapolation (Figure 4.8).

A

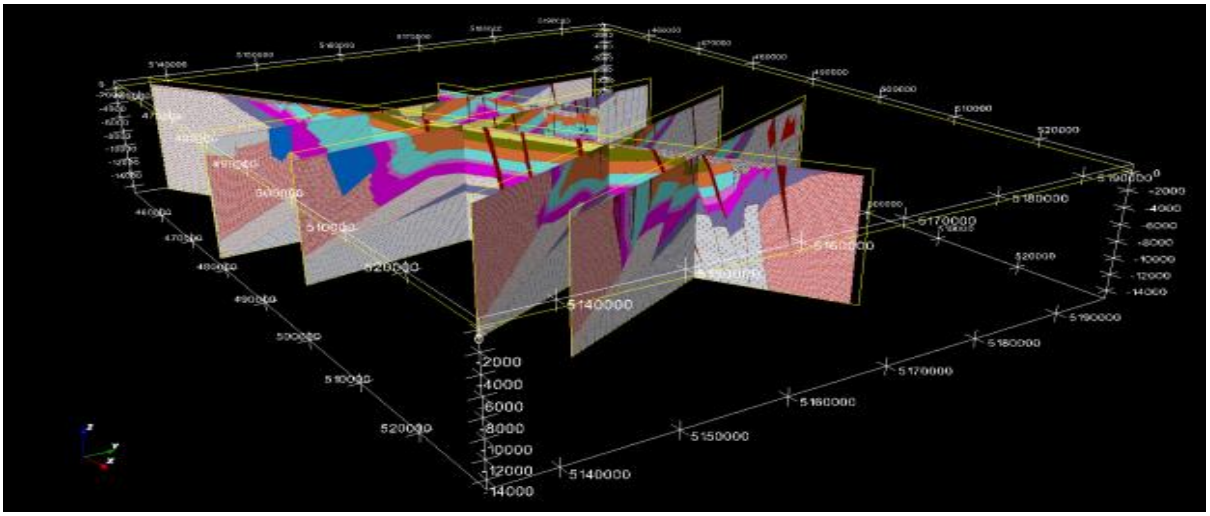

B

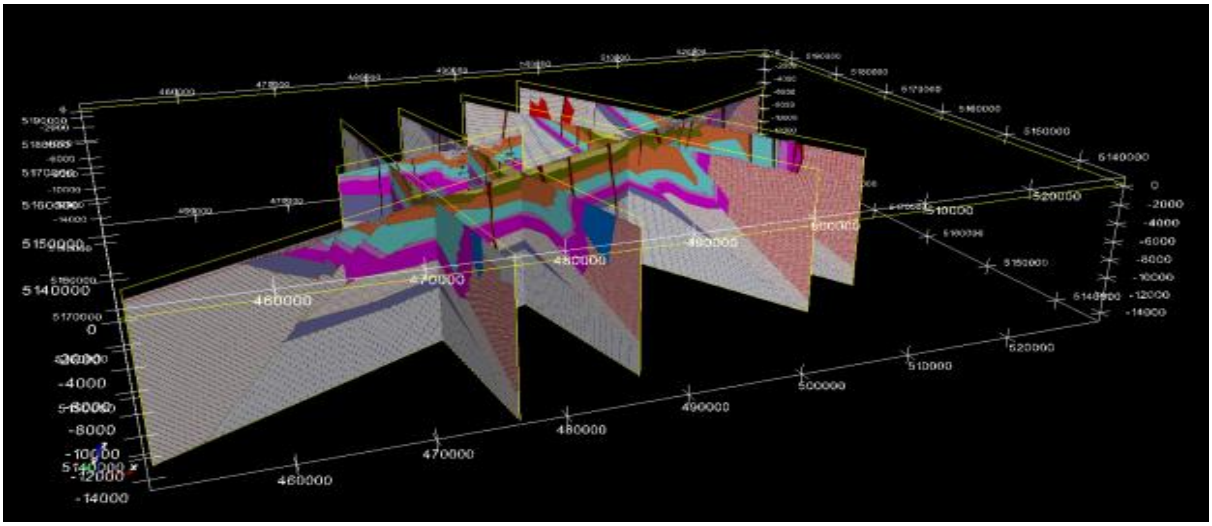

Legend

Chelmsford (0.003 SI, 2.70 g/cm^3)	Granophyre (0.022 SI, 2.70 g/cm^3)	Elliot Lake Group (0.029 SI, 2.80 g/cm^3)
Onwatin (0.015 SI, 2.68 g/cm^3)	Quartz Gabbro (3.58 SI, 2.88 g/cm^3)	Huronian sediments and volcanics (0.014 SI, 2.71 g/cm^3)
Onaping (0.018 SI, 2.76 g/cm^3)	Norite (3.58 SI, 2.81 g/cm^3)	Archean Gneisses (0.045 SI, 2.73 g/cm^3)
Cartier Granite (0.011 SI, 2.71 g/cm^3)	Creigthon (0.026 SI, 2.72 g/cm^3)	Dense Levack Gneiss (0.068 SI, 2.88 g/cm^3)

CCF- Cameron Creek Fault, CLF- Cameron Lake Fault, TF- Thrust Faults, FLF- Fairbank Lake Fault.

Figure 4.7 (a-b): Different perspectives of the litho-fence diagram that forms the framework of the 3-D geological volume. a) looking North west and b) looking north east,

The generated 3-D geological model provides insights into some of the unexplained regional geophysical anomalies within the SIC. Visual inspection of the SIC from any perspective in space is possible in this 3-D mode, making it easier to evalute the proposed hypothesis and past intepretations related to the deformation and geological setting of the SIC. At this regional scale, the resolution of the derived 3-D volume does not accommodate most of the known and interpreted fault displacements and some of the down-thrown blocks evident in the 2.5-D sections. Unconsolidated sediments that have accumulated in the depressions created by the normal faults are difficult to model as it was necessary to specify constant topography for each 2.5-D image in Geomodeller.

Regionally, the 3-D geological model illustrates that the increased thickness of the LGC in the western half appears to explain the higher magnetic and gravity fields observed in this part of the SS (Olaniyan et al. 2013b). There appears to have been some relative movement of basement rocks in the central portion of the SIC marked by a series of growth faults as expressed by gradual changes in the potential field data (Olaniyan et al. 2013b) around the Sandcherry fault in the North Range. Growth faults appear to have downthrown the basement and the SIC rocks resulting in a low gravity field around the Sandcherry fault. However, geophysical signatures of the growth fault system does not occur on the more southern longitudinal profile F-F', which suggest the faults were active in the North Range of the SIC and likely originate from a location around the Sandcherry fault. A series of converging faults mapped at surface around the Sandcherry fault may be related to this system (Ames et al, 2005). Depending on the timing of these faults, they could have acted as conduits for hydrothemal/ mineralised fluids within the Sudbury basin and perhaps the SIC (Ames and Farrow, 2007). As projected from the subsurface, the thicknesses of the SIC rocks vary between geographical areas. There is more volume of SIC

rocks at depth in the South Range compare to the North Range, likely because the South Range has undergone greater tectonic shortening (Shanks and Schwerdtner, 1991a).

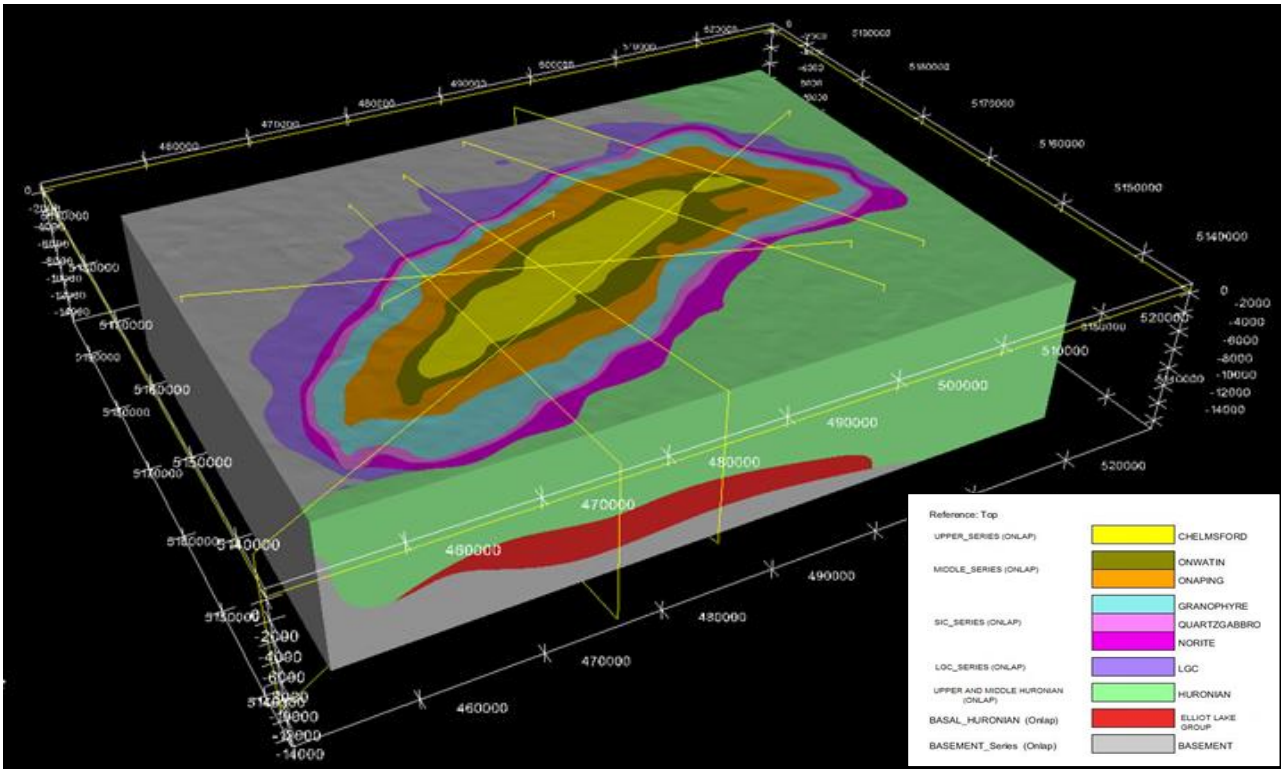

Figure 4.8a: Derived 3-dimensional geologically constrained model of the Sudbury structure that is consistent with the surface geological map, orientation data and subsurface geometry along the interpreted 2.5-D geological sections. Creighton and Muray plutons were not computed.

4.5.3 Three- dimensional forward modelling

Computation of the gravity field for the 3-D geological model allows evaluation of the applicability of the geological interpretations presented and provides additional constraints on the geological setting to reduce the misfit between the measured and the predicted fields. The high resolution measured bouguer gravity response along the selected profiles was also compared to the computed field. Although this approach was able to highlight area of misfit along the profiles, it does not provide the regional synoptic view required to assess the continuity

of geological features away from the profiles. For example, Figure 4.9 shows the broad correlation of the measured and computed gravity response along profile B-B', but it also highlight areas of misfits.

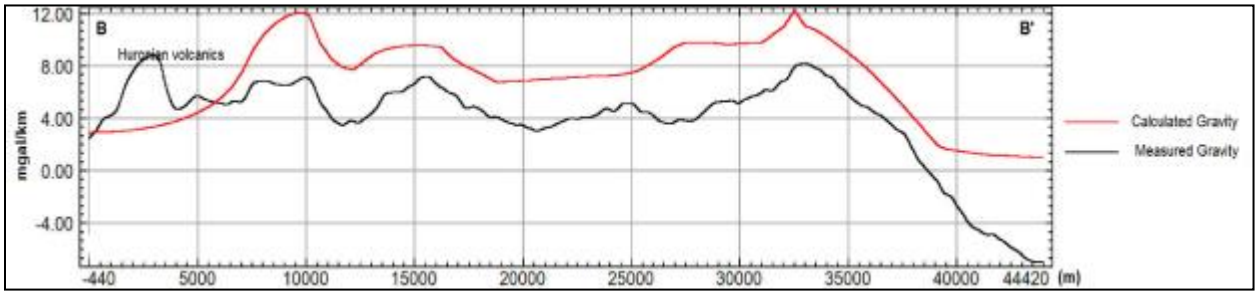

Figure 4.9: Plot of the measured bouguer versus the calculated gravity response of the 3-D geological model along profile B-B'. The calculated response is consistent with the measured gravity field but exhibit higher intensity. The measured field was bouguer corrected using 2.91 g/cm^3, which is much higher than the reference background density of 2.73 g/cm^3. Gravity high observed before 5000 m along the profile are due to mafic volcanic rocks in the Huronian sediments, which were not included in the model.

The computed gravity map (Figure 4.10) was quantitatively assessed by comparing it to the available low resolution, free-air gravity data of the Geological Survey of Canada (GCS) database (Figure 4.11). Vale's proprietary high resolution gravity grid was not used because of confidentiality restrictions. The geometry of the initial 3-D geological model and density values were iteratively adjusted and recomputed, until a predicted field broadly similar to the measured gravity field was attained.

High gravity field intensity delineates the elliptical rim of the Sudbury structure in the South Range and East Range in both the measured and the calculated gravity response. This broad response is attributed to the norite (2.81 g/cm^3), quartz gabbro (2.88 g/cm^3) and basal Huronian

tholeiitic basalt of the Elliot Lake Group (2.80 g/cm^3) and other mafic intrusions such as the Nipissing diabase and trap dykes, which were not included in our geological model. The basal mafic volcanic rocks at the base of the Huronian sequence appears to have been thrusted northwards to under the Sudbury Basin, where it is wedged beneath the SIC resulting in north-verging fold and deformation of the basal part of the SIC in the South Range. The presence of this highly dense mafic rock (2.80 g/cm^3) and relatively shallowness of the SIC rocks at the southern border of the Sudbury Basin is able to generate the linear gravity high (XXX).

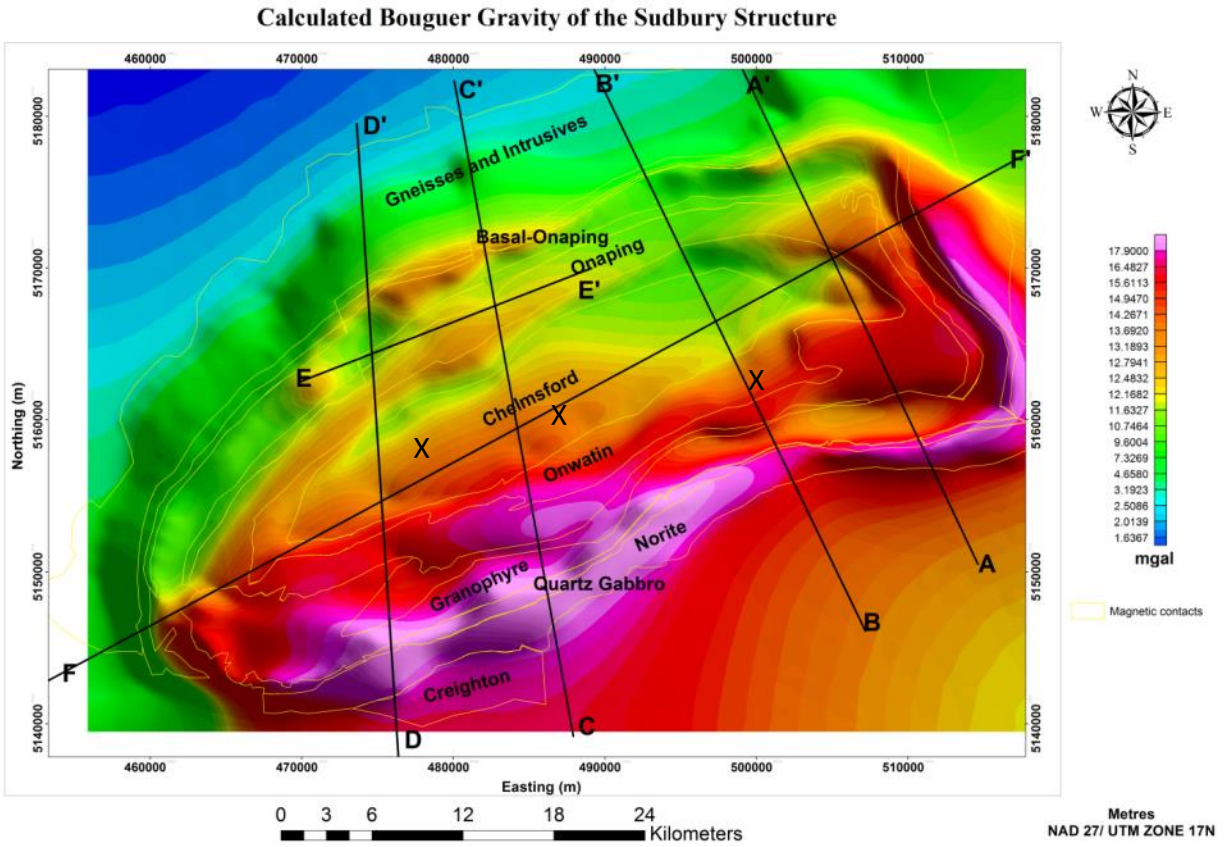

Figure 4.10: Computed gravity response of the 3-D geological model spatially computed at 1 m distance above the surface. The discontinuity of the linear gravity high feature labelled XXX across the B-B' profile is due to the misfit introduced by the chosen constant topography.

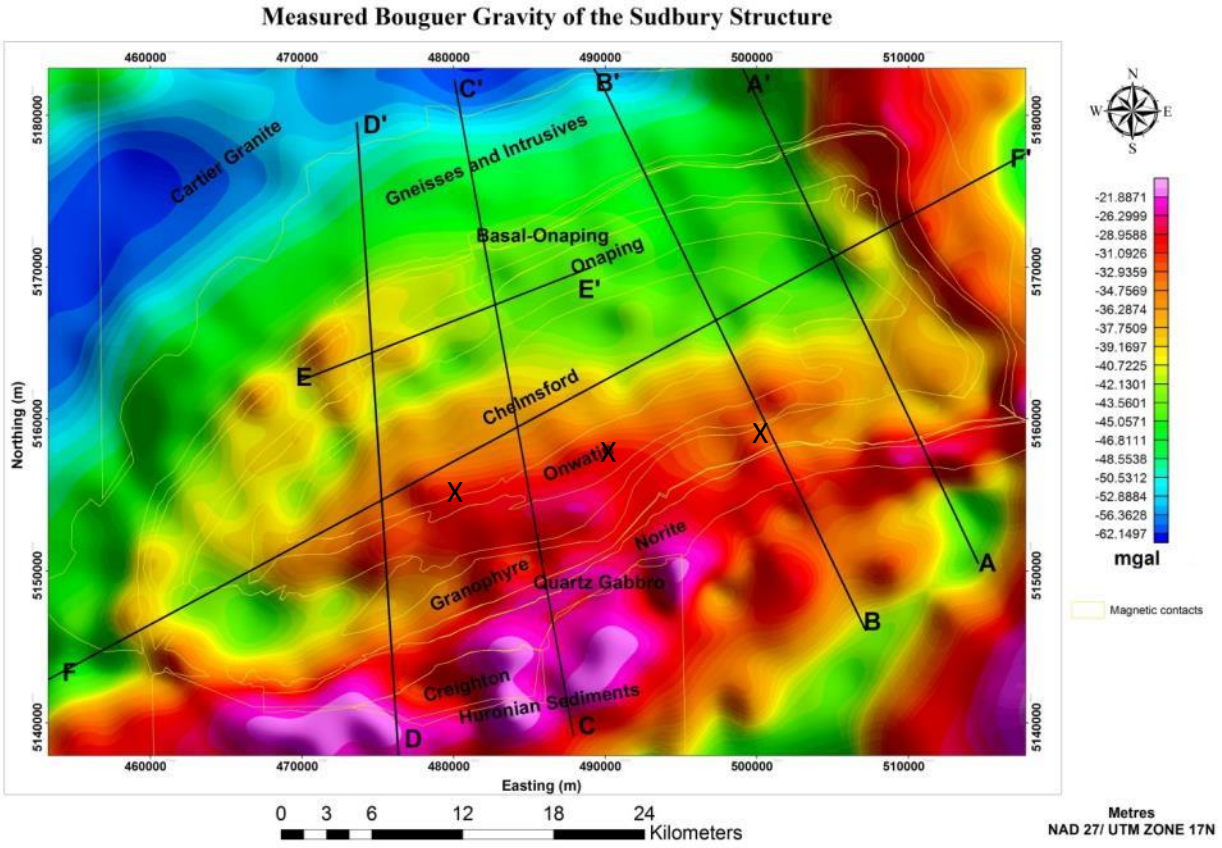

Figure 4.11: Measured Bouguer gravity anomaly of the Sudbury structure.

The western part of the North Range contains dense LGC up to 4 km in thickness, which results in a high gravity response seen in the calculated and the observed sections or profiles. A low gravity zone dominates the eastern portion of the North Range at the junction with the East Range. This zone is faulted (see Profile F-F') and hosts the Joe Lake mafic intrusion in the footwall contact. As expected, the North Range portion of the Whitewater group exhibits a relatively low gravity field even though it dips more gently (average 30^0) than in the South Range (average 55^0). The gravity low in the NW portion of the map is due to the Archean basement (2.73 g/cm^3).

4.5.3.1 *Area of Misfit*

The junction of the East Range and the North Range has been highly faulted and downthrown (see F-F'). This resulted into the low gravity field observed in this region. This structural deformation is difficult to incorporate in this model, since the reference surface was the top of each unit and a constant elevation was specified for each geological section. Therefore, the youngest unit that can be delineated in the model is the Onwatin Formation, while the Chelmsford formation is occupying all spaces above it. This misfit due to the assumed constant elevation used to calculate the gravity response, also introduced a discontinuity (low gravity) in the linear gravity anomaly marked XXX (Figure 4.10). The gravity high in the SE of the map is caused by the Grenville Front and the gravity low east of the SIC is caused by the younger Wanapitei impact crater.

Hydrothermal alteration and metamorphism have differentially altered the mineralogy of the SIC and has resulted in the magnetic properties varying within the same rock type in different parts of the SIC, especially in the South Range and East Range, where remanence magnetisation is dominant. In other to assign the magnetic susceptibility and NRM values, an 'unconformity' was introduced between the North Range and the South Range at depth, while the magnetic properties of the North Range and the East Range were assumed to be the same. Attempts to forward model the magnetic data did not yield meaningful results.

4.6 Discussion on the Basal Deformation

In timing the deformational events associated with the Sudbury structure using the Lithoprobe seismic section, Wu et al. (1995) identified prominent north-dipping reflections under the

Sudbury Basin related to the change in dip of the North Range at depth, but did not provide a geological interpretation for these features, though they speculated they could be due to back faulting or fracturing. Olaniyan et al. (2013b) re-interpreted these north-dipping reflectors as caused either by basement thick skinned deformation or by the formation of a north-verging fold due wedging of basal Huronian volcanic rocks at the SIC-basement contact. Geochemical and geological field evidence that explain the deformation history and patterns of the SIC have been previously described (Cowan, 1996; Riller, 2005; Riller and Schwerdtner, 1997; Shanks and Schwerdtner, 1991 and references therein). Here, the derived 3-D geological model and forward computation was used to evaluate these hypotheses and present a new geophysical interpretation of the development of structures at the base of the Sudbury structure.

4.6.1 Testing of basal deformation

The hypothesis proposed to explain the linear high gravity anomaly under the Sudbury basin, that is the northwards folding of the basal SIC rocks, is consistent with the known pre- and post-impact geological history of the Sudbury area. Other possible geological models to explain the high gravity trend, were considered including proposed hidden layered mafic/ultramafic intrusions as suggested by Gupta et al., (1994). Small bodies of mafic intrusions such as Chicago (at the junction of the South and North Ranges), Norduna (at the junction of the East and South Ranges) and Joe Lake in the North Range occur around the SIC. We suggest that the event that deformed the SIC is more probably a late Proterozoic Penokean deformation, as it is interpreted to have affected both the basal part of the SIC and the transitional zone. The ages of these small mafic plutons around the SIC predate the emplacement of the SIC. A recent study indicates the Joe Lake intrusion to be Archean in age (2657 ± 9 Ma, Ames et al., 2013), and Norduna is dated at 2450 Ma (Prevec 1993). Having stated that, mafic rock pre-existing at the

target site of the meteorite impact, would probably have been highly brecciated and melted in the crater, therefore might not have resulted into folding or any kind deformation at the basal part of the SIC. Also, a mafic intrusive event after the SIC emplacement will probably have intruded fault zones and result into intrusive contacts like the olivine diabase, rather than the folding. Lastly, this kind of intrusion would have probably be more restrained in size, causing a circular or oval shaped gravity response and not a 42 km linear gravity high in the Sudbury Basin.

Basement thick-skinned deformation resulting in thrusting and uplift of the basement (Olaniyan et al., 2013b) was also tested using a 3-D forward modelling approach. This can be modelled by changing the density (2.80- 2.83 g/cm^3) of the block A (Figure 3.4b) at the basal part of the SIC to the Archean basement density (2.73 g/cm^3, Gupta et al., 1994), while every other parameters remain same. The resulting test grid should also further isolate the gravity response due to the relatively dense Onaping Formation (2.77 g/cm^3) and also evaluate the influence of other deep seated dense sources on the gravity field in the Sudbury Basin. This rapidly computed 3-D forward gravity response (Figure 4.12) is devoid of the long wavelength gravity high that is observed within the Sudbury Basin (Figure 4.11), which also extends to the footwall of the South Range over the Huronian metasediments. Likewise, it shows the gravity response due to the Onaping formation is limited and sits on a broader anomaly.

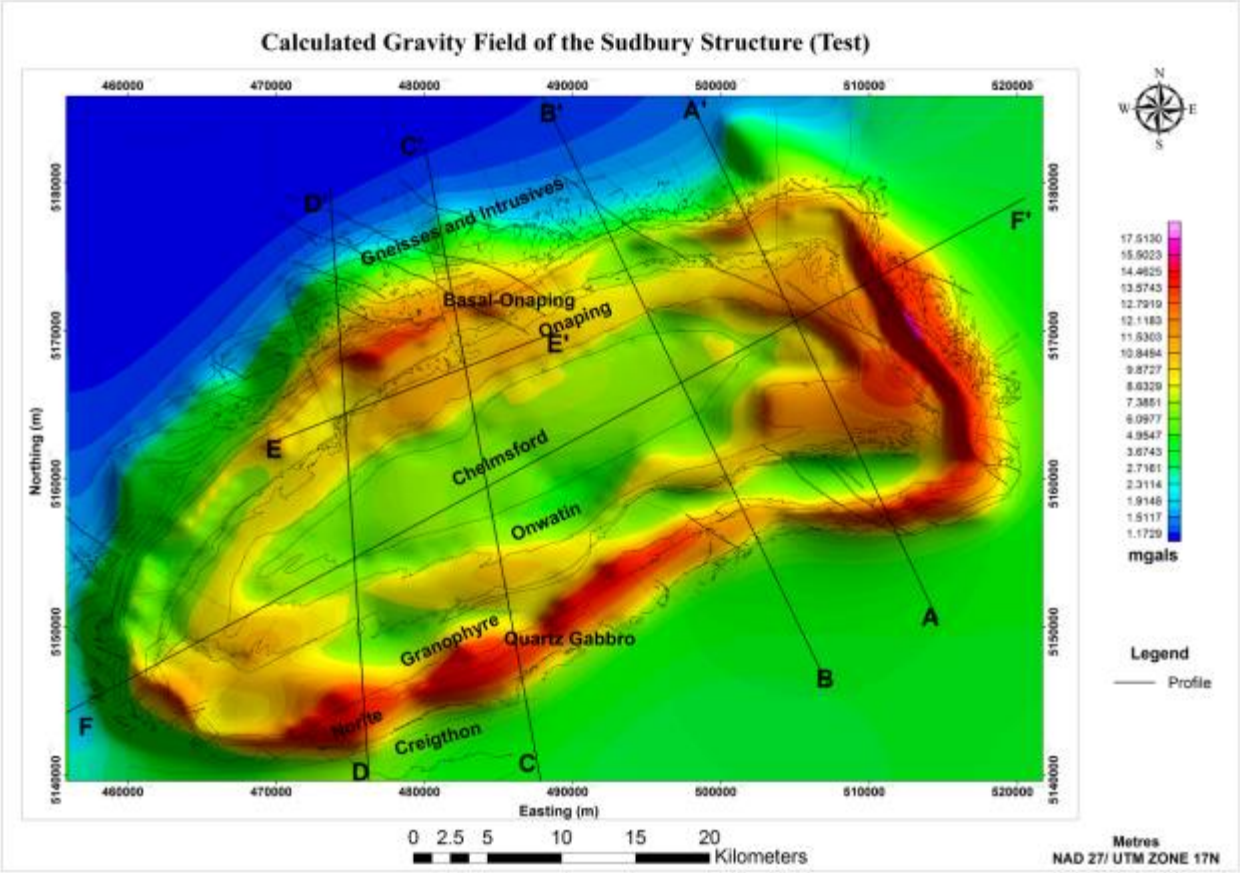

Figure 4.12: Test grid of the forward gravity response assuming the density of the wedge is same as the density of the basement (2.73 g/cm^3).

The result of the 3-D forward modelling clearly illustrates the existence of a deeper dense source under the Huronian metasedimentary rocks, which further extends to the north and gets shallower under the southern part of the Sudbury basin (Figure 4.13).

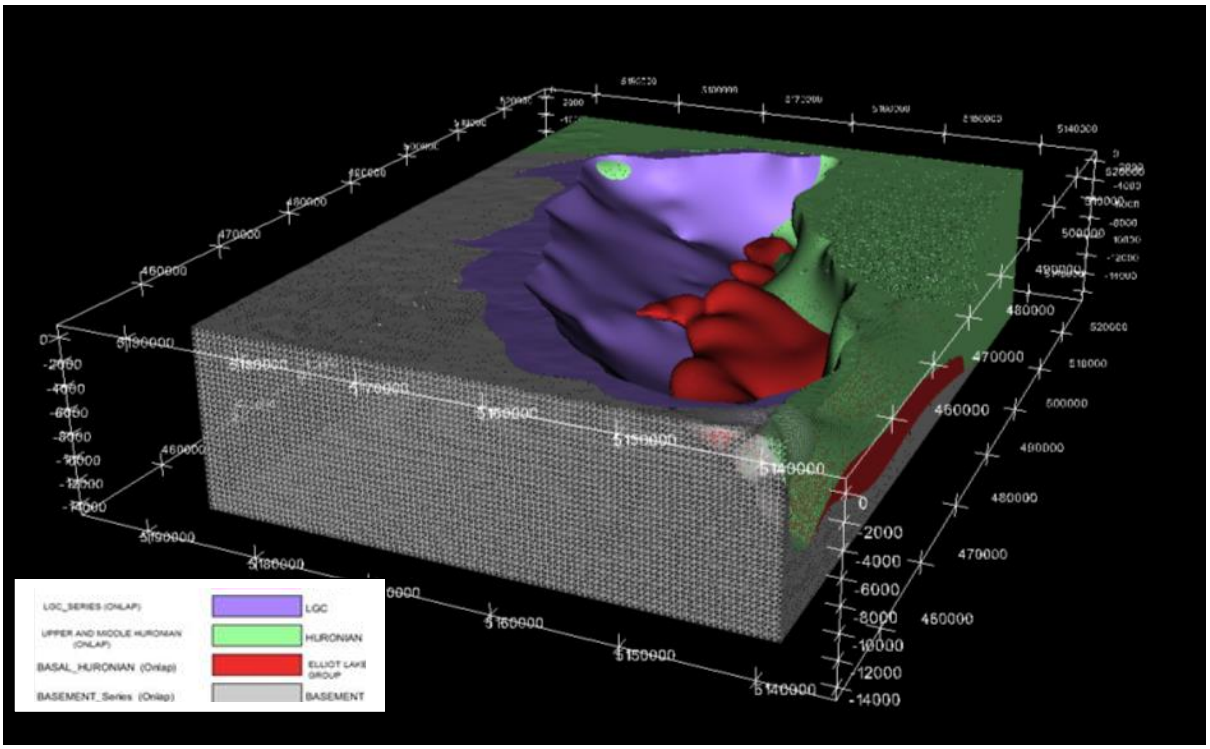

Figure 4.13: Wireframe 3-D geological model of the Sudbury structure illustrating the interpreted occurrence of the thrusted Elliot Lake mafic volcanic rocks and other intrusions at the base of the SIC (not shown) in the South Range.

4.6.2 Timing and implication of the basal deformation

Recent reconstructions of the pre-deformation geometry of the SIC suggests that it had an initial circular geometry with a minimum diameter of 60 km and differentiated from a melt sheet of about 2.5 km thickness (Roest and Pilkington, 1994). Due to its large crater size, the thickness of the melt sheet (~2.5 km) and the post-impact breccias and deposits (~3 km), it was suggested that and the differentiation process would have lasted up to 500 million years. (Grieve et al., 1991; Ivanov and Deutsch 1999), allowing for multiple, syn-emplacement modifications. A more recent study at the Garson Mine on the South Range argued that Penokean deformation in the Sudbury area started shortly after the emplacement of the SIC (Mukwakwami et al., 2014).

Either way, the compressive Penokean regime was NW-directed and resulted in the compressive tectonic structures observed in the South Range of the SIC (Shanks and Schwerdtner, 1991).

The suggestion that deformation at the base of the SIC contributed to its present post-impact shape only requires simple changes to present interpretations of the post-impact deformation of the Sudbury structure. Our model proposes that some geological features observed within the SIC, such as in-basin NE open folds and longitudinal south-dipping Vermillon fault set, have deep seated origins. The model is consistent with post-impact Penokian inversion of pre-impact Huronian rift basins along the continental margin of the Superior craton. Post-impact reverse movement along the syn-depositional Murray fault set has been reported by Raharimahefa et al. (in review). Simplified geologic cross-section diagrams are used to illustrate how the normal faults bounding Huronian rift margin basins could have been reactivated as reverse faults that deformed the basal part of the SIC. The proposed sequence of events (A-F) is presented in Figure 4.12 below and described as follows:

A. The development of the Huronian continental rift margin likely to have been initiated by an impinging hot spot (Heaman, 1997) or in response to the tensional force in crust and lithospheric mantle (Dunbar and Sawyer, 1988).
B. Deposition of supracrustal rocks during rifting began with conglomerates of the Livingstone Creek Formation and uranium-rich Matinenda Formation of the Elliot Lake Group. In the Sudbury region, a thick package of volcanic rocks interbedded with minor stratified metasedimentary rocks (Elsie Mountain, Stobie and Copper cliff formations) was emplaced early during rifting. These volcanic rocks underlie a 12 km thick sequence of Huronian sedimentary rocks that was deposited as the Superior margin evolved from a rifted margin to a stable continental margin (Long and Lloyd, 1983; Long et al., 1999;

Young et al., 2001). Although not illustrated in the cartoon, the Huronian rocks were intruded by the felsic plutons- Murray (2477 Ma, Krogh et al., 1996) and Creighton (2333 Ma, Frarey et al., 1982) as well as the Nipissing diabase sills and dikes (2219 Ga, Corfu and Andrews, 1986).

C. At 1850 Ma, an extraterrestrial bolid collided with Superior continental margin. Our model assumes that the SIC was initially 2.5 km thick and was circular with a minimum 65 km diameter (Roest and Pilkington,1994). The Onaping and Onwatin formations were deposited in the depression formed by the crater, which sits on gently south-dipping Archean gneisses (AG) that are covered to the south by a southward thickeneing sequence of Huronian sedimentary rocks (Milkereit et al., 1992).

D. The post-impact, NW-directed, Penokean Orogeny re-activated normal faults below the Huronian sequence as reverse faults thereby thrusting the faulted basement and the Elliot Lake group mafic volcanic rocks northwards below the SIC. A Penokean mountain chain formed that shedded sediments of the Chelmsford Formation into a basin, the Sudbury basin, overlying the SIC and impact-related breccias of the Onaping Formation (Young et al., 2001). The SIC norite acted as a competent mechanical anisotropy (Boerner et al., 1999) that buckled during deformation resulting in the formation of a north-verging ductile fold at the base of the SIC. This resulted in the formation of broad open anticlinal and synclinal folds in the Sudbury basin (Shanks and Schwerdtner, 1991). The north limb of the anticlinal structure corresponds to the north dipping reflectors in the Lithoprobe section under the Sudbury Basin.

E. Continued shortening during the Penokean deformed the SIC into its present elliptical shape (Grieve et al., 1991; Milkereit et al., 1992; Wu et al., 1995; Deutsch et al., 1995) and

resulted into the tightening of the folds in the Sudbury basin, the overturning of the SIC-basement contact in the South Range, and formation of thrust faults in the South Range and Sudbury basin.

F. Erosional activity reduced the elevated part of the South Range to the current level. This current state of the SIC explains most of the reflectors interpreted in the Lithoprobe transect (Olaniyan et al., 2013b).

Proposed deformational sequence of the Sudbury structure (Cartoon, not to scale).

(A)

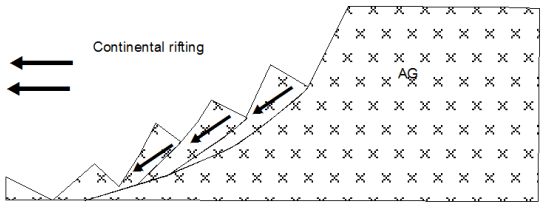

i) Development of the Huronian continental rift margin along the boundary of the Superior and the Southern Provinces

ii) Opening of the ocean

(B)

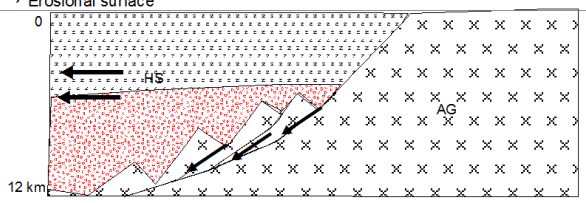

i) Continental rifting continues

ii) Emplacement of the Huronian volcanics and sedimentary rocks (2.4 to 2.2 Ga)

iii) Intrusion of Huronian rocks by Murray (2.4 Ga) and Creigthon (2.3 Ga) and Nippissing diabase (2.2 Ga) (not shown)

iv) Transition from rift margin to passive margin and sinistral movement

(C)

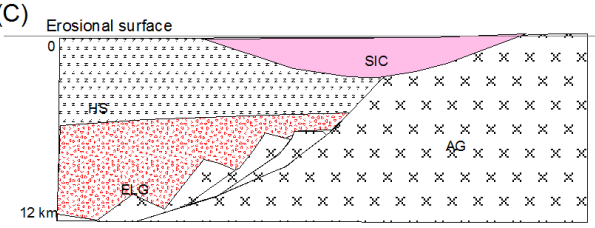

i) Impact event occured at the margin of Archean and Proterozoic rocks (1850 Ma).

ii) Impact melt in a saucer shaped crater with flat surface and curved bottom

(D)

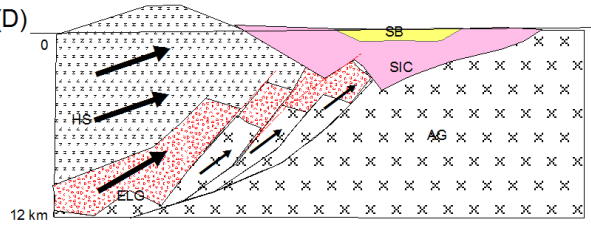

i) Volcanic activities and explosive interaction of magma with water led to deposition of the Onaping Formation and Onwatin Formation was later deposited in a more quiescent environment.

ii) Post-SIC Penokean orogeny began shortly after the impact melt has differentiated.

iii) Transition from Passive margin into foreland margin system

iv) Northwards thrusting of the basal Huronian mafic rocks and other mafic intrusive rocks.

v) Deformation of the basal portion of the SIC

vi) Development of a north-vergent fold at the base of the SIC

(E)

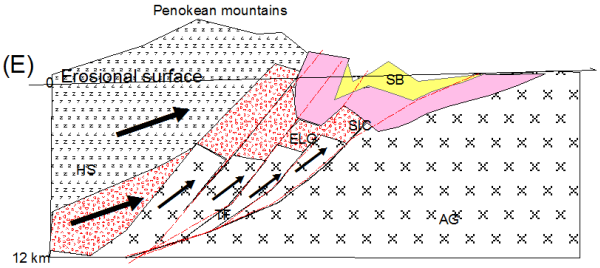

Further compressional deformation during the Penokean orogeny might have resulted into:

i) deformation of the initial geometry of the SIC

ii) tigthening of the open folds.

iii) overturning of the SIC in the South Range.

iv) development of fractures and joints in the NW direction.

v) Development of Penokean mountains and deposition of the Chelmsford Formation

vi) thrusting of the Elliot Lake northwards to south of the SIC and the felsic plutons

(F)

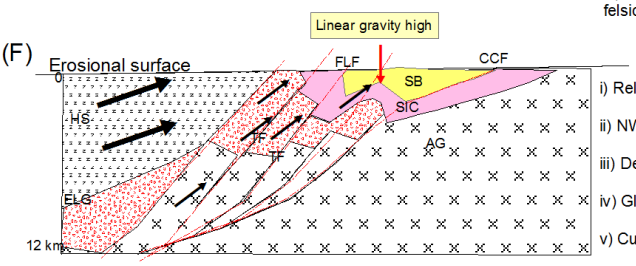

i) Relative movement along the fractures and joints

ii) NW thrusting of the South Range rocks and Onaping Formation

iii) Development of Vermilon Lake fault set

iv) Glacial and erosional activities

v) Current geometry of the SIC consistent with the Lithoprobe seismic section

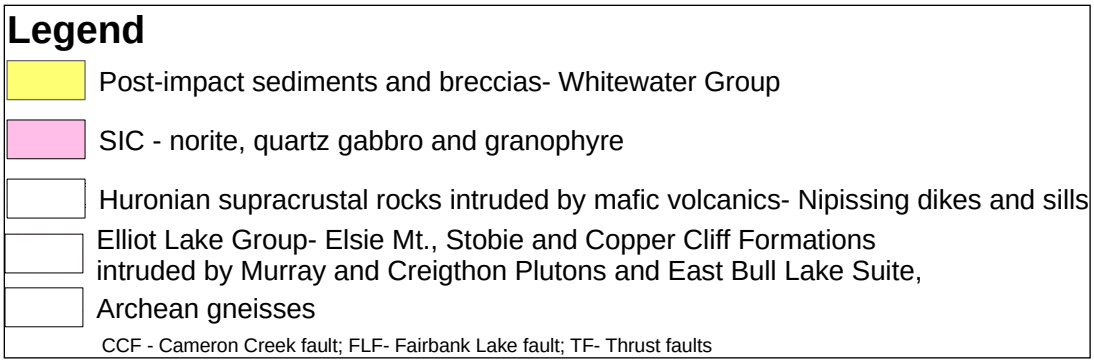

Figure 4.14: Proposed timing and sequence of the deformation of the Sudbury structure

The possibility of deep contact deposits at 4 to 6 km depth was highlighted in a previous paper (Olaniyan et al., 2013b). Our 3-D geological forward modelling further constrains the possible sources of the linear gravity high below the Sudbury structure. However, the calculated broad linear anomaly at 4-5 km is less strong than the observed anomaly (Figure 10). This could imply that the folded portion of the SIC rocks is shallower under the Sudbury basin or it is due to the presence of the xenolith bearing Sublayer, in both cases are of mineral exploration interest.

4.7 Conclusions

Our proposed 3-D geological model, which is based on prior geological knowledge, a seismic section and available potential field data, has provided insights into the sources of previously unexplained geophysical anomalies in the Sudbury structure. The linear gravity high under the Sudbury basin is related to the north-verging folding and deformation at the base of the SIC due to the reversal of normal faults as reverse faults that thrusted Huronian mafic volcanic rocks below the SIC. Having developed a 3-D model for the Sudbury structure, this model can continually be updated as more detailed subsurface information such as more reflection seismic data across the SIC and /or drilling a deep borehole become available.

References

1. Ames, D.E., Davidson, A.J., Buckle, L., and Card, K.D. 2005. Geology, Sudbury bedrock compilation, Ontario. Geological Survey of Canada, Open file 4570, Scale 1:50,000.
2. Ames, D.E., and Farrow, C.E.G., 2007, Metallogeny of the Sudbury mining camp, Ontario, *in* Goodfellow, W.D., ed., Mineral Deposits of Canada: A Synthesis of Major Deposit-Types, District Metallogeny, the Evolution of Geological Provinces, and Exploration Methods. Geological Association of Canada, Mineral Deposits Division, Special Publication No. 5, p. 329-350.
3. Ames, D.E., Hanley, J.J., Tuba, G., Bleeker, W., and Kamo, S. 2013. Primitive Source Revealed in the Sudbury Impact Structure: Implications for Cratering and Metal Sources. Large Meteorite Impacts and Planetary Evolution V, Proceedings of the conference held 5-8 August 2013, in Sudbury, Canada. LPI Contribution No. 1737, p.3099
4. Boerner, D.E., and Milkereit, B. 1999. Structural evolution of the Sudbury Impact Structure in the light of seismic reflection data. *In* Impact cratering and Planetary Evolution II, Boulder Colorado. *Edited by* B. Dressler, and V.L. Sharpton. Geological Society of America, Special Paper 339**,** pp. 419-430**.**
5. Card, K.D., 1964, Geology of Sudbury- Mautoulin area: Ontario Geological Survey, Report 166.
6. Card, K.D. 1965. Geology of the Hyman and Drury townships; Ontario Department of Mine, Geological report 34, 38p.

7. Card, K.D., and Jackson, S.L. 1995. Tectonics and Metallogeny of the Early Proterozoic Huronian foldbelt and the Sudbury structure of the Canadian Shield, Field Trip Guide Book, Geological Survey of Canada, Open File 3139.
8. Corfu, F. and Andrews, A. 1986. A U-Pb age for mineralized Nipissing Diabase Gowganda, Ontario. Canadian Journal of Earth Sciences, **23**: 107-112.
9. Cowan, E.J. 1996. Deformation of the eastern Sudbury Basin; unpublished PhD thesis, University of Toronto, Toronto, Ontario, 322p.
10. Deutsch, A., Grieve, R.A.F., Avermann, M., Bischoff, L., Brockmeyer, B., Buhl, D., Lakoomy, R., Muller- Mohr, R., Ostermann, M., and Stoffer, D. 1995. The Sudbury structure (Ontario, Canada): a tectonically multi ring impact basin. Geologische Rundschau, **84**: 697-709.
11. Dietz, R.S. 1964. Sudbury structure as an astrobleme. Journal of Geology, **72**: 412-434
12. Dressler, B.O. 1984. General Geology of the Sudbury area. *In* The Geology and Ore Deposit of the Sudbury structure, Ontario Geological Survey, Special Volume **1**: 57-82.
13. Dunbar, J.A., and Sawyer, D.S., 1988. Continental rifting at pre-existing lithospheric pressure weaknesses. Nature, 333, 450-452.
14. Dressler B. O. and Sharpton V. L. 1999. Large Meteorite Impacts and Planetary Evolution II. Geological Society of America Special Paper 339. Boulder, Colorado, USA. Geological Society of America. 464 p.
15. Frarey, M.J., Loveridge, W.D., and Sillivian, R.W. 1982. A U-PB age for the Creighton granite, Ontario. *In* Rb-Sr and U-Pb isotope age studies, Report 5, Current Research, Part C, Geological Survey of Canada paper, **82**, pp. 129-132.

16. Galdeano, A., Andreoli, M.A.G., Hart. R. J. 2008. Magnetic Imaging of the Vredefort Dome: Implications for the size and geometry of the Vredefort Crater. *In* Large Meteorite Impacts and Planetary Evolution IV.
17. Grieve, R.A.F., Stoffler, D., and Deutsch, A. 1991. The Sudbury structure: controversial and misunderstood? Journal of the Geophysical Research, **96**: 22753-22764.
18. Gupta, V.K., Grant, F.S., and Card, K.D. 1984. Gravity and magnetic characteristics of the Sudbury structure. *In* The Geology and Ore Deposits of the Sudbury structure: Ontario Geological Survey. *Edited by* E.G. Pye, A. J. Naldrett and P. E. Giblin. Special Volume **1**, pp. 381-410.
19. Heaman, L.M., 1997. Global mafic magmatism at 2.45 Ga: remnants of a large igneous province: Geology, **25**, 295-298.
20. Hearst, R.B. and Morris, W.A. 2001. Regional gravity setting of the Sudbury structure: Geophysics, **66**: 1680-1690
21. Hearst, R.B., Morris, W.A. and Thomas, M.D. 1994. Magnetic interpretation along the Sudbury structure Lithoprobe Transect. *In* Proceedings of the Sudbury-Noril'sk Symposium Ontario Geological Survey. *Edited by* P.C. Lightfoot, and A. J. Naldrett. Special Volume **5**, pp. 33-43.
22. Ivanov B.A. and Deutsch, A, 1999. Sudbury impact event: cratering mechanism and thermal history. *In* Large Meteorite Impact and Planetary Evolution II, Geological Society of America, Special Paper 339, p 389- 398.
23. Lane, R., and Guillen, A., Geologically-inspired Constraints for a Potential Field Litho-inversion Scheme. Proceedings of IAMG'05: GIS and Spatial Analysis, Vol.1, 181-186.

24. Long, D.G.F. and Lloyd, T.R. 1983, Placer gold potential of basal Huronian of the Elliot Lake Group in the Sudbury Area, Ontario: Ontario Geological Survey Miscellaneous paper 126, 256- 258.
25. Lajaunie, C., Courrioux, G., Manuel, L., 1997. Foliation fields and 3-D cartography in geology: principles of a method based on potential interpolation: Mathematical Geology **29**, 571-584.
26. McGrath, P.H., and Broome, H. J. 1994. A gravity model of the Sudbury structure along the Lithoprobe seismic line: Geophysical Research Letters, **21**: 955-958.
27. McInerney, P., Guillen, A., Courrioux, G., Calcagno, P. and Lees, T., 2005, Building 3-D geological models directly from data? A new approach applied to Broken Hill, Australia: Digital Mapping Techniques 2005 Workshop in Baton Rouge.
28. Milkereit, B., Green, A., and Sudbury working group 1992. Deep geometry of the Sudbury structure from seismic reflection profiling: Geology, **20**: 807-811.
29. Mukwakwami, J., Lafrance, B., Lesher, C.M., Tinkham, D.K., Rayner, N.M., Ames, D.E. 2014. Deformation, metamorphism and mobilisation of Ni-Cu-PGE sulfides ores at Garson Mine, Sudbury: Minerallum Deposita, **49**: 175- 198.
30. Naldrett, A.J., Bray, J.G., Gasparrini, E.L., Podolsky, T. and Rucklidge, J.C. 1970. Cryptic variations and the petrology of the Sudbury Nickel Irruptive: Economic Geology, v.65, p 122-155
31. Naldrett, A. J. and R. H. Hewlins, 1984. The main mass of the Sudbury structure. *In* The Geology and Ore Deposit of the Sudbury structure: Ontario Geological Survey, Special volume **1**, 231-251.

32. Olaniyan, O.F., Smith, R.S., and Morris, W.M. 2013a. Qualitative interpretation of the Sudbury structure. Interpretation, **1**: 25-43.
33. Olaniyan, O.F., Smith, R.S., Lafrance B. 2013b. A constrained potential field data interpretation of the deep geometry of the Sudbury structure: Canadian Journal of Earth Sciences (Submitted)
34. Polzer, B., 2000, The role of borehole EM in the discovery and definition of the Kelly Lake Ni-Cu deposit, Sudbury, Canada, Society Economic Geologists Technical Program, Expanded Abstracts, 1063-1066
35. Pye, E.G., Naldrett, A.J., and Giblin, P.G. 1984. The Geology and Ore Deposits of the Sudbury structure. Ontario Geological Survey, Special Volume **1**: 603p.
36. Riller, U., 2005 Structural characteristics of the Sudbury impact structure, Canada: impact induced and orogenic deformation: Meteoritics and Planetary Science, **40**, 1723-1740.
37. Riller, U., and Schwerdtner, W.M. 1997. Mid-crustal deformation of the southern flank of the Sudbury Basin, central Ontario, Canada: Geological Society of America Bulletin, **109**: 841-854.
38. Rousell, D. H, 1984b, Onwatin and Chelmsford formations, *in* the Geology and Ore Deposit of the Sudbury structure: Ontario Geological Survey, Special volume **1**, 211-218.
39. Roest, W. R., and Pilkington, M. 1994. Restoring post-impact deformation at Sudbury: A circular argument, Geophysical Research Letters, 21, pp. 959-962
40. Schwarz, E.J and Buchan, K.L. 1982. Uplift deduced from remanent magnetization; Sudbury area since 1250 Ma ago: Earth and Planetary Science Letters, **58**, 65-74.

41. Shanks, W.S., and Schwerdtner, W.M. 1991. Structural analysis of the central and southwestern Sudbury structure, Southern Province, Canadian Shield: Canadian Journal of Earth Sciences, **28**: 411-430.
42. Spray, J.G., Butler, H.R., and Thompson, L.M. 2004. Tectonic influences on the morphometry of the Sudbury impact Structure: implication for terrestrial cratering and modeling: Meteoritics and Planetary Science, **39**: 287-301.
43. Veermeesch, P.M and Morgan, J.V. 2008. Structural uplift beneath the Chicxulub impact structure: Journal of Geophysical Research, vol. 113, B07103.
44. Watts, A., 1997, Exploring for Nickel in the 90s, or 'til depth us do part', *in* A.G. Gubins ed., Proceedings of Exploration 97: Fourth Decennial International Conference on Mineral Exploration.
45. Wu, J., Milkereit, B. and Boerner, D. 1995. Seismic Imaging of the enigmatic Sudbury structure: Journal of Geophysical Research, **100**: 4117- 4130.

CHAPTER 5: Future Outlook of the Research work.

5.1 Regional physical property studies of the Sudbury structure

This study relied mostly on published physical petrophysical data, which were obtained from borehole and surface rock samples from the Sudbury area (Gupta et al., 1994; McGrath and Broome, 1994; Hearst et al., 1994). Density values appear to be more reliable and consistent because the mass per unit volume of the individual rock unit does not change much from one location to another. But due to diffrentian alteration pattern and remanence magnetisation, the magnetic susceptibility of rocks in the Sudbury structure varies largely from location to location and even within individual rock unit (Morris 1981). This is further complicated by the presence of remanence magnetisation in the East and South Ranges. The magnitude of remanence magnetisation used in this study was selected to fit the measured data, even though the direction of inclination and declination were kept constant (Hearst et al., 1994). The collection and statistical analysis of physical rock properties from samples collected systematically from outcrop and core samples would enhance knowledge about the distribution of the these properties and improve the quality of this data in future studies.

5.2 Additional Lithoprobe seismic section across the Sudbury structure

This research benefitted greatly from the re-interpreted, merged Lithoprobe section 40 and 41 (Milkereit et al., 1992). As described in Chapter 3, the merging of the section 40 and 41 is not consistent with the North Range rock lithological contacts. The other seismic sections 1, 43, 44 also acquired during the Lithoprobe project did not provide much additional information due to the short length of the sections or the level of processing. Seismic is the only geophysical method

that can provide a high resolution image of complex subsurface geological structures. Since the initial Sudbury surveys, the processing techniques for hardrock terranes has been improved (Eaton, et al., 2003). Hence, it is recommended that more seismic data be acquired across the eastern and western parts of the SIC and probably across the longitudinal section. The 3-D model developed in this study is generated within Geomodeller by interpolation algorithms that are guided by field geological observations and measurements. The addition of new subsurface geometry information provided by seismic or borehole data will lead to a more refined 3-D geological model.

5.3 3-D lithological inversion modelling

The approach adopted in this study was to build a 3-D geological model based on the geometry interpreted for five constrained 2.5-D sections. These sections comprise polygons with different shape and physical properties and were developed from limited subsurface geological information. 3-D forward modelling enabled the computation of the spatial response of the constrained geological model using the same density values as were derived in the 2D models. This methodology generally assumed that the 2.5-D and 3-D geological units defined with the polygonal shapes had a constant physical property. This is not always true, as studies within the Sudbury structure have shown variations in the magnetisation and remanent magnetisation in same rock unit (Morris, 1981).

This study resulted in a 3-D geological model that is consistent with all the available geological constraints and consistent with the measured gravity data. This model can be used as a reference model in a litho-based inversion process that uses a statistical or probability algorithm to determine the subsurface distribution of physical properties of a voxelised Earth, which will

generate the measured gravity field. This will test the model presented and also provide more insight into the subsurface distribution of physical properties in the Sudbury structure. Guillen et al. (2008) applied a Monte Carlo sampling inversion technique in 3-D Geomodeller to a multidisciplinary dataset from the French Massif Central. The dataset was constrained by geological and geostatistical information to demonstrate that a probabilistic distribution of granites and leucogranites in the sub-surface can be established along the Sillion-Houllier Fault. Fullagar et al. (2008) describe the VPmg software, which could be used to invert the gravity and magnetic data. Some preliminary results of an on-going, three-dimensional litho-constrained inversion study, which uses the 3-D geological model presented and the Geological Survey of Canada's (GSC) low resolution bouguer gravity data to model the most probable density distribution model for the Sudbury Structure are presented below (Figure 5.1 and 5.2).

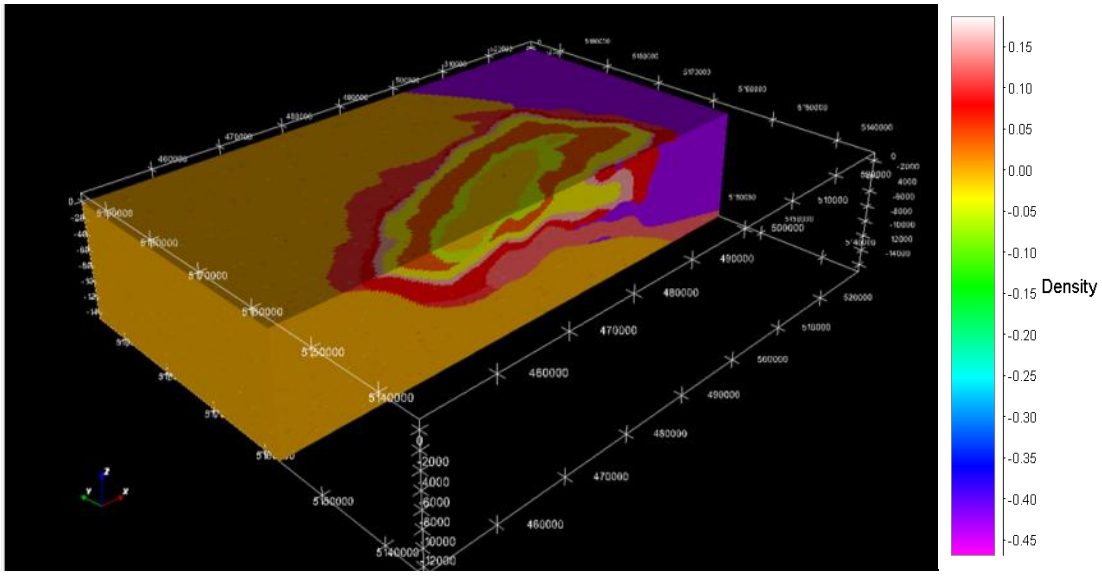

Figure 5.1: North-east view of the most probable 3-D density distribution model clipped across southern portion of the Whitewater Group and the South Range. The density voxel volume was specified to be 150 x 150 x 100 number of cells in the x, y and z directions. Legend shows for each lithological unit and basement (2.73 g/cm^3) the density contrast in mgal. The density

distribution model illustrates the a dense and elongated body stretching from under the Sudbury basin into the eastern axis of the SIC.

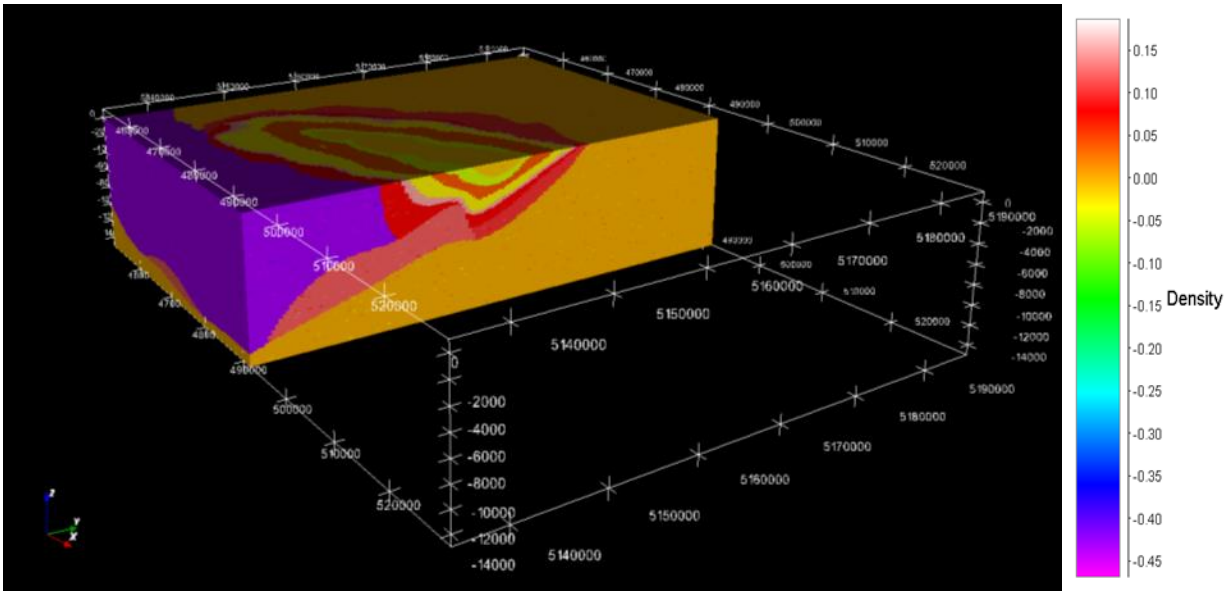

Figure 5.2: North-west view of the most probable 3-D density distribution model clipped across the SIC in a north-south direction. The density voxel volume was specified to be 150 x 150 x 100 number of cells in the x, y and z directions. Legend shows for each lithological unit and basement (2.73 g/cm^3) the density contrast in mgal. The density distribution volume illustrates the interpreted deformation of the basal part of the SIC by dense body.

5.4 High resolution ground geophysical survey (E-W direction)

The airborne geophysical dataset used in this research work was acquired mostly in the NNW direction across the strike of the SIC. Although this survey design is able to resolve the regional trend of the SIC, this study has shown what appears to be sub-parallel geological features, such as the interpreted growth faults located near the centre of the SIC in the North Range. The occurrence of these structures and perhaps their significance in localizing minerlaization could be tested by acquiring ground geophysical surveys in an E-W direction over this area. Ground

gravity and magnetic surveys would help to explain the gradual reduction in the gravity and magnetic fields across the centre of the SIC.

5.5 Topographic correction

One difficulty encountered during this research that required significant effort and time to overcome was the lack of a data exchange format between the Geosoft Gmsys and 3-D Geomodeller software. This deficiency required the conversion of the 2.5-D models in Gmsys format to an image format, thereby losing the topographical information of the geological section during the 3-D modelling in Geomodeller. This introduced inconsistencies into the 3-D geological model, especially in areas with substantial differences between the chosen and actual topographical height. Intrepid, the developer of Geomodeller is working on interoperability "gaps" between the Gmsys and Geomodeller (Personal communication, Desmond Fitzgerald). When achieved, it will be interesting to re-import the 2.5-D models into the modelling environment and correct topographic inconsistencies in the data.

5.6 Deep geological investigation

This study has proposed that the folding interpreted to have affected the footwall rocks and the SIC may have resulted in the emplacement of sulfide-rich sublayer at depths of about 5-6 km under the southern portion of the Sudbury Basin in the South Range. There is need to further investigate this interpretation either by a deep drilling or by using some other less expensive, but deep penetrating geophysical method such as magneto-telluric (MT) to test the presence of conductive bodies at this location.

5.7 **Explaining features outside the basin**

This study focused on explaining geophysical gravity and magnetic anomalies along the elliptical axis of the SIC. The geological model in Geomodeller could be augmented to explain the gravity anomaly associated with the Wanapitei structure and the linear gravity anomaly located south of the Sudbury Structure. This would require incorporating geological models, which best explain these anomalies into the 3-D geological model developed in this study.

References

1. Eaton, D.B., Milkereit, B., and Salisbury, M. 2003. Hardrock seismic exploration: Mature technologies adapted to new exploration targets, Foreword to hardrock seismic exploration. SEG, 1-6.
2. Fullagar, P.K., Pears, G.A., and McMonnies, B. 2008. Constrained inversion of geologic surfaces – pushing the boundaries. The Leading Edge, **27**, 98-105.
3. Guillen, A., Calcagno, Ph., Courrioux, G., Joly, A., and Ledru, P. 2008. Geological modelling from field data and geological knowledge Part II. Modelling validation using gravity and magnetic data inversion. Physics of the Earth and Planetary Interiors, **171**, 158-169.
4. Gupta, V.K., Grant, F.S., and Card, K.D. 1984. Gravity and magnetic characteristics of the Sudbury Structure. *In* The Geology and Ore Deposits of the Sudbury Structure: Ontario Geological Survey. *Edited by* E.G. Pye, A. J. Naldrett and P. E. Giblin. Special Volume **1**, pp. 381-410.
5. Hearst, R.B., Morris, W.A., and Thomas, M.D. 1994. Magnetic interpretation along the Sudbury structure Lithoprobe Transect. *In* Proceedings of the Sudbury-Noril'sk Symposium Ontario Geological Survey. *Edited by* P.C. Lightfoot, and A. J. Naldrett. Special Volume **5**, pp. 33-43.
6. McGrath, P.H., and Broome, H. J. 1994. A gravity model of the Sudbury Structure along the Lithoprobe seismic line. Geophysical Research Letters, **21**: 955-958.

7. Milkereit, B., Green, A., and Sudbury working group 1992. Deep geometry of the Sudbury structure from seismic reflection profiling. Geology, **20**: 807-811.
8. Morris, W.A. 1981. Intrusive and tectonic history of the Sudbury micropegmatite; the evidence from paleomagnetism. Economic Geology, **76**: 791-804.